5-2010

Mathematical Modeling of Light Utilization and the Effects of Temperature Cycles on Productivity in a Steady-State Algal Photobioreactor

Peter Edwin Zemke
Utah State University

MATHEMATICAL MODELING OF LIGHT UTILIZATION AND THE EFFECTS OF TEMPERATURE CYCLES ON PRODUCTIVITY IN A STEADY-STATE ALGAL PHOTOBIOREACTOR

by

Peter E. Zemke

A dissertation submitted in partial fulfillment
of the requirements for the degree

of

DOCTOR OF PHILOSOPHY

in

Mechanical Engineering

Approved:

_____	_____
Byard Wood Major Professor	Brent Stucker Committee Member
_____	_____
Barton Smith Committee Member	Ronald Sims Committee Member
_____	_____
Heng Ban Committee Member	Byron Burnham Dean of Graduate Studies

UTAH STATE UNIVERSITY
Logan, Utah

2010

ABSTRACT

Mathematical Modeling of Light Utilization and the Effects of Temperature Cycles on Productivity in a Steady-State Algal Photobioreactor

by

Peter E. Zemke, Doctor of Philosophy

Utah State University, 2010

Major Professor: Dr. Byard D. Wood
Department: Mechanical and Aerospace Engineering

The work presented here investigated two methods of improving productivity in microalgal photobioreactors: applying temperature cycles intended to maximize photosynthesis and minimize respiration, and development of a mathematical model that predicts improvements in photon utilization using temporal light dilution (flashing).

The experiments conducted on diurnal temperature cycles with *Dunaliella tertiolecta* in 30-L outdoor photobioreactors showed that a properly chosen temperature cycle can improve mass and energy productivity by 18% over an identical photobioreactor with a constant temperature. However, excessively large temperature cycle amplitudes reduced productivity. A 4-7% increase in energy content was observed in microalgae exposed to temperature cycles. The physiological reason for this could not be established.

A relationship similar to the Bush Equation was obtained that related photon utilization efficiency to flashing frequency, load factor, Photosystem II (PSII) concentration and reaction frequency, and chlorophyll content. The model was validated by the experimental data of a number of researchers.

(153 pages)

ACKNOWLEDGMENTS

This work would not have been possible without all of my family, mentors, friends, and coworkers encouraging me, helping me, and supporting me.

I wish to thank the LORD God, for "with man this is impossible, but with God all things are possible."

I am deeply grateful to my wife, Cindy, whom I love coming home to every day, and to the rest of my family, Daniel, Glenda, Elizabeth, and Tom, for their love, patience, and help.

I am indebted to my advisor and mentor, Dr. Byard Wood, for encouraging me to embark on this endeavor and investing so much of his time, resources, and energy into me. I also wish to thank my committee, Dr. Bart Smith, Dr. Heng Ban, Dr. Brent Stucker, and Dr. Ron Sims, for their lectures, help, and input, inside the classroom and out.

To my coworkers, friends, and staff - Dan Dye, Stephen Merrigan, Shaun Dustin, Brad Wahlen, Shatanu Wahal, Mike Morgan, Mikey Morgan, Curtis Carrigan, Nathan Phillips, Tracy Pace, and Bonnie Ogden - I could not have done this without them and I thank them for making this experience enjoyable, or at least for having someone to laugh with when it was not.

Finally, I wish to acknowledge Dr. Brett Barney for providing me with many of the ideas and materials for this research and the Utah Science Technology and Research program for funding this research.

Peter Edwin Zemke

CONTENTS

LIST OF TABLES

LIST OF FIGURES

NOMENCLATURE

c	Volumetric photosynthetic content (μmol m^{-3})
e	Uncertainty
f	Photosynthetic unit turnover frequency (s^{-1})
k	Total Absorbitance (m^2 g^{-1})
k_{LHP}	Absorbitance of light-harvesting pigment (m^2 g^{-1})
m_s	Algal sample dry mass (g)
p	Probability
r	Respiration rate (g day^{-1})
s_2	Transition depth from partial to full light dilution (m)
s_3	Transition depth from ineffective to full light dilution (m)
t_f	Duration of light flash (s)
t_d	Duration of dark period (s)
u_P	Photon utilization fraction
$u_P^{(2)}$	Photon utilization for partially light diluted cultures
$u_P^{(3)}$	Photon utilization for culture with ineffective light dilution
z	Distance into algal culture (m)
C	Areal photosynthetic unit density (μE m^{-2})
C_p	Specific heating value (kJ kg^{-1} K^{-1})
C_T	Total inorganic carbon concentration (mol kg^{-1})
E	Energy productivity (kJ day^{-1})

F	Flow rate (L day^{-1})
H_T	Total energy content of dry algae (kJ g^{-1})
I	Light intensity (μE m^2 s^{-1})
I_a	Average incident light intensity for intermittent light (μE m^{-2} s^{-1})
I_{abs}	Absorbed light (E day^{-1})
I_f	Intensity of light flashes (μE m^{-2} s^{-1})
I_I	Average incident light intensity scaled to full sunlight
I_o	Incident continuous light intensity, (μE m^{-2} s^{-1})
I_s	Saturation light intensity, (μE m^{-2} s^{-1})
I_u	Rate of light utilized by algae (μE m^{-2} s^{-1})
I_w	Rate of light wasted by an algal culture (μE m^{-2} s^{-1})
I_z	Light intensity inside an algal culture (μE m^{-2} s^{-1})
P	Algal productivity (g day^{-1}),
Q	Thermal energy requirement (kJ day^{-1})
T	Temperature (K)
V_p	Volume of algal culture removed from the photobioreactor (L)
V_R	Photobioreactor volume (L)
V_s	Algal culture sample volume (L)
X	Cell concentration (g L^{-1})
Y	Algal yield, (s m^2 E^{-1})
α	Photobioreactor absorbtivity

χ	Volume of photosynthetic units per chlorophyll area (m)
ε	Photosynthetic yield (g E^{-1} day^{-1})
ϕ	Flashing load factor
γ	Photosynthetic unit excitation requirement (E mol^{-1})
η	Land use efficiency
κ	I_s correction factor
μ	Specific growth rate (day^{-1})
μ_{max}	Maximum specific growth rate (day^{-1})
ν	Flashing frequency (s^{-1})
θ	Hydraulic retention time (day)
ρ	Media density (g L^{-1})
ρ_{LHP}	Density of light-harvesting pigments (g m^{-3})
τ	Photosynthetic unit turnover period (s)
Δt	Elapsed time between samples (day)
OD	Optical density
PSU	Photosynthetic unit
PSII	Photosystem II
TEC	Total energy content
AFEC	Ash-free energy content
LED	Light-emitting diode
GC	Gas chromatography

NTC	No temperature control
CTC	Constant temperature control
VTC	Variable temperature control
HRT	Hydraulic retention time
LHP	Light harvesting pigment
TAG	Triacylglycerol
FFA	Free fatty acid

CHAPTER 1

INTRODUCTION

Current changes in perspectives on fossil fuels have generated interest in obtaining fuels from biomass. While many sources of biomass are available for biofuels, microalgae (henceforth referred to as algae) are of special interest. These photosynthetic microorganisms are capable of producing biomass at rates orders of magnitude higher than terrestrial plants. Thousands of species of algae exist that possess a variety of characteristics that permit them to be grown in a wide range of conditions, and their cell compositions can be manipulated by environmental conditions to produce compounds such as starches or lipids that are of interest as a feedstock for biofuels [1].

The production of algae has seen intermittent interest only since World War II and the technology has not evolved significantly since then. For biofuels from algae to become competitive with fossil fuels, it will need to be produced very efficiently in terms of energy and economics [2]. This research explores two factors that are relevant to improving biomass productivity in photobioreactors (henceforth referred to as reactors): 1) light utilization, and 2) temperature cycles. The results of the research can be used toward designing and optimizing a reactor for photosynthetically producing algae.

This dissertation has been divided into two sections: chapters 2 through 5 discuss the experiments on temperature cycles in reactors while chapters 6 through 10 discuss the development of the light utilization relationship.

CHAPTER 2

TEMPERATURE CYCLES IN PHOTOBIOREACTORS

The productivity of an algal reactor can be generally expressed as [3]:

$$P = I_{abs}\varepsilon - r \tag{1}$$

From Eq. 1, it is apparent that increasing algal productivity, P, can be increased by increasing the efficiency, ε, and/or reducing the respiration rate, r. For healthy outdoor algal cultures, $I_{abs}\varepsilon$ is significantly higher than r during daylight, but r dominates during dark periods. Since both ε and r increase with increasing temperature over the functional range of the algal cells, P can in theory be increased by increasing temperature during the daytime and reducing temperature during the nighttime.

While much is known about the photosynthetic and respiratory responses of algae to temperature, research on the value of thermal cycles for increasing productivity is very limited.

2.1 Literature Review

The correlation between increasing algal photosynthesis and respiration with increasing temperature has been demonstrated in the literature [4-6]. Yet, the influence of temperature cycles on algal productivity has been given very little attention despite some intriguing results.

Davis et al. [7] were the latest to publish results on the influence of temperature cycles on algal productivity. They cultivated *Chlorella pyrenoidosa* in small tubular reactors submerged in outdoor temperature-controlled water baths. During the day, the

reactors were subjected to a different temperature than the night. The experiments produced three major findings:

1. The described temperature cycle improved productivity by as much as 33% over reactors grown with a constant temperature.
2. An optimal daytime and nighttime temperature exists for maximizing productivity.
3. The optimal daytime temperature is higher with temperature cycling than the optimal constant temperature.

Davis et al.'s results support the theory that cooling an algal culture to a certain temperature at night reduces nighttime respiration and warm daytime temperatures improve photosynthesis. The results are not totally conclusive, as it is not known if similar results would be attainable for other species of algae operating at different photosynthetic and respiratory rates.

2.2 Research Scope

While Davis et al. [7] presented results that supported the use of diurnal temperature cycles for improving productivity, they left many questions unanswered. Do the resulting optimal temperatures apply to other algae species in different reactors with different photosynthetic efficiencies? If not, how much different are the results? While mass productivity (mass / area – time) improved, does the energy productivity (energy / area – time) improve correspondingly? What would have been the yield if the algae culture was subjected to natural thermal cycles? The experiments described herein:

- compared the improvement in algal productivity of a different species of algae in a different reactor configuration to the results obtained by Davis et al. [7],
- quantified the value of diurnal thermal cycles by comparing the productivities of outdoor reactors subjected to thermal cycles to a reactor maintained at constant temperature, and
- provided knowledge of the type of thermal controls necessary for the design of an efficient reactor.

2.3 Thermal Cycling Experiment Description

The experiments consisted of three 30-L modified vertical plate reactors (VPR's) in an outdoor setting. This type of reactor was selected because Richmond and Cheng-Wu [8] obtained very high productivities and cell densities using similar reactors and stable semi-continuous production has been attained at the USU Biofuels Center for several months in an outdoor VPR.

The VPR's were modified from the reactors described by Richmond and Cheng-Wu [8] to be capable of more rigorous temperature control. Each VPR consisted of a rectangular chamber 10 cm in depth and approximately 60 cm square. Water from a temperature control circulator was pumped through approximately 2 m of 0.625-cm-diameter stainless steel tubing in the chamber to add/remove heat (Fig. 2.1). The chamber contained the algal culture, an aeration device, a pH probe, and a thermocouple.

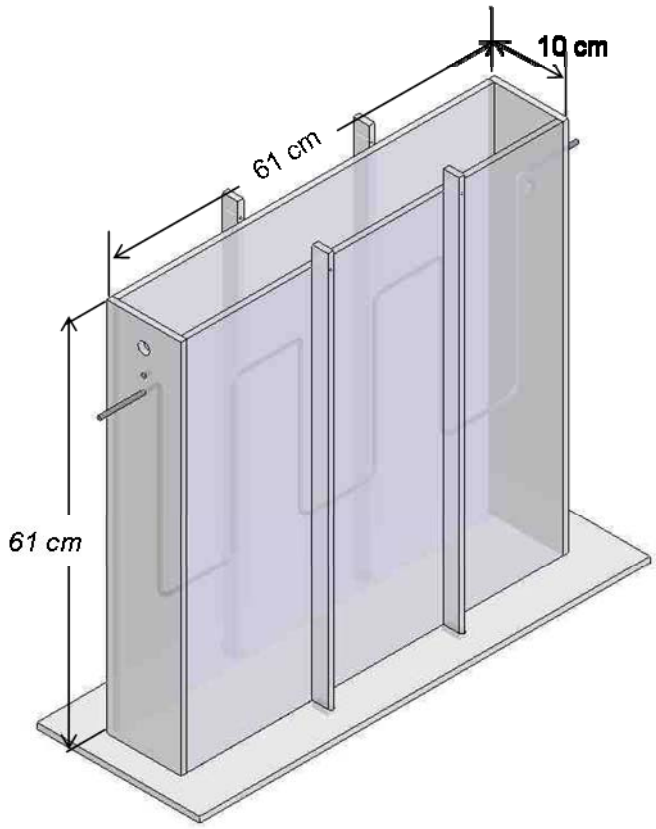

Figure 2.1. Solid model of a modified VPR used for the thermal cycle experiments.

For the experiments, *Dunaliella tertiolecta* was used. Because this strain is a halophile, the risk of contamination by predators or other species of algae was reduced, and dense healthy cultures have been routinely obtained in the laboratory. The pH of the cultures was controlled by CO_2 injection into the cultures. This method also maintained a constant CO_2 concentration in the media as well as pH. The reactors were operated on approximately a 13-day hydraulic retention time (HRT). This retention time produced a reasonable cell density without risking nutrient limitation in previous outdoor experiments.

The first VPR did not have any thermal control except a water spray system that cooled the reactor via evaporative cooling when a media temperature of 30 °C was reached. The temperature of this VPR was expected to follow a cycle similar to that of the environment. The second VPR was attached to a programmable heated/refrigerated circulator. The circulator was programmed to heat the VPR to 30 °C during daylight hours and cool it to 15 °C during dark hours. This temperature cycle was the optimal cycle determined by Davis et al. [7]. The third VPR was attached to a standard heated/refrigerated circulator set to constantly maintain the reactor as close to 22.5 °C as possible, the average of the hot/cold temperatures of the second reactor. The functional temperatures of *Dunaliella tertiolecta* are similar to *Chlorella pyrenoidosa* [9], thus these temperatures provided a direct comparison of the results obtained here to Davis et al.'s.

VPR and outdoor temperatures were monitored with K-type thermocouples attached to a Fluke Hydra II Data bucket programmed to record temperatures every 30 minutes. The daily biomass productivities were determined by centrifuging and freeze-drying 1.5-L samples on a daily basis. The energy content of the samples was determined by combustion in a bomb calorimeter.

The reactors were continuously operated and data collected over the course of 39 days.

2.4 Experimental Uncertainty

The experimental results (mass, P, and energy, E, production) were determined from experimental data as follows:

$$P = \frac{V_p m_s}{V_s \Delta t} \quad (2)$$

and

$$E = PH_T \quad (3)$$

Thus, the variables that directly contribute to experimental uncertainty were the volume of media removed from the reactor, V_p, the mass of algae in the sample, m_s, the sample volume, V_s, the time elapsed between samples, Δt, and the determined energy content of the algae samples, H_T.

The maximum uncertainties of these measurements are given in Table 2.1. The variable that contributed the most significant uncertainty is the sample mass. This was not due to instrumentation limitations, but unknown losses of algae mass during the centrifugation process. The resulting measurement uncertainties were less than 6%.

Other variables that cannot be factored may contribute to the uncertainty of the results, such as unequal shading of the three reactors by nearby objects, aeration rate, and unequal hydraulic retention times. These variables were closely observed to assure that the reactors were being operated under very similar conditions.

Table 2.1. Measurement Uncertainties of Thermal Cycling Experiments.

Variables	Expected Values		Maximum Uncertainty
E	37	kJ day^{-1}	**5.6%**
- H_T	16	kJ g^{-1}	1.5%
- ***P***	2.3	g day^{-1}	**5.4%**
- V_p	3	L day^{-1}	0.21%
- m_s	1.75	g	5.00%
- V_s	1.5	L	0.14%
- Δt	24	h	2.08%

Because the experiments were conducted outdoors, sunlight exposure and ambient temperature were beyond the control of the experiment. To compensate for variation of these factors, samples were repeated over the course of more than 39 days to obtain a statistical sample. This period covered three HRT's of the reactors (39 days / 13-day HRT = 3 cycles).

Unless otherwise stated, all experimental results are reported with 95% confidence.

CHAPTER 3

TEMPERATURE CYCLE EXPERIMENT DESCRIPTION

The goal of these experiments was to maintain three algal reactors with identical conditions, except the temperatures at which the reactors were maintained.

3.1 Location

The experiment was located on the roof of the USU Biofuels Center in North Logan, Utah. The roof was equipped with a galvanized steel mezzanine suspended above a white flat membrane roof. Below the mezzanine five tubes 5 cm in diameter protruded from the roof surface into the ceiling above the lab. These tubes allowed for hoses and wires to be connected between the reactors on the mezzanine to instrumentation and equipment in the laboratory.

The three reactors were located on the southwest corner of the mezzanine where sunlight exposure was the least obstructed by surrounding structures. The reactors were faced due south and arranged in a line about 30 cm away from each other. The central reactor was offset 60 cm behind the two outer reactors to avoid shading (Fig. 3.1).

3.2 Photobioreactor Construction

Each reactor was constructed of 1-cm-thick polycarbonate. The inside of each reactor was 61 cm x 61 cm x 10 cm. The reactors were intended to contain 30 L of media. A hole was drilled into the sides of each reactor with the bottom of the hole 48 cm

Figure 3.1. Experimental reactors located on the mezzanine[1]. From left to right: NTC, CTC, and VTC reactors.

above the bottom of the reactor such that any media in excess of 30 L would drain out of the reactor.

On the opposite wall of the drain hole was located a 1/8" NPT hole 53 cm above the base of the reactor and a 2.5-cm hole 3.8 cm above it. A fitting was threaded into the 1/8" NPT hole into which fresh media would be pumped. The 2.5-cm hole was intended for passing instrumentation and air tubing into the reactors.

On two of the reactors, two 0.32-cm holes were drilled into each end of the reactor through which a radiator was run to heat/cool the media. On the remaining reactor, small polycarbonate plates with holes were glued horizontally from the two

[1] Mezzanine was located on the roof of Building 620, located at 1600 N., 620 E., North Logan, UT.

south-facing beams. Each plate had a hole in it through which sprayers were suspended to provide cooling water to the face of the reactor.

3.3 Instrumentation

Temperature in each reactor was recorded every 15 minutes using a single Type K thermocouple in each reactor. The mixing in the reactors was such that the temperature could be considered constant throughout. The thermocouples were connected to a Fluke Hydra II Data Bucket. The thermocouple wires were soldered together with rosin core solder. To protect from corrosion, the ends of the thermocouples were coated with a thin coating of silicone sealant. The data bucket recorded readings from the thermocouples accurate to ±0.3 ^{o}C.

The pH of the samples were checked with a Mettler Toledo InLab ® Versatile Pro probe. The probe was checked against a pH 4.00, 7.00, and 10.00 standard daily and was calibrated or replaced as necessary.

Three different mass scales were used, depending on the accuracy and mass being weighed. Samples being measured to the nearest 1 g were measured with a Denver Instruments MXX-10. Samples measured to the nearest 10 mg were measured using a Sartorius U 3600 P. Samples being measured to the nearest 0.1 mg were measured with a Mettler Toledo AB 204-S/FACT.

Optical density was measured using a Shimadzu UV-1800 spectrophotometer with 3-mL cuvets. The samples were well shaken and diluted one part in 10 with media standard. Optical density was measured at 806 nm, a notable absorbance peak (Fig. 3.2) that gave good correlation to cell density.

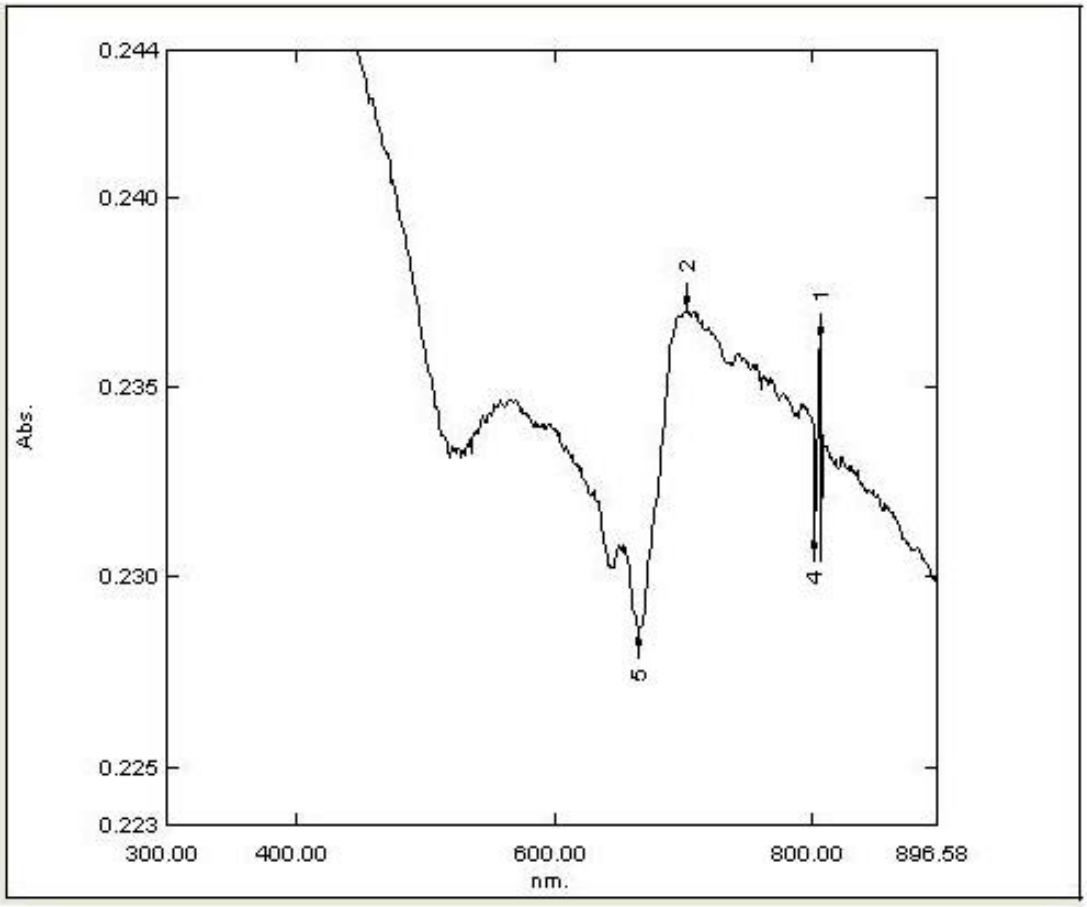

Figure 3.2. Spectral absorbance of *Dunaliella tertiolecta*. The peak notated by the number 1 was the wavelength used to measure optical density.

3.4 Sample Preparation

Samples (2 L) were removed daily from each reactor. The samples were taken around 3 PM. The samples were placed in water-tight containers and transported from the roof to the lab. The pH of each sample was taken and recorded, along with the optical density. The samples were then loaded into 500-mL polycarbonate centrifuge tubes and centrifuged at 7000 rpm for 10 minutes using a Thermo Sorvall RC6 Plus with a Piramoon F10-6x500y rotor (approximately 8000 g's). The supernatant was poured off of

the centrifuged algae and not used for any type of analysis. The supernatant was typically clear, but sometimes slightly white or green. The centrifuged algae was removed from the centrifuge bottles using a small stainless steel scoop and placed into a 50-mL centrifuge tube. Algae remaining in the centrifuge bottles was washed with a salt solution consisting of 90 g l^{-1} NaCl, 3 g l^{-1} KCl, and 0.2 g l^{-1} $CaCl_2$ dihydrate and scraped from the bottle sides. A salt solution was used instead of washing with filtered water because fresh water caused the cells to lyse. The algae-laden solution was poured into the 50-mL centrifuge tube. The tube was filled to 50 mL with salt wash and centrifuged at 3600 rpm for 20 minutes in a Thermo EIC Multi (approximately 2400 g's). The supernatant was poured off of the algae. The centrifuged algae was left in the 50-mL tube and placed in a –80-^{o}C freezer until it could be lyophilized.

Samples were lyophilized inside their centrifuge tubes. The caps were removed from the tubes and a piece of tissue paper was placed over the opening and secured with a rubber band. The samples were lyophilized at -50 ^{o}C and 4 Pa using a Labconco FreeZone 4.5 freeze-dryer for two or more days. When lyophilization was complete, the caps were replaced on the tubes and they were placed in a freezer at approximately –18 ^{o}C until the samples were consumed for bomb calorimetry tests or lipid extractions.

Procedures were developed for consistent sample preparation; they can be found in Appendix A.

3.5 Media

Media was prepared in batches of 10 L. The media composition can be found in Table 3.1. This media was developed by Dr. Brett Barney at the University of Minnesota

and has been successful at growing high-density cultures of *Dunaliella tertiolecta.* Morton solar salt was used in place of pure NaCl, Morton Potassium Chloride in place of KCl, and Epsom Salt in place of $MgSO_4$ for cost efficiency and to provide trace metals to the media, making the explicit addition of trace metals unnecessary. Media components were measured to within 1% of the specified amounts.

Water used for the media was filtered by reverse osmosis. An additional 100 mL of water was added for every 1 L of media to compensate for evaporation during preparation and in the reactors. The media was autoclaved at 121 ^{o}C for 45 minutes, then cooled to room temperature before being added to the reactors. The pH of the media was typically between 7.6 and 8.0 after autoclaving. No pH adjustment was performed on the media prior to loading the media into the reactors.

Foaming in the reactors was a frequent occurrence at the beginning of the experiments, particularly in the NTC and VTC reactors. The foaming was very undesirable because it caused overflow of the media contents out of the reactors and frequently accompanied the flocculation of the algae in the reactors and deposition of

Table 3.1. Description of Brine Media Used for the Described Experiments.

Component	Concentration (g L^{-1})
NaCl	90
KCl	3
$NaNO_3$	5[2]
$MgSO_4*7H_2O$	1.25
K_2HPO_4	0.5
$CaCl_2*2H_2O$	0.2
Ferric Ammonium Citrate	0.005

[2] While the original formulation specifies 2 g L^{-1} $NaNO_3$, it was intended for indoor light conditions. 5 g L^{-1} was used instead to insure no nitrogen limitation.

large quantities of biomass on the walls of the reactor. This was remedied by the addition of 6-10 ppm Emerald Performance Products Foam Blast ® 882 to each reactor whenever foaming was observed (approximately every other day). Application of the anti-foam immediately dispersed foam in the reactors.

3.6 Influent Supply Equipment

Fresh media was pumped into each reactor using a system described in Fig. 3.3. An LMI AA171 metering pump lifted media from a 20-L bucket at a rate of 1.5 L min^{-1} into a PVC manifold to which three Orbit automatic sprinkler valves (Model 57101) were attached. From the valves, 6.35-mm black vinyl tubing transported the media into each reactor. Each valve was opened twice for approximately 1 h each night to inject approximately 3 L of media into each reactor. The open/close time of the valves were adjusted to compensate for evaporative losses in the reactors.

This system was used for the first several weeks of the experiment. After approximately 28 days the valve feeding the VTC reactor lost seal and overfed the VTC reactor. This continued for seven days with various attempts to rectify the problem. After 35 days, the automatic feed system was abandoned in favor of a manual feed operation in which fresh media was manually poured into each reactor after sampling.

3.7 Aeration

Each reactor was aerated using weighted stainless steel spargers placed at the bottoms of the reactors. Each sparger was 56 cm long. Nine tapered 3.2-1.6 mm holes

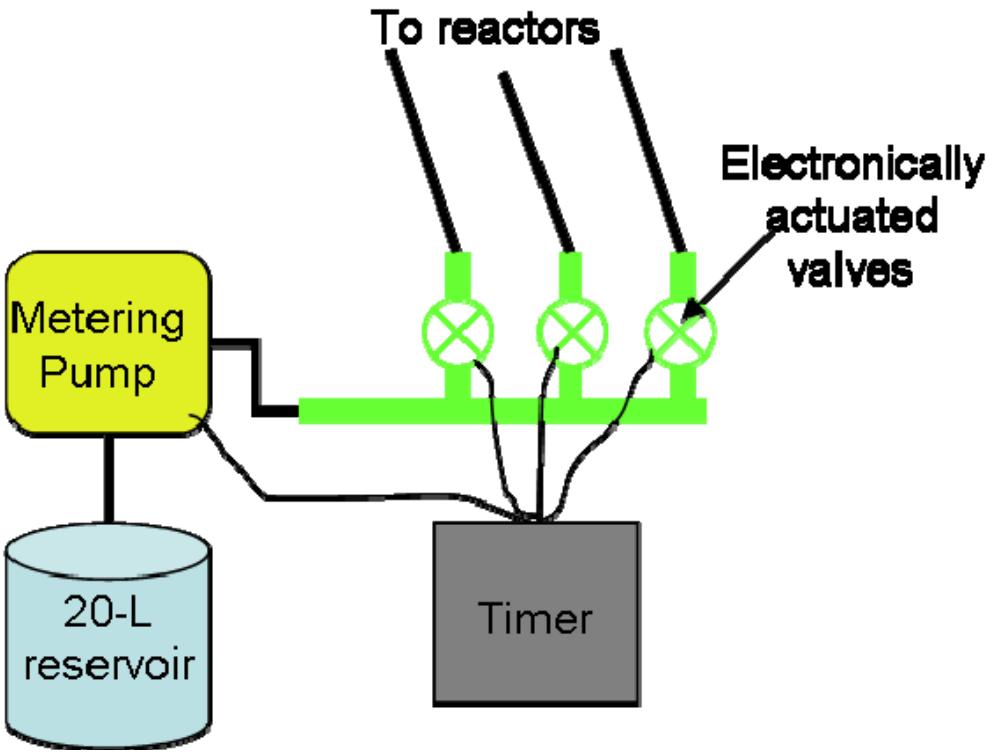

Figure 3.3. Schematic of the feed system for delivering fresh media to the reactors.

were drilled into each sparger at equal spacing. 35 g of galvanized steel washers were placed on each sparger end between two of the holes and secured in place with silicone tubing. Silicone tubing linked each end of the sparger to a VWR FR2A17 flow meter[3] located in a sealed PVC box next to the reactors. The flow meters were fed from a 6-port manifold connected to a 6.35-mm vinyl hose that transported compressed air from the building compressed air distribution manifold. An oil filter removed oil from the air and a regulator compensated for pressure fluctuations in the compressed air manifold.

Over the course of the experiments, the aeration system provided 20 – 24 L min^{-1} of air to each reactor. The sparger holes were cleaned out and flow rates were checked

[3] Range: 4-50 L min^{-1} of air; Resolution: 1 L min^{-1}

and adjusted daily to ensure that the flow into each reactor was the same.

3.8 CO_2 / pH Control

The method for controlling pH and CO_2 in the reactors requires some description of the relationship between pH and CO_2 content. The removal of CO_2 from, or diffusion into, water results in a respective increase or decrease in pH. For these experiments, this phenomenon was capitalized upon for monitoring and maintaining pH and CO_2 content in the reactors simultaneously. A Sensorex S650CD submersible pH probe was connected to an Omega pHCN-201 pH controller that opened and closed a valve on a compressed CO_2 tank. As the algae in the reactor consumed the CO_2 for photosynthesis, the pH increased. When the pH value exceeded 7.8, the controller opened the CO_2 valve, introducing the gas into the reactor aeration system. The valve remained open until the pH value decreased to 7.4, then the controller closed the valve.

A target pH of 7.6 was selected because it was the pH at which *Dunaliella tertiolecta* was successfully grown previously. The target pH is arbitrary with regard to CO_2 availability because its solubility in the media is independent of pH [10]. It is necessary to point out that the solubility of total inorganic carbon increases with pH, but CO_2 solubility remains the same regardless of pH (Fig. 3.4). The ability of algae to utilize HCO_3^- and $CO_3^=$ is disputed [11]. It will be assumed that only the CO_2 content is of importance.

Only one pH probe and controller was used for the following reason: CO_2 use will be highest in the highest-producing reactor. By placing the pH probe in the highest producing reactor, it will receive the CO_2 it demands while the other two lesser producing

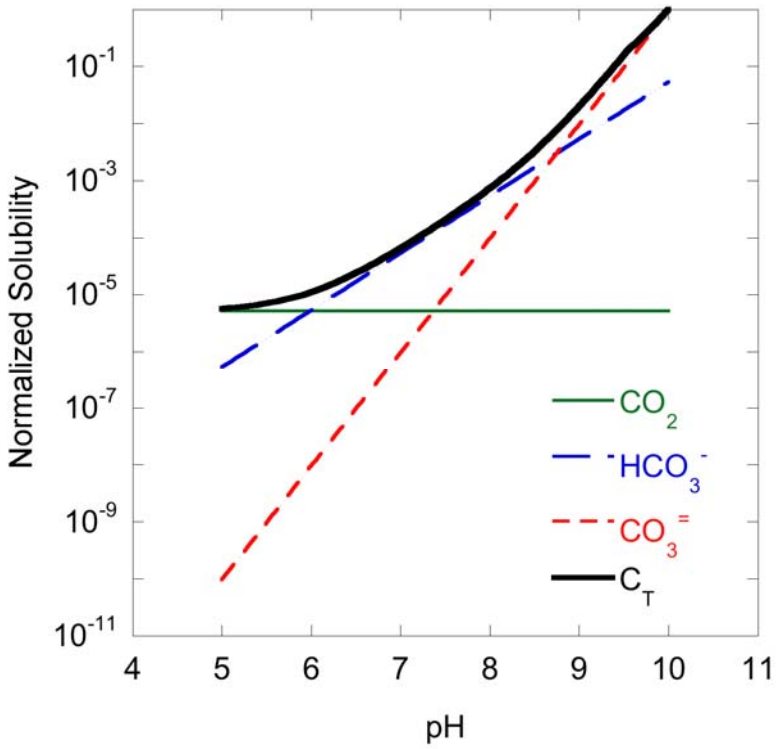

Figure 3.4. Normalized solubility of carbon dioxide (CO_2), bicarbonate (HCO_3^-), carbonate ($CO_3^=$, and total inorganic carbon (C_T) as a function of pH [10].

reactors will receive excess CO_2. Therefore, the two under-performing reactors must be limited by some means other than CO_2 availability. Because of the calibration drift frequently observed in pH probes operating under such conditions, independently controlling the pH in each reactor could not have insured this.

3.9 Temperature Control

Three independent temperature control units were used to regulate temperature in each reactor. The NTC reactor was placed in a 40-L acrylic basin, approximately 10 cm in height, and the basin was filled with water. A small pump was located in the basin to pump water up to sprinklers suspended above the reactor. The sprinklers applied water to

the south-facing plate of the reactor to provide evaporative cooling when the temperature of the reactor exceeded 26 ^{o}C. The temperature of the reactor generally continued to climb with the cooling unit running, but the evaporative cooling system limited the temperature to approximately 35 ^{o}C.

The CTC reactor contained 2.8 m of 6.35 mm stainless steel tubing through which a propylene glycol / water solution was pumped. A 13-L VWR Digital Temperature Controller heated and cooled the solution as necessary to maintain the reactor at approximately 22.5 ^{o}C.

The VTC reactor contained a cooling / heating system similar to that of the CTC reactor, except that a 13-L VWR Programmable Temperature Controller was used to heat / cool the solution and the controller was programmed to maintain the temperature at 30 ^{o}C during daylight hours and 15 ^{o}C during nighttime hours. This cycle was successfully maintained for the duration of the experiment, except for two days in which a power outage caused the controller to heat and cool at the wrong times.

3.10 Determination of Energy Content

Energy content of the samples was determined using bomb calorimetry. Samples that had been lyophilized were ground to a powder using a mortar and pestle. One third or less of the sample was weighed and placed in a Parr 1108 oxygen combustion bomb. The bomb was detonated inside a Parr 1241 adiabatic oxygen bomb calorimeter. The ash remaining in the crucible after combustion was weighed to determine an ash-free energy content. Sulfur content was not determined for the samples, thereby biasing the results on the high side. However, this bias is negligible (see Appendix B).

The test was repeated three times for each mass sample to determine variability in of the experiment.

3.11 Gas-Liquid Chromatography

For reasons that will be discussed in the following chapter, free fatty acid (FFA) and triacylglycerol (TAG) content of the samples were determined using gas-liquid chromatography (GC) with a Shimadzu GC-2010. The lipids were extracted using a chloroform-hexane-tetrahydrofuran solvent extraction method developed at USU by Dr. Brett Barney. The procedures are detailed in Appendix A.

To determine the precision of the method, the protocol was carried out for three samples from the same sample of algae. The three results were all within ±5% of the average value (e.g. the sample contained 20±1% TAG).

CHAPTER 4

EXPERIMENT RESULTS

This chapter describes the conditions each reactor observed and the resulting cell densities, production rates, and mass energy contents.

Each reactor was inoculated on Jul. 15, 2009 with 10 L of *Dunaliella salina* that had been previously cultivated in an outdoor reactor. The inoculum was diluted with 5 L of fresh media that day, then with 3 L for the following five days until the reactors were full. The reactors were operated in continuous batch mode after that and were sampled daily for 3 HRT's (39 days) from Aug. 1 to Sep. 8. The reactors required approximately 20 days of this period to reach stable production. Consequently production from the reactors was only considered for the last HRT (13 days) of the experiment. The measurements of variables such as temperature, insolation, pH, HRT, and aeration over the entire course of the experiment are discussed to demonstrate consistent control of these variables, but only the last 13 days of the resulting optical and cell densities, and mass and energy productivities were considered, except to show that steady-state conditions were reached.

The reactors were operated after Sep. 8 until Sep. 26, but under different conditions that will be described in Section 4.11.

All results are presented with uncertainty bars. If no bar is present, the uncertainty was smaller than the data point, unless otherwise stated. Uncertainty analyses are detailed in Appendix B. All results are tabulated in Appendix C.

4.1 Temperature

The CTC reactor temperature as a function of the time of day is given in Fig. 4.1 for the duration of the experiment. It was desired that the reactor be maintained at 22.5 ^{o}C at all times. The actual reactor temperature did follow ambient temperature trends slightly, increasing or decreasing by a few degrees throughout the day, but the reactor was almost constantly maintained between 20 and 25 ^{o}C. Figure 4.2 shows the daily distribution of CTC temperatures for the duration of the experiment. From this data, it can be seen that temperatures were outside 20 and 25 ^{o}C less than 5% of the time with no significant deviations from the mean temperature.

The temperature controller of the VTC reactor was programmed to maintain the

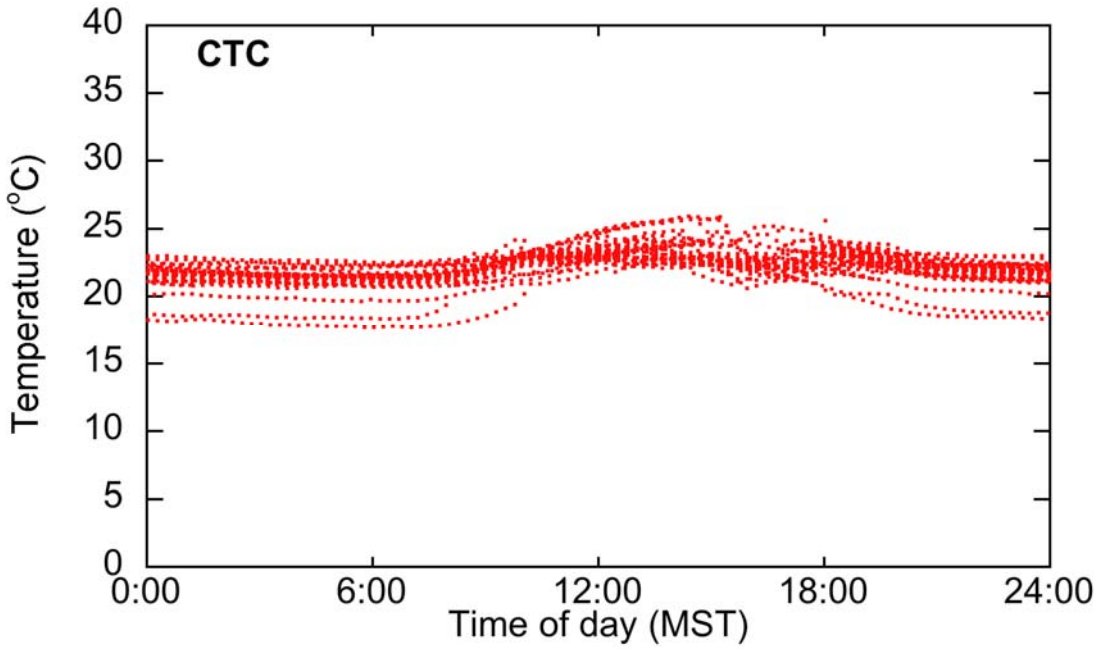

Figure 4.1. Complete set of CTC reactor temperature measurements from Aug. 1 to Sep. 8 with respect to the local time of day. With a few exceptions, the temperature of the reactor was maintained close to 22.5 ^{o}C.

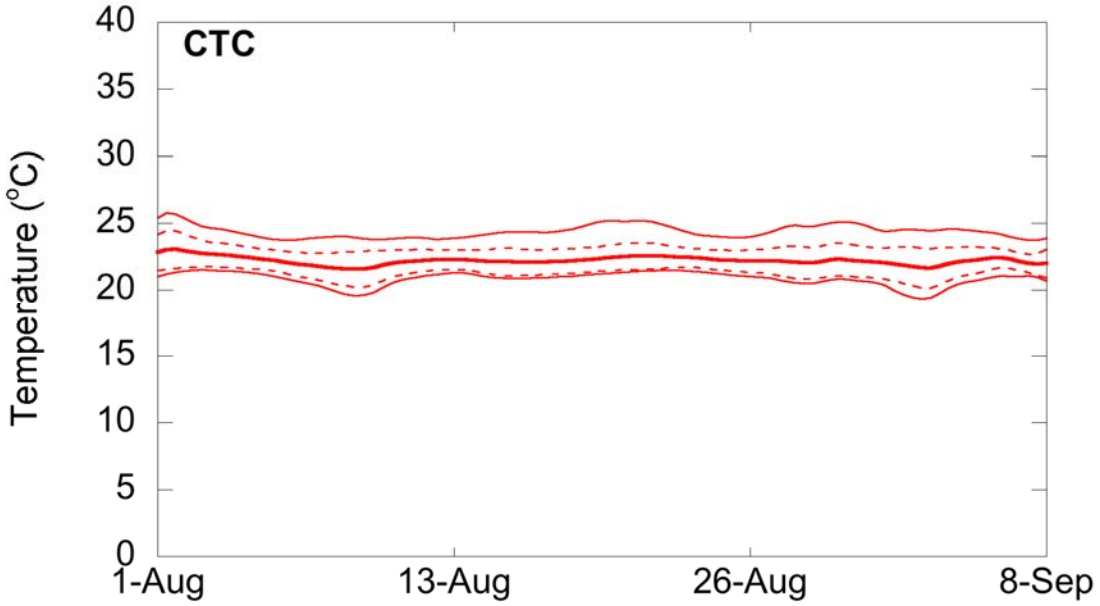

Figure 4.2. Minimum, maximum, and average CTC temperatures for the duration of the experiment. Dashed lines represent one standard deviation away from the mean temperature. Note that no significant trend in temperatures occurs for the duration of the experiment.

reactor temperature at 15 ^{o}C during dark hours, then begin heating the reactor to 30 ^{o}C approximately one half hour before sunrise and maintain that temperature until sunset.

An average sunrise and sunset of 6:45 am and 8:15 pm, respectively, were assumed for the duration of the experiment. Figure 4.3 shows that, with a few exceptions, this temperature cycle was maintained very well. The exceptions are labeled by date and were the result of power outages in the lab that reset the temperature controller.

The reactors were heated and cooled at approximately the same rate every day. Heating during sunrise occurred at an average rate of 9.3 ^{o}C h^{-1}, and sunset cooling occurred at an average rate of -13.3 ^{o}C h^{-1}. This resulted in the reactor being completely heated or cooled to the specified temperature within 60 to 90 minutes.

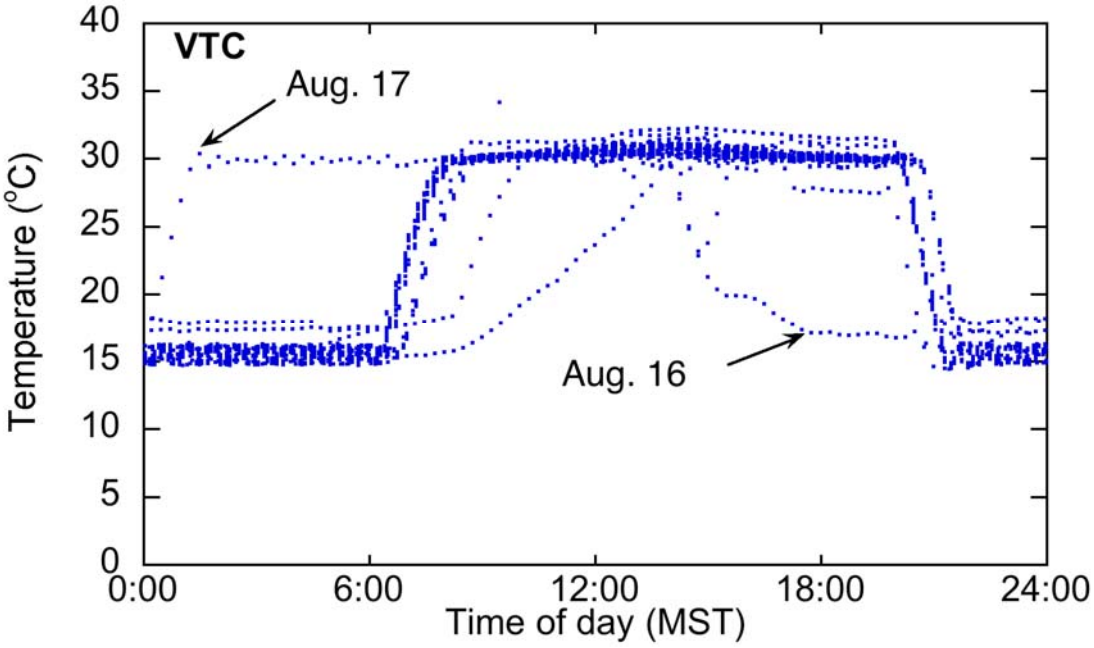

Figure 4.3. Complete set of VTC reactor temperature measurements from Aug. 1 to Sep. 8 with respect to the local time of day. With a few exceptions, the temperature of the reactor was maintained at the specified 30/15-°C temperature cycle.

The NTC reactor mimicked outdoor temperature trends, following a sinusoidal-like fluctuation with a maximum at approximately 4 to 5 pm and a minimum between 7 and 8 am (Fig. 4.4). The evaporative cooling system did not appear to augment the temperature cycle noticeably, and temperature consistently exceeded the intended maximum of 30 °C. However, since the higher temperature was not significantly degrading the cell density and productivity, the temperature cycle was allowed to continue. The temperature of the NTC remained between 10 and 35 °C 98% of the time. Figure 4.5 shows that there was no significant trend in the NTC temperatures throughout the duration of the experiment.

Figure 4.6 compares the histograms of the temperature data for the three reactors.

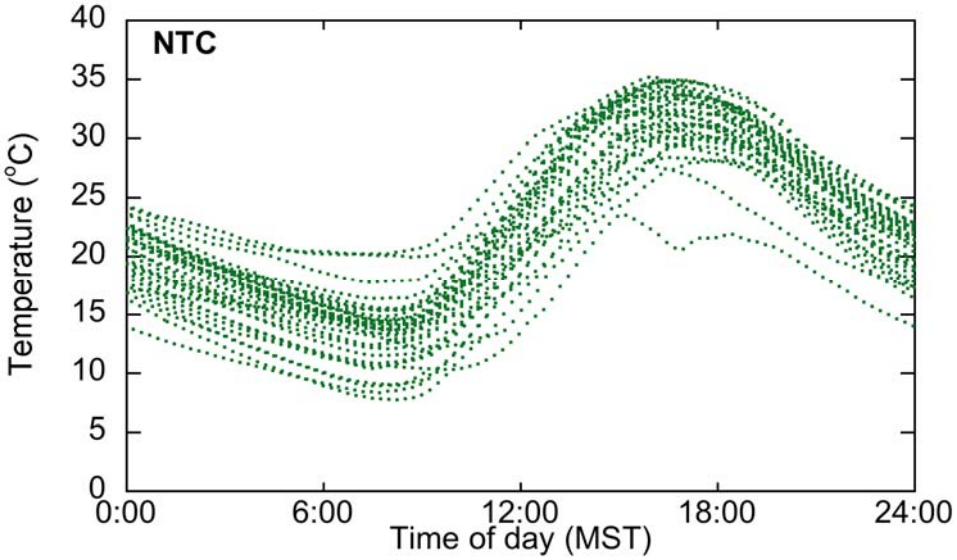

Figure 4.4. Complete set of NTC reactor temperature measurements from Aug. 1 to Sep. 8 with respect to the local time of day. The sinusoidal-like fluctuations in temperature mimicked the ambient temperature fluctuation.

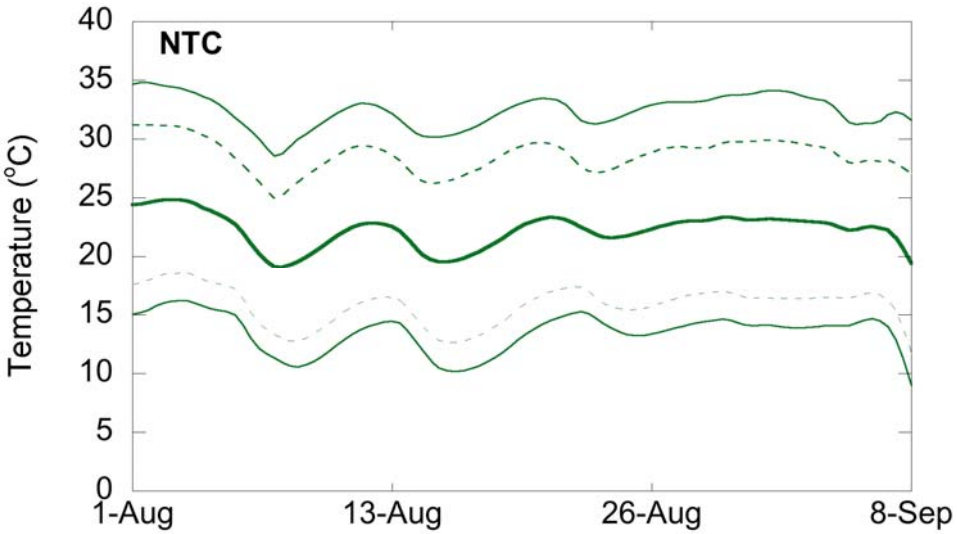

Figure 4.5. Minimum, maximum, and average NTC temperatures for the duration of the experiment. Dashed lines represent one standard deviation from the mean temperature. Note that no significant trend in temperatures occurred for the duration of the experiment.

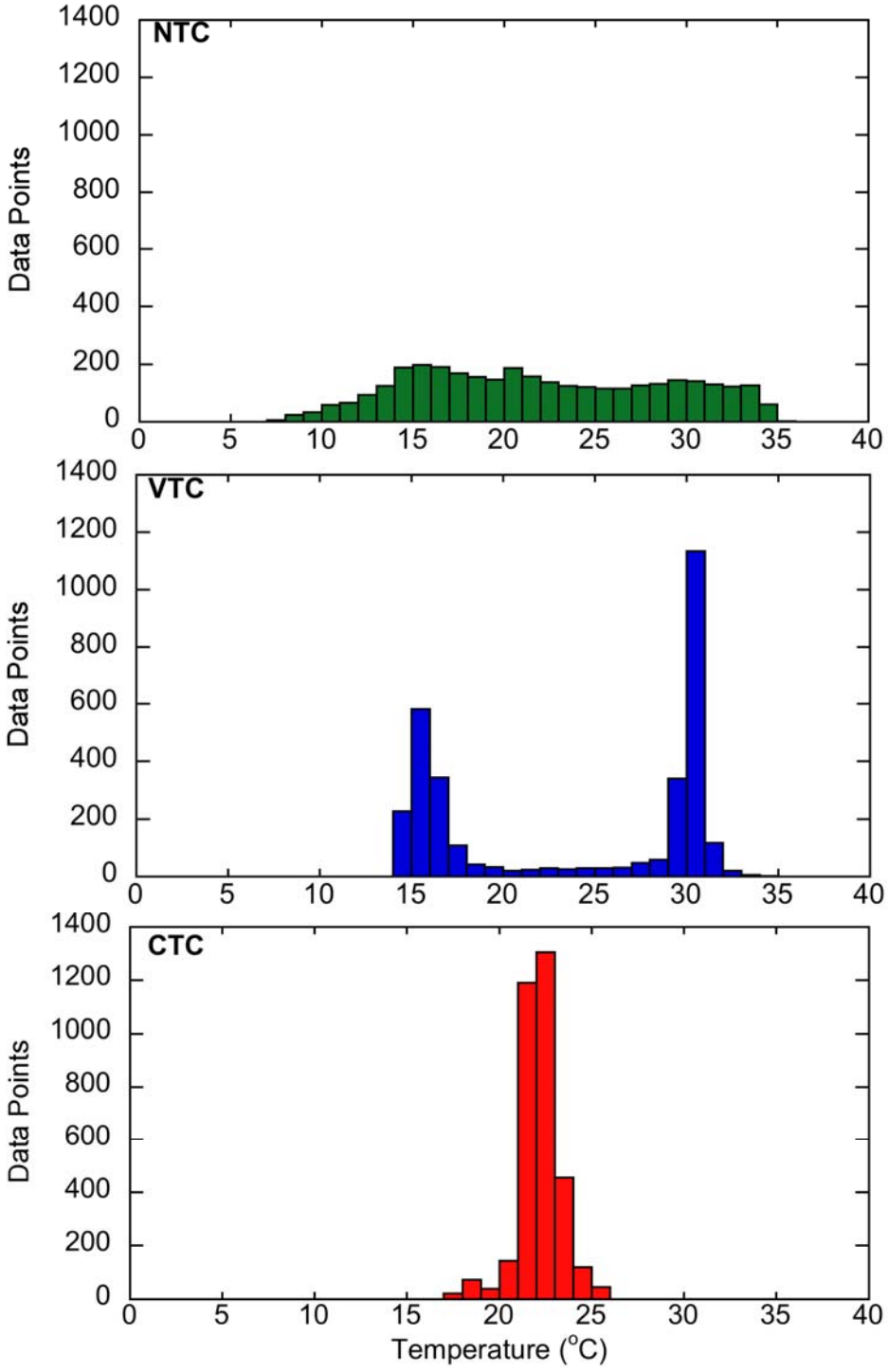

Figure 4.6. Temperature histograms for the NTC (top graph), VTC (middle graph), and CTC (bottom graph) reactors over the course of the experiments.

4.2 Insolation

The available solar radiation for the duration of the experiment was typical of the region, providing 20 - 25 MJ m^{-2} day^{-1} of mean total global insolation on most days (Fig. 4.7).

4.3 pH

The pH values of the reactors during the experiment were quite varied. These fluctuations were due primarily to calibration drift in the pH sensor. However, the range of pH values that each reactor observed over the course of the experiment were similar:

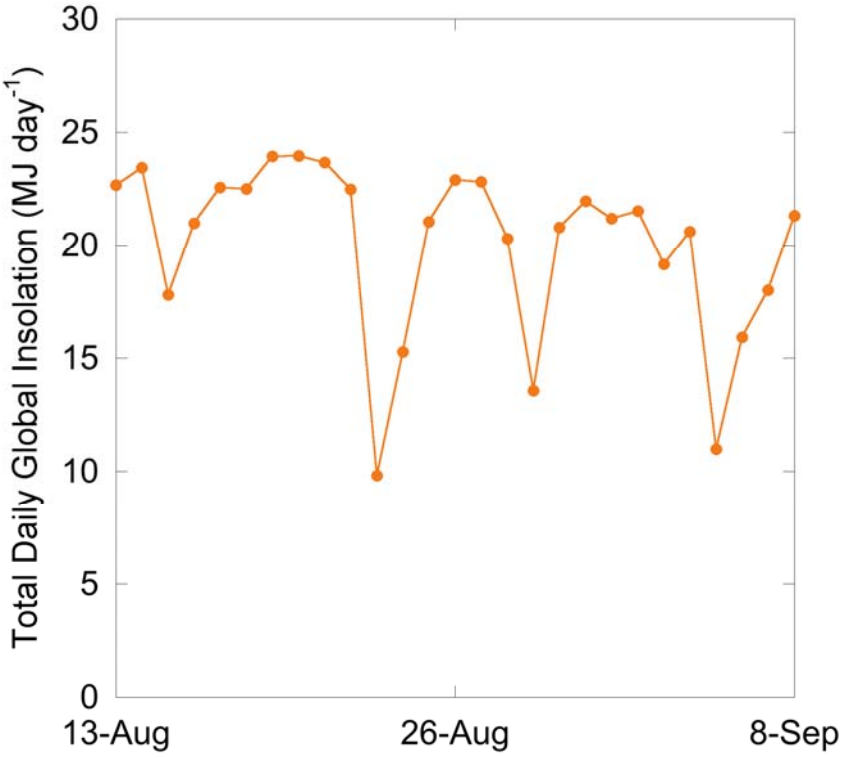

Figure 4.7. Mean total daily global insolation for from Aug. 13 to Sep. 8. Data from before Aug. 13 was unavailable.

7.0 – 8.1, 6.9 – 7.8, and 6.9 – 8.0 for the CTC, NTC, and VTC reactors, respectively.

As was discussed in Section 3.8, the objective of the pH control system was to maintain the less productive reactors at a lower pH than the most productive reactor, thus making more CO_2 available to them. Figure 4.8 shows the pH of the harvested samples from each of the reactors relative to the reactor with the highest cell density. The CO_2 control system was effective at maintaining more CO_2 in the less productive reactors, except for the latter third of the experiment in which the NTC reactor consistently displayed a higher pH and therefore less available CO_2. However, as will be discussed in

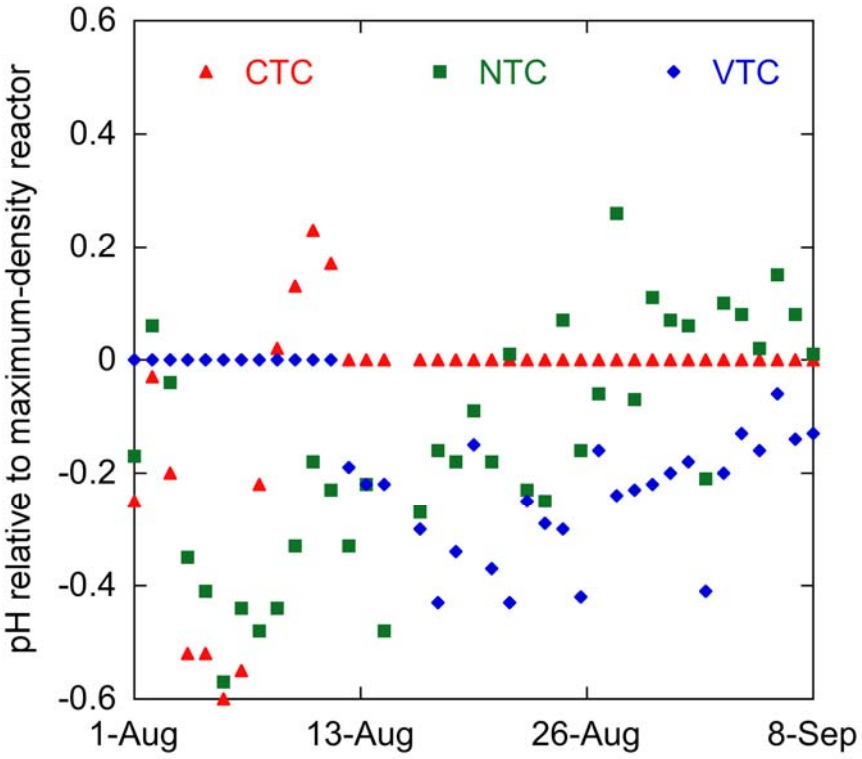

Figure 4.8. pH values of harvested samples relative to the pH of the reactor with the highest density. Most of the relative values are negative, indicating that the pH of the lower-producing reactors were lower and therefore more CO_2 was available to the algae.

Section 4.7 below, the lower CO_2 availability evidently did not limit productivity.

4.4 HRT

The hydraulic retention time of each reactor was determined by dividing the wetted reactor volume by the volume of effluent harvested each day ($HRT = V_R / V_P$). Although the flow rate of media fed to each of the reactors was identical during the beginning of the experiment, water evaporation on the order of 0.5 to 1 L day^{-1} caused varied and higher-than-anticipated HRT's because the evaporation resulted in less water volume in the effluent (Fig. 4.9). To compensate for this, media flow was increased slightly to the VTC and NTC reactors. However, since the evaporation was dependent on environmental conditions, and therefore unpredictable, obtaining stable HRT's during the experiment was challenging. The HRT's of all three reactors were maintained on average at 13.2 days with each reactor within 0.5 days of the others.

Figure 4.9 shows a few incidences where very low HRT's were observed (Aug. 13 and 25) because of control valve failures. The valve that failed on Aug. 10 was replaced with an identical valve. When a valve on Aug. 25 failed, the automated media feed system was discontinued and replaced with daily manual media feeds.

4.5 Aeration

Aeration remained relatively constant, only increasing slightly from about 20 L min^{-1} per reactor at the beginning of the experiment to 22 L min^{-1} per reactor at the end, producing a mean aeration flow rate of 20.8 L min^{-1} for each reactor.

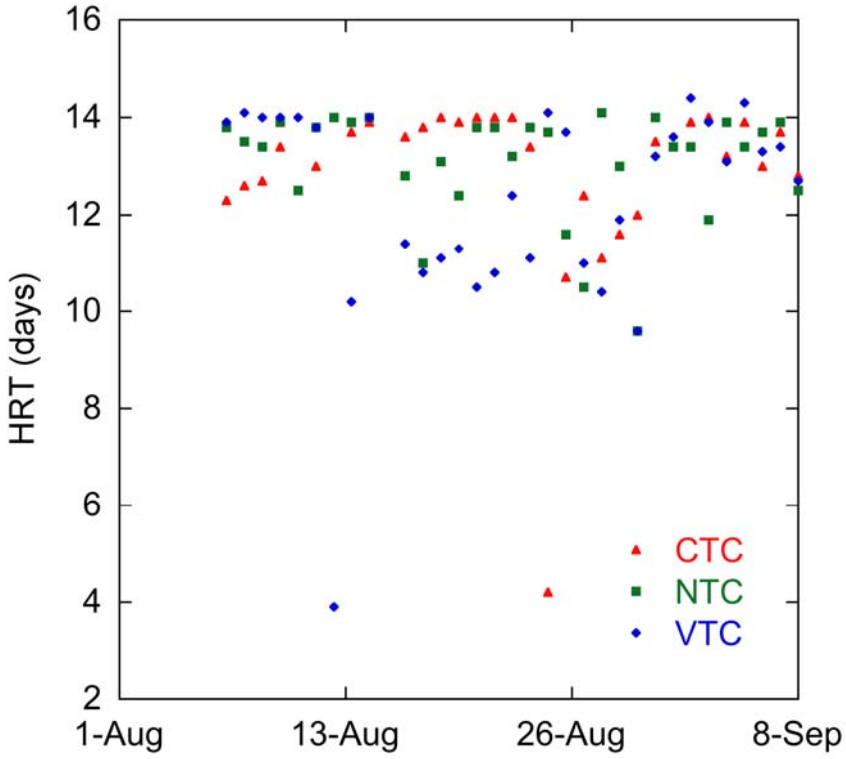

Figure 4.9. HRT measured as reactor volume / daily harvested volume. The harvested volumes were not measured until Aug. 5, hence the lack of data prior to that date. Fluctuations were largely due to constantly varying evaporation rates.

4.6 Optical and Cell Density

The optical densities (measured at 806 nm) of the daily samples are shown in Fig. 4.10. For the first week of the experiment, the VTC reactor had a higher OD than the other two reactors. However, while the OD of the VTC reactor remained fairly constant, the OD's of the CTC and NTC reactors slowly increased throughout the experiment. The CTC reactor exceeded the OD of the VTC reactor on Aug. 14 and the NTC reactor exceeded the VTC reactor OD one week later. Dry cell mass densities confirmed this trend, except with the NTC reactor exceeding the VTC reactor four days earlier (Fig. 4.11).

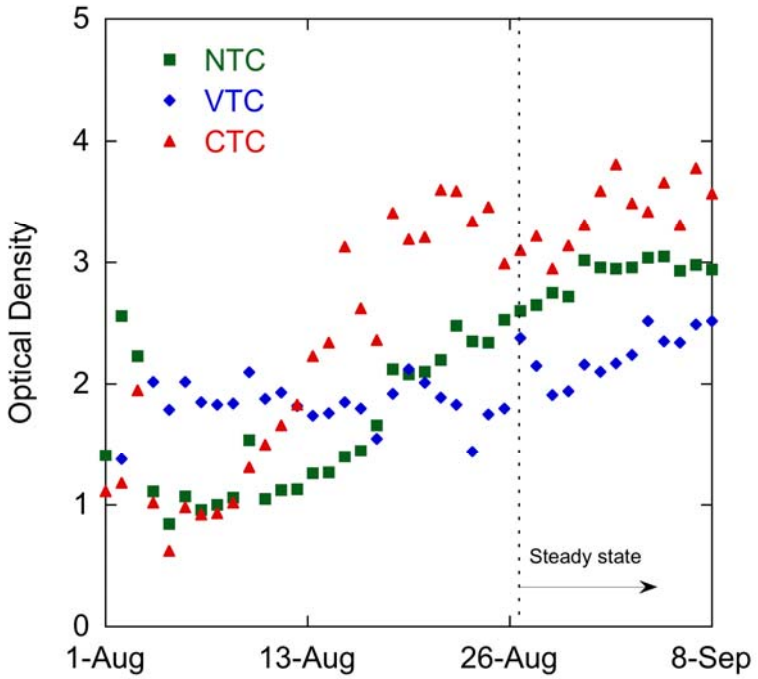

Figure 4.10. Daily optical density measurements. Optical density was determined at 806 nm. Steady-state conditions were considered to begin on Aug. 27, as indicated.

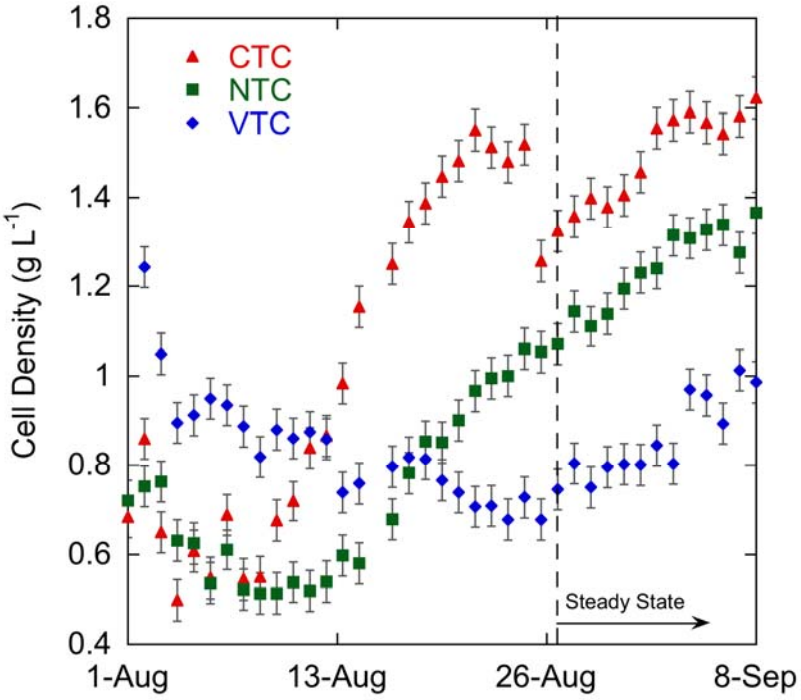

Figure 4.11. Cell densities of each reactor over the course of the experiment. Steady-state conditions were considered to begin on Aug. 27, as indicated.

Figure 4.12 shows good linear correlation between cell mass density and OD, adding reliability to the results.

From Fig. 4.11, a sharp drop in cell density on Aug. 25 is evident. This was caused by a failed feed valve injecting excessive media into the reactor and washing about 25% of the cell mass out of the reactor.

4.7 Productivity

Productivity was calculated from the results as $P = V_R X / \theta = FX$. The calculated productivities for each of the reactor for the duration of the experiment are shown in

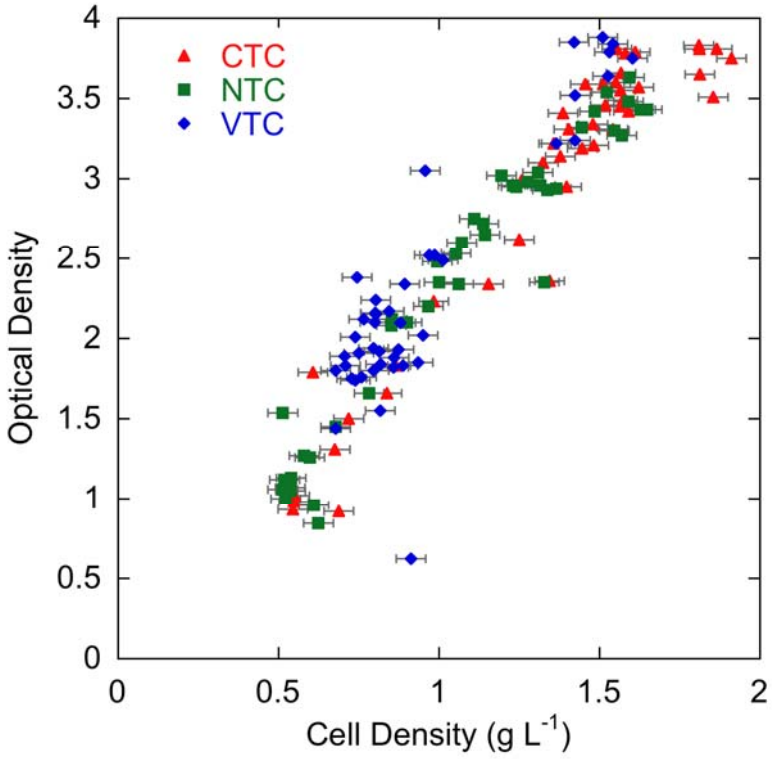

Figure 4.12. Optical density versus cell density. Good linear correlation was obtained between the two, adding reliability to the results. The cluster of CTC results that deviated from the trend in the upper right corner is the result of skew in the optical density reading above values of 0.4.

Fig. 4.13. Since, with few exceptions, θ was similar for each of the reactors, the productivity trends are similar to the cell mass density results of Fig. 4.11.

The optical and cell densities increased steadily in the CTC reactor for approximately 26 days before stabilizing, whereas the VTC reactor was relatively stable for the entire experiment and the NTC reactor continued to gradually increase. For this reason, stable production was only considered for the last HRT (13 days) of the experiment. Productivity data in this region appear to be randomly distributed and were treated as such.

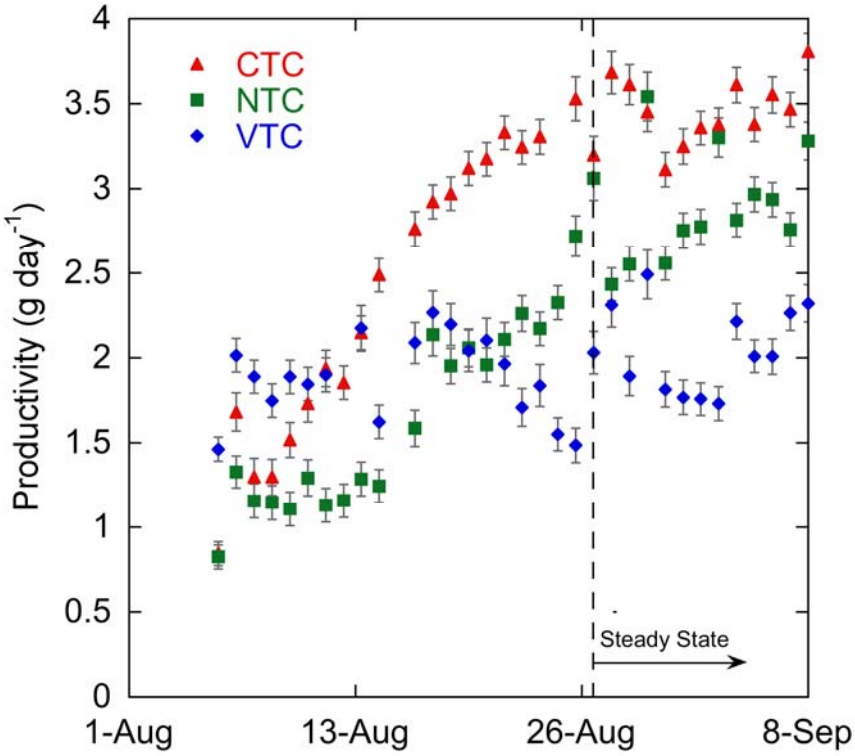

Figure 4.13. Total daily algal productivity from each reactor. Values before Aug. 5 were unavailable because the harvested volume was not measured until then. Steady-state conditions were considered to begin on Aug. 27, as indicated.

The continual increase in the mass productivity of the NTC reactor is an indication that, despite its pH value being regularly higher than the CTC reactor (Fig. 4.8), there was adequate CO_2 available to the algae. If CO_2 was limiting, the productivity would have leveled off or decreased when the NTC reactor pH value exceeded the CTC pH.

4.8 Energy Content and Productivity

Algae samples from every third day starting Aug. 27 during the steady-state period were analyzed for energy content. Each sample was analyzed three times to observe the variability of the results from identical samples. Only one third of the available samples were analyzed, the rest were preserved for other experiments such as lipid and chlorophyll content.

The total energy content (TEC) and ash-free energy content (AFEC) results are given in Table 4.1. The energy contents did not appear to display any trend during steady state conditions (i.e. the energy contents were randomly distributed). It was not expected that the samples from the NTC and VTC reactors consistently contained more energy than the CTC samples. Thus, although the CTC reactor out-produced the other two reactors, the mass it produced was of lesser energy quality than the other two reactors. On average, the ash-free energy content of the VTC samples were 7.6% higher and the NTC samples were 4.1% higher than the CTC samples.

The daily energy productivity of the reactors is calculated as $E = PH_T$. It is important to note that the calculation uses *total* energy content, as opposed to the *ash-free*

Table 4.1. Total and Ash-free Energy Contents of Samples During Steady-state Production. Energy contents given are the average of three tests; standard deviations are given in parentheses.

	CTC		VTC		NTC	
	Total Energy Content (kJ g^{-1})					
8/27	16.57	(0.27)	17.19	(0.42)	17.30	(0.58)
8/30	15.39	(0.39)	17.82	(0.24)	16.90	(0.19)
9/2	16.41	(0.28)	17.15	(0.09)	17.37	(0.31)
9/5	15.85	(0.38)	17.23	(0.49)	17.44	(0.22)
9/8	15.12	(0.20)	17.61	(0.39)	16.98	(0.33)
Avg.	15.87	(0.64)	17.40	(0.41)	17.20	(0.36)
	Ash-free Energy Content (kJ g^{-1})					
8/27	20.79	(0.79)	22.52	(0.56)	21.55	(1.02)
8/30	19.75	(1.72)	21.93	(1.25)	21.64	(1.09)
9/2	21.15	(0.35)	22.59	(0.48)	21.88	(0.40)
9/5	21.30	(0.09)	22.31	(1.01)	22.28	(0.27)
9/8	20.89	(0.44)	22.45	(0.30)	20.87	(0.70)
Avg.	20.78	(0.94)	22.36	(0.72)	21.64	(0.73)
	Energy Productivity (kJ day^{-1})					
Avg.	54.80	(3.79)	34.90	(5.02)	49.70	(5.54)

energy content. The resulting energy productivity (Table 4.1) indicates that the CTC reactor was 57% more efficient than the VTC reactor and 10% more efficient than the NTC reactor. That is, despite the higher energy content of the VTC and NTC reactors, the CTC reactor was more efficient.

The energy content results are very interesting in indicating that the energy content and dry cell mass productivity are inversely related. The higher energy content

may be an indicator of higher lipid content [12]. If so, it appears that temperature fluctuations are imposing a stress condition that is lowering mass productivity but increasing the lipid content, a phenomenon frequently encountered by researchers during the ASP [1] using nitrogen or silica limitation. If lipid production is the primary goal of an algal production operation, permitting or inducing temperature cycles may be a viable method for increasing lipid production.

Given that the energy content of carbohydrates and proteins are approximately 17 kJ g^{-1} and triacylglycerols are 38 kJ g^{-1} [13], an increase of 1 kJ g^{-1} would correspond to a nearly 5% increase in lipids. Therefore, the difference in lipid content between the VTC and CTC reactor should be approximately 7%. Experimental work by Illman et al. [12] suggested a difference of approximately 5%.

4.9 Gas Chromatography Results

The higher energy contents of the NTC and VTC samples disclosed in Section 4.8 may not be directly correlated to higher free fatty acid (FFA) or triacylglycerol (TAG) content. It may also indicate a differing content of other compounds. To investigate the reason for the increased energy content, lipids were extracted from one third of the algae samples and processed with a gas chromatograph to evaluate the lipid compounds contained in the samples. Every third sample from the steady-state period starting from Aug. 26 was used for the analysis.

The combined FFA and TAG contents were quite small, and the average values were nearly identical, 2.24% (0.19%), 2.14% (0.33%), and 2.13% (0.33%), for the CTC, NTC, and VTC samples, respectively (standard deviations given in parentheses). No

significant difference in any other compound, such as glycerol, could be found either. Octacosane content of the samples, a compound injected into the samples to indicate proper operation of the GC, were consistent, indicating that the samples were analyzed properly.

4.10 Results Summary

The results of the experiment are summarized in Table 4.2. The precisions represent 95% confidence. Chauvenet's criterion was used to eliminate anomalous data points [14]. While the CTC reactor significantly out-produced the mass productivity of the NTC and VTC reactors by 20% and 67%, respectively, the difference in energy productivities was less significant, with the NTC and VTC reactors producing only 9% and 36% less energy, respectively. Combined FFA and TAG content was nearly identical among the three reactors, at about 2.2%.

Table 4.2. Summary of Experimental Results. Precisions represent 95% confidence.

Parameter	CTC	VTC	NTC
Temperature, ^{o}C	22.1±1.1	23.8±6.7	22.0±13.3
Total global insolation, MJ day^{-1}		20±8	
pH	7.49±0.41	7.26±0.50	7.49±0.56
HRT, day	13.1±1.7	13.0±2.7	13.2±2.3
Air flow rate, L min^{-1}		21±4	
Optical Density	3.41±0.58	2.24±0.46	2.83±0.45
Cell density, g l^{-1}	1.49±0.23	0.86±0.20	1.24±0.21
Ash-free Energy Content, kJ g^{-1}	20.8±0.9	22.4±0.7	21.6±0.7
FFA & TAG content, %	2.24±0.62	2.13±1.05	2.14±0.91
Mass productivity, g day^{-1}	3.42±0.39	2.05±0.55	2.85±0.60
Energy productivity, kJ day^{-1}	54.8±3.8	34.9±5.0	49.7±5.5

To quantify whether these differences are real, or are only due to variability of the experiment, a statistical significance test was conducted. A standard normal variable, t_o, was calculated by comparing two data points:

$$t_o = \sqrt{n}\,\frac{\bar{x}_1 - \bar{x}_2}{\sqrt{s_1^2 + s_2^2}} \tag{4}$$

where n is the number of data points, $\bar{x}_1$ and $\bar{x}_2$ are the mean values of the samples being compared, and s_1 and s_2 are the standard deviations of the respective samples. Given t_o, a probability from the normal curve could be determined, resulting in a probability that the two results were not equivalent. The differences of the results between the CTC and NTC and CTC and VTC reactors were all statistically significant (Table 4.3), with confidences greater than 99%.

4.11 Reduced Temperature Amplitude Experiments

While the results showed conclusively that, at steady-state conditions, constant temperature control produced more algae than either variable or no temperature control while increasing the energy content of the less productive reactors, some broader conclusions were desirable. Was it the amplitude of the temperature cycle, or the cycle itself, that inhibited production in the VTC reactor? How would a different temperature

Table 4.3. Statistical Significance of Results Presented in Table 4.2.

Parameter	P(CTC≠VTC)	P(CTC≠NTC)	P(VTC≠NTC)
Optical Density	~100%	99.3%	99.8%
Cell density	~100%	99.5%	~100%
Energy Content	~100%	95%	71%
Mass productivity	~100%	99.4%	99.94%
Energy productivity	~100%	99.8%	~100%

affect the energy content? To answer these questions and obtain some broader conclusions about temperature cycles, the experiments were continued for several more weeks. The temperature cycle of the VTC reactor was changed to 27.5 ^{o}C during the day and 17.5 ^{o}C at night. While no changes were made to the NTC reactor, September weather incurred an average temperature that was 2 ^{o}C cooler and had a 2-^{o}C-larger temperature amplitude in the reactor (Fig. 4.14).

The second experiment was conducted for 18 days, one HRT (13 days) was allowed for the VTC reactor to reach stable production, followed by five days of sampling. A longer sampling period was desirable, but data during an ensuing unstable weather pattern may have skewed the results. Optical and cell density and pH were each taken every other day until the last five days of the experiment, in which samples were acquired each day. Figure 4.15 depicts the optical densities of the three reactors throughout the course of this experiment. While the CTC and NTC reactors remained generally the same density, the VTC reactor steadily increased for the duration of the experiment, indicating that a well-chosen variable temperature cycle can improve productivity of *Dunaliella salina* under these conditions.

Table 4.4 presents the mean experiment values. Except for the temperatures of the VTC reactors, the other conditions were comparable to the previous experiment. However, Table 4.5 shows that with the reduced temperature amplitude the mass and energy productivities of the VTC reactor were nearly doubled, without a significant decrease in energy content. The increase in the CTC and NTC productivities was due to increased insolation incident on the south-facing plates of the reactors. It is evident from

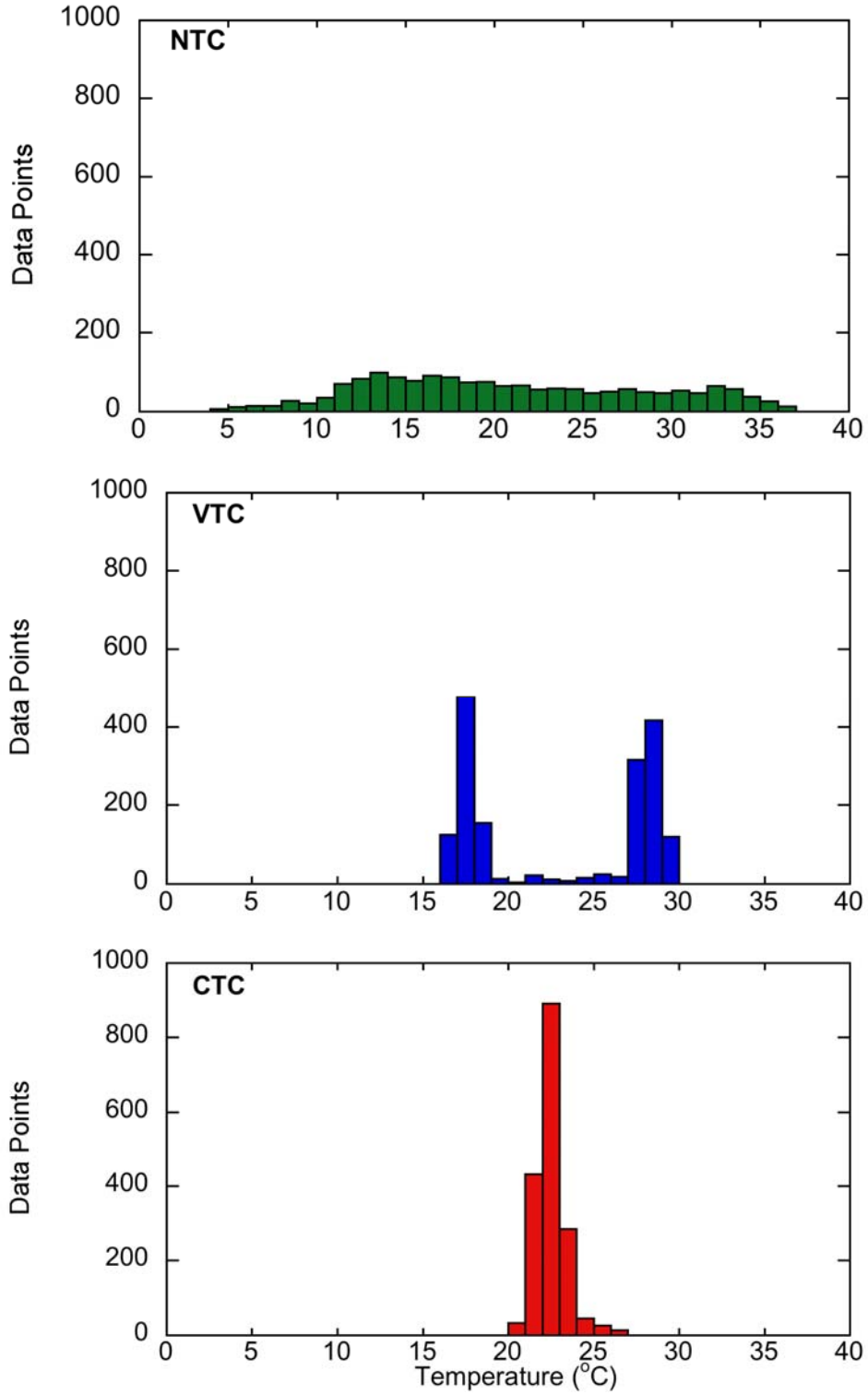

Figure 4.14. Temperature histograms for the NTC (top), VTC (middle), and CTC (bottom) reactors for the duration of the reduced temperature amplitude experiments.

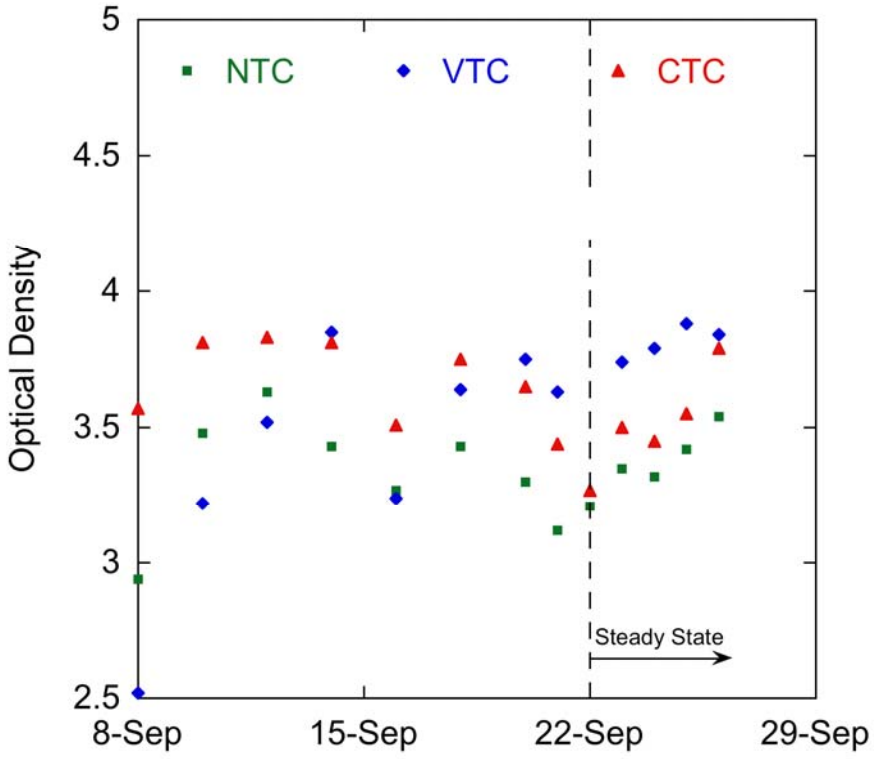

Figure 4.15. Optical densities after the VTC temperature amplitude was reduced. Note the steady increase the VTC data. Steady-state production was assumed after 1 HRT (13 days) of the new temperature conditions.

Table 4.4. Mean Parameters for the Reduced Temperature Amplitude Experiment. Precisions represent 95% confidence.

Parameter	CTC	VTC	NTC
Temperature, ^{o}C	22.5±1.8	23.3±10.3	20.9±15.0
pH	7.26±0.46	7.25±0.50	7.30±0.29
HRT (days)	12.6±1.2	12.4±2.2	12.6±1.3
Air flow rate (l m^{-1})	24.4±1.9	24.3±2.8	25.0±3.2

Table 4.5. Change in Reactor Production During the Reduced Temperature Amplitude Experiment. Only small changes were observable in the CTC and NTC reactors, whereas large improvements occurred in the VTC reactor due to the change in temperature amplitude.

Result	CTC	VTC	NTC
Optical Density	3.0%	70.2%	19.0%
Dry cell mass density	6.0%	77.5%	19.9%
Mass Production	11.4%	87.8%	24.6%
Energy Content	0.6%	-0.7%	0.32%
Energy Production	14.5%	103.5%	36.5%

these results that an optimal temperature cycle exists for maximizing mass productivity while also resulting in improved energy content over algae grown under constant temperature conditions.

4.12 Additional Experiments

In addition to the routine experiments detailed above, experiments were devised to determine the density of the media, compare the salinity of the media in the three reactors, and determine the nitrogen content of the medias in the reactors. In addition, the results of a reactor maintained under constant 30-^{o}C-conditions is discussed.

4.12.1 Media Density

The density of the growth media was determined by measuring the mass of 1 to 7 mL of media on a mass scale. The density of the media was determined to be 1061 ± 4 g L^{-1}.

4.12.2 Nitrate Consumption

The quantity of nitrate in each of the reactors was determined on Aug. 28 using a Cd reduction method. The tests indicated a quantity of approximately 1 g L^{-1} with all three reactors within 10% of each other. Thus 4 g L^{-1}, 80% of the nitrogen supplied, was consumed by the algae.

4.12.3 Salinity

Not long after the experiments were initiated, it was noticed that the evaporation rates from each reactor were different due to the differing temperature profiles of the reactors. To ensure that the salinities of each reactor were not significantly different as a result of the evaporation rates, a test was devised. Samples (100 mL) were withdrawn from each reactor and dried in pre-weighed aluminum pans at 100 ^{o}C until dry (about 24 hours). The pans were then placed in a muffle furnace at 550 ^{o}C for 20 minutes to remove any organic components. The pan was weighed again and the original pan weight was subtracted to obtain the salt mass. From this, a salt concentration could be determined.

The salinities of the NTC and VTC reactors were identical, at 11.4%. The CTC reactor had a slightly lower salinity at 10.7%, but this difference was not considered significant.

4.12.4 High-temperature Experiment Results

During the development phase of the experiments (early July, 2009), the VTC reactor was set up to operate on a 30/15-^{o}C day/night cycle. However, due to a programming error in the temperature controller, the reactor was maintained at 30 ^{o}C

continuously. After only four days, these conditions caused an originally healthy culture of algae to perish. Similar results were observed by Davis et al. [7]. Noting that the VTC consistently produced algae with the proper temperature cycle, reducing the temperature of an algal culture overnight that periodically or routinely observes overheating may prove to be an effective method of retaining the culture.

4.13 Energy Efficacy

With the exception of the NTC reactor, energy was required to maintain the temperatures of the reactors through cooling or heating. This section will compare those energy requirements to improvements in biomass energy productivity over the NTC reactor.

To assess the thermal energy requirements of the reactors, the mean temperatures of the NTC, CTC, and VTC reactors were calculated through the course of the experiment. From this data, the thermal energy requirement for the CTC reactor, Q_{CTC}, was determined as

$$Q_{CTC} = \rho C_p V_R \sum_{t=1}^{96} \left[T_{CTC}(t) - T_{CTC}(t-1) - T_{NTC}(t) + T_{NTC}(t-1) \right] \tag{5}$$

and similarly for the VTC reactor (both temperature amplitudes). This is the minimum thermal energy requirement; it does not include heat losses from piping and associated processes.

Differentiation was made for cooling and heating requirements. The daily thermal requirements are presented in Fig. 4.16 and are compared to improvements in biomass energy productivity over the NTC reactor. While the constant and variable temperature

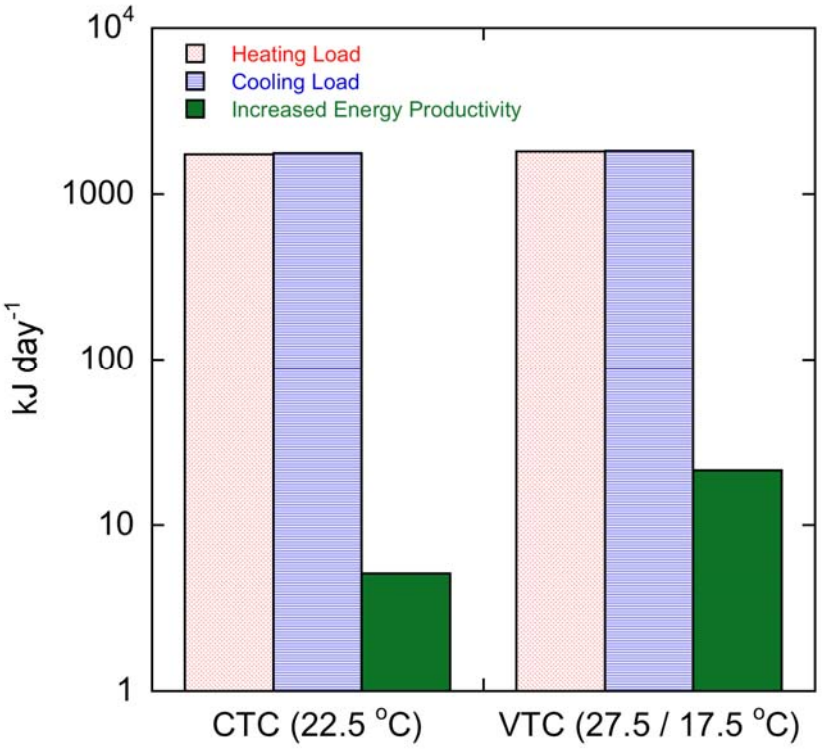

Figure 4.16. Heating and cooling requirements for the CTC and VTC reactors compared to their improvements in biomass energy productivity of the NTC reactor.

cycles improved energy productivity 5 kJ day^{-1} and 21 kJ day^{-1}, respectively, the heating and cooling loads required to maintain these temperatures were approximately 1800 kJ day^{-1} each. Thus, even if improvements in energy productivities were 100 times what these experiments yielded, they would hardly compensate for the thermal loads necessary to maintain the reactors.

CHAPTER 5

TEMPERATURE CONTROL EXPERIMENT SUMMARY, CONCLUSION, AND FUTURE WORK

Three approaches to maintaining the temperatures in 10-cm-thick, continuous batch, outdoor, vertical plate reactors were experimentally investigated for maximizing mass and energy productivity. Each reactor contained 30 L of media and had a lit surface area of 0.75 m^2. The three temperature cycles considered were a constant temperature control (CTC), a variable temperature control (VTC) in which the reactor was heated in the day and cooled at night, and no temperature control (NTC) in which temperatures mimicked ambient temperature cycles. The three reactors were operated in otherwise near identical conditions (pH, CO_2, HRT, mixing, aeration, insolation, and media). A brine microalgae, *Dunaliella tertiolecta*, was used for the experiments.

The CTC reactor temperature was maintained at 22.1 ± 1.1 ^oC throughout the duration of the experiments (from Jul. 15 through Sep. 26, 2009). The VTC reactor was operated on a 30/15-^oC day/night cycle from Jul. 15 to Sep. 8, then a 27.5/17.5-^oC day/night cycle for the remainder of the experiment. The 30/15-^oC VTC cycle resulted in mass and energy production rates 40% and 36% less, respectively, than the CTC reactor. However, by decreasing the temperature amplitude to 27.5/17.5 ^oC, the VTC reactor increased in mass and energy productivity by 88% and 104%, respectively, over the course of 18 days. This dramatic change observed from the simple reduction of the

temperature amplitude showed that the performance of the reactors was responding primarily to temperature conditions, and not some other factor.

The NTC reactor followed a sinusoidal-like temperature cycle with a mean temperature of 22.0 ^{o}C and an amplitude of 13.3 ^{o}C throughout the course of the experiment. These conditions resulted in mass and energy production rates 17% and 9% less, respectively, than the CTC reactor.

It was unexpected that the algae produced by the NTC and VTC reactors were of higher energy quality than the CTC reactor, containing 4% and 7% more kJ g^{-1} AFDW, respectively. Higher energy content has been linked with higher lipid content, but FFA and TAG content of the algae from the three reactors were not significantly different, each at approximately 2.2%, despite literature and calculations that suggest there should exist a difference of 5 - 7%. *Dunaliella tertiolecta* is known to produce β-carotene, a long-chain hydrocarbon ($C_{40}H_{56}$), under stress conditions such as nutrient limitation [15]. It is possible that the extreme temperatures in the NTC and VTC reactors induced β-carotene production in the algae that may have contributed to higher energy contents.

A 27.5/17.5-^{o}C day/night cycle produced the highest mass and energy productivity. Similar results were obtained by Davis et al. [7], but for a different algae species and a higher temperature amplitude. The improvement in energy efficiency was 13% over the same culture grown at constant temperature.

The NTC reactor fell short of the efficiency of the CTC reactor due to the extreme temperatures (as high as 35 ^{o}C and as low at 5 ^{o}C) that it experienced. However what is not accounted for by mass and energy productivities is the quantity of auxiliary energy

required to maintain controlled temperature cycles. In order to maintain the temperatures of the CTC and VTC reactors, heating and cooling loads 100 times any improvements in energy productivity over the NTC reactor were required, as mentioned in Section 4.13. While limiting the high and low temperatures of a reactor was shown to be important to maximizing the productivity, limiting these conditions must be considered with regards to auxiliary energy requirements. A more efficient method of controlling the temperature in a reactor may be to allow the temperature to follow ambient temperature trends until it reaches a maximum or minimum temperature at which point a heat exchange system can remove or add heat to or from a large thermal reservoir, thereby limiting the temperature fluctuation of the reactor while retaining thermal energy inside the system.

While properly varying the temperature with diurnal light and dark cycles clearly improves algal productivity, a few questions remain that should be addressed in the future:

- What influence did the rate of heating and cooling in the VTC reactor have on the efficiency of the reactor? Would it have produced more algae if heating and cooling were not as rapid?
- A temperature cycle, whether natural or forced, was shown here to result in algae with up to a 7% higher energy content, indicating changes in the chemical makeup of the algae, likely a higher concentration of reduced compounds. This difference could not be identified with GC analysis, but if this change in

composition can be identified and shown to yield greater amounts of any compound of value, it may be of interest to the biochemical industry.

The experimental reactors used during these experiments were far from optimized. Their mass and energy productivities were only 3% of what is theoretically possible [16], likely because the reactor was too thick and the HRT was too long for optimal productivity. When the feed valves failed and fed the CTC and VTC reactor excessive media, the proceeding productivities and cell densities recovered quickly. Thus, more media (and algae) could have been replaced each day with little corresponding decrease in cell density. In the future, reactors should be operated in a tubidostat fashion in which the optical density is maintained at a constant and the HRT is varied. This approach provides a means to account for environmental fluctuations such as insolation and temperature in the quantity of harvested algae, thereby allowing a higher rate of algae can be removed without risking washing out the reactor.

A major technical difficulty of algae is that an optimal condition (e.g. temperature) is dependent on nearly every other environmental condition (pH, incident light intensity, HRT, reactor thickness, light utilization, nutrient availability, etc.). Thus, a more nearly optimized reactor may be more sensitive to thermal cycles. But, this is not known.

CHAPTER 6

LIGHT UTILIZATION IN PHOTOBIOREACTORS

The production of 1 kg of algae requires approximately 1.3 kg of carbon dioxide, 0.54 kg of water, 75 g of ammonia, 25 g of phosphate, and 250 MJ of terrestrial solar energy [16,17]. Because of the diffuse nature of solar energy relative to the availability of the nutrients, reactors optimally provide the algae with adequate nutrients, making light the growth-limiting constituent.

The specific growth rate (μ) of algae is dependent upon the light intensity to which it is exposed (see Fig. 6.1). For light intensities between zero and the saturation intensity, I_s, μ is proportional to light intensity. Increasing light intensity beyond this point results in no further increase in μ. Although the rate of absorbed photons is proportional to the light intensity, only a fraction of I_s/I is utilized by the algae due to rate-limiting reactions in the photosynthetic process. If light intensity is increased significantly beyond I_s for a prolonged period of time, photoinhibition - irreversible damage to the cells' photosynthetic apparatuses - occurs and μ proceeds to decrease [18,19].

For wild strains of algae, the value of I_s is typically 2.5 – 20% of full sunlight, thus much of the light absorbed by the algae in full sunlight is wasted before it can contribute to the photosynthetic process.

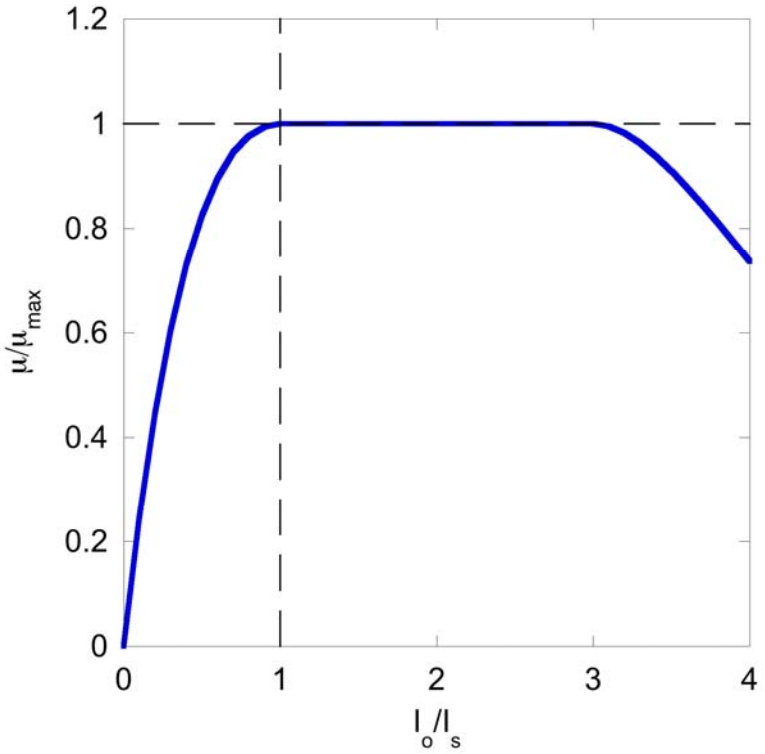

Figure 6.1. General specific growth rate curve as a function of light intensity for optically thin cultures of algae [18].

In order to absorb most of the incident light, algal cultures are necessarily deep and/or dense. Since light intensity decreases exponentially with cell density and culture depth, light intensity cannot be treated as a constant value throughout the culture. Rather, light through the depth of an algal culture generally follows the Beer-Lambert Law:

$$I_z(z) = I_z(z=0)e^{-k \cdot X \cdot z} \tag{6}$$

Therefore, the specific growth rate of a particular algae cell is a function of incident light intensity, pigment concentration, and its location in the algal culture.

It is the convoluted relationships between light intensity, culture depth, and specific growth rate that makes mathematical modeling of light utilization in reactors complicated, but also provides potential for maximizing the use of light in reactors.

6.1 Literature Review

Over the past 70 years, a large number of publications have detailed the production rates of numerous algal reactors and explored various phenomena related to algal growth. A number of mathematical relationships have also been published, some using experimentally established relationships to derive more general relationships [20,21], some with correlating experimental data [3,22-24], and some with only a theoretical basis [25-27].

6.1.1 The Bush Equation

The earliest relationship for determining photon utilization in an algal culture was attributed to V. Bush by Burlew [25]. The Bush equation was derived by assuming an infinitely thick culture (complete photon absorption into the culture) and that all photons were utilized when the light intensity was less than I_s, but when the light intensity was above I_s, only the rate of photons I_s was utilized (Fig. 6.2). The resulting equation for photon utilization is

$$u_p = \begin{cases} \frac{I_s}{I_o}\left(\ln\left(\frac{I_o}{I_s}\right)+1\right) & I_o > I_s \\ 1 & I_o \le I_s \end{cases} \tag{7}$$

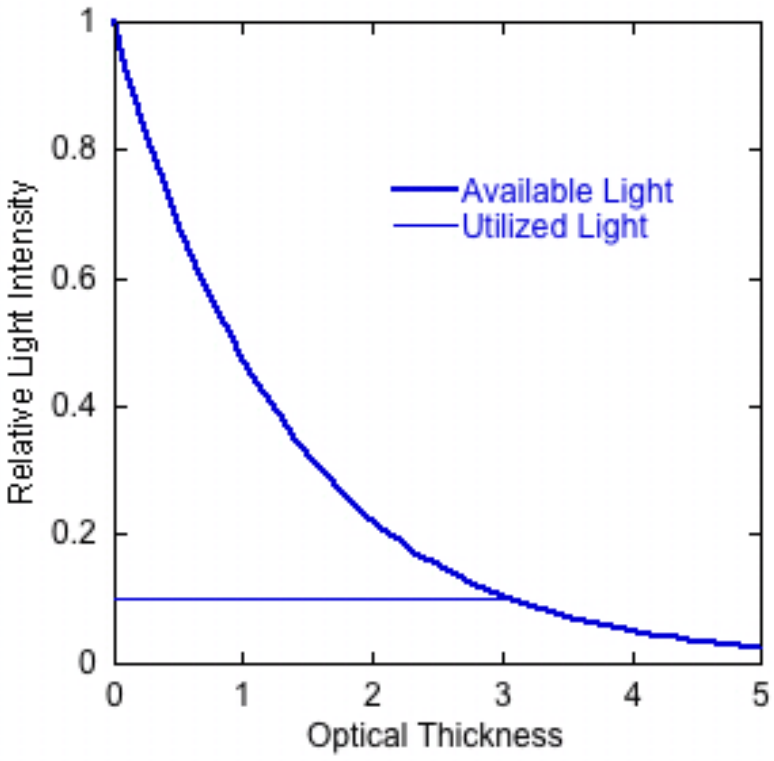

Figure 6.2. Available and utilized light through an algal culture.

Equation 7 does not take into account light escaping through the culture or photoinhibition. The Bush equation has never explicitly been compared to experimental data. A few articles have indicated the u_p is never equal to unity and the right-hand side of the Bush equation should be multiplied by a constant (such as 0.85) [28-30]. Melis et al. [31] obtained photon utilization values in an algal culture for various light intensities, but they did not compare the Bush equation to the results. Figure 6.3 shows the Bush equation curve fitted to Melis et al.'s data, indicating that the data and equation correlate very well.

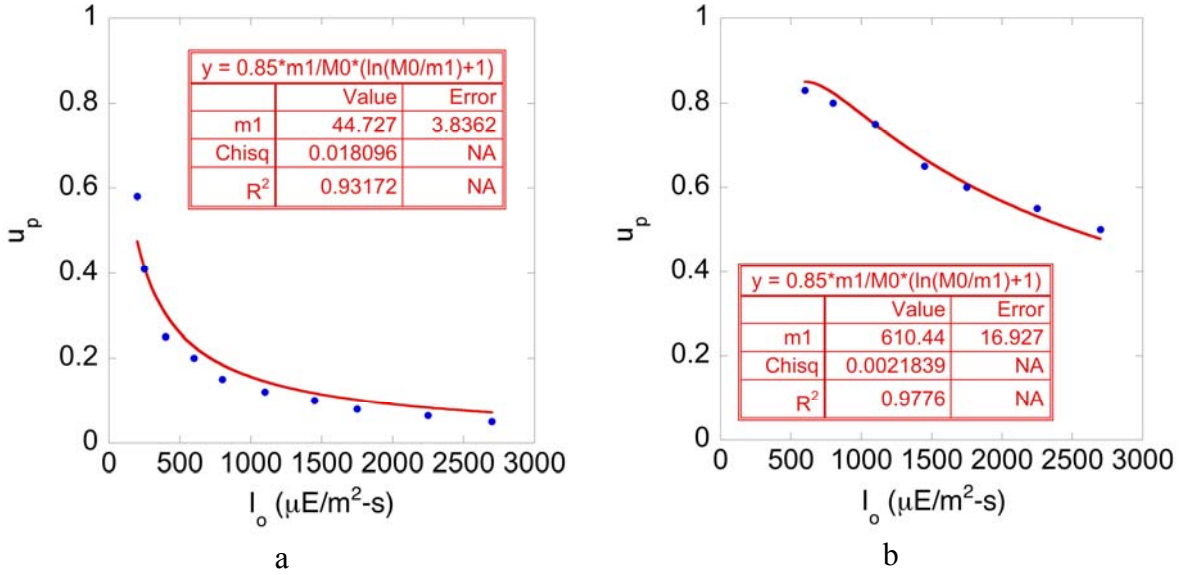

Figure 6.3. Comparison of the Bush equation to data adapted from Melis et al. [31] for a) low-light adapted algae and b) high-light adapted algae.

6.1.2 Improving Light Utilization

The inability of algal cultures to use full sunlight at maximum efficiency has motivated researchers to find ways of diluting incident sunlight since the 1950's [32-37]. There are two general methods of doing so: spatial light dilution, and temporal light dilution. The approach of spatial dilution is simply to increase the area of algal culture to which the sunlight is exposed. This effectively decreases I_o in Eq. 7, driving u_p toward its maximum value.

The second approach, temporal light dilution, exposes algal cells to intense light very briefly, then moves the cells to darkness to give the dark reactions in photosynthesis time to utilize the captured photons while cells in darkness are moved to the light; the cycle is then repeated, creating what is termed the "flashing effect". Hu and Richmond, and Hu et al. [35-37] demonstrated the full potential of the temporal dilution, obtaining

algal productivities that were linearly proportional to light intensities up to full sunlight in thin, very dense, rapidly mixed cultures of *Spirulina platensis*.

6.1.3 Temporal Light Dilution

Researchers agree that the flashing frequency, *f*, light intensity, *I*, and load factor (the fraction of time the algae is exposed to light per cycle), ϕ, are relevant factors to maximizing photosynthesis with temporal dilution [21,32,38-46], but experimental and theoretical results have yielded a wide range of optimal values for these parameters. Table 6.1 lists a number of research papers with optimal values of *I, f,* and ϕ.

Table 6.1. Optimal Values for Maximizing Photosynthesis Using Temporal Dilution.

Reference	I ($\mu E\ m^{-2}\ s^{-1}$)	f (Hz)	ϕ	Organism
	Experimental			
Emerson & Arnold [42]	N/A	>28	0.03%	*Chlorella pyrenoidosa*
Clendenning & Ehrmantraut [43]	N/A	25	0.03%	*Chlorella pyrenoidosa*
Weller and Franck [44]	1250*	15	7%	*Chlorella pyrenoidosa*
Rieke and Gaffron [45]	2200*	35	14%	*Scenedesmus Obliquus*
Phillips and Myers [39]	1000	50	5%	*Chlorella pyrenoidosa*
Terry [21]	500	<10	25%	*Phaeodactylum tricornutum*
Tennessen et al. [40]	5000	90	2%	Tomato leaf
Kok [38]	1800	>50	20%	*Chlorella pyrenoidosa*
Matthijs et al. [46]	500	<20	0.01%	*Chlorella pyrenoidosa*
Park et al. [41]	N/A	50 000	10%	*Chlorella kessleri*
	Theoretical			
Gorden and Polle [32]	2000	1-10 000	N/A	N/A

*Calculated light intensity assuming 1 $\mu E\ m^{-2}\ s^{-1}$ = 72 lux.

The majority of the results indicate that the flashing frequency need only be on the order of 10 to 100 Hz. Higher frequencies did not necessarily reduce photon utilization, nor did they yield significant improvements. Park et al. showed some improvement at frequencies in the range of 10 – 50 kHz, but the experimental uncertainty exceeded any trends [41]. Lower frequencies of 0.004 – 1 Hz did not have any detectable improvement in productivity [47].

Terry experimentally obtained a relationship for photon utilization as a function of flashing frequency, light intensity, and load factor, but only for one species of algae and suggested that a fundamental model rather than an empirical relationship would be more beneficial [21].

The majority of the mathematical models that have been developed contain means of describing phenomena such as photoinhibition, photoacclimation (slow changes in the photosynthetic units to accommodate the existing light conditions), and slowly varying light cycles that are relevant to phytoplankton production in the seas [23,24,27]. Eilers and Peeters and Rubio et al. described models that were capable of predicting production with temporal light dilution [23,27]. Both models were necessarily very complex. The model of Eilers and Peeters was not compared to any experimental data. Rubio et al. demonstrated their model mimicked the experimental data of Phillips and Myers [39], but the unknown coefficients were determined by curve-fitting the model to fit the data. The only model to be based on measurable parameters was Zonneveld [48].

Zonneveld's model took into account physical parameters of the algae, such as chlorophyll content and PSII content per cell, photosynthetic unit (PSU) cross-sectional

area, absorption coefficient of the chlorophyll, and PSU turnover time (minimum time a PSU needs between receiving photons to fully utilize them). His model without photoacclimation was relatively simple. However, his model was not applied to consider temporal light dilution and it was not compared to any experimental data.

6.2 Research Scope

There are two methods for improving light utilization in reactors grown in full sunlight: spatial light dilution and temporal light dilution. Light utilization using spatial dilution can be effectively modeled, as was shown in the previous section. While a variety of models exist that describe photosynthetic productivity as a function of intermittent light, the models are unnecessarily complex for application to reactor design. Most of the models contain a number of coefficients such that the models cannot predict productivity a priori – the models must be curve fitted to existing data to determine the coefficient, or the models do not consider temporal light dilution. A simplified model tailored to light conditions expected in reactors that is based on measurable characteristics of the algae, such as chlorophyll content, Photosystem II (PSII) content, I_s, and PSU turnover frequency would significantly advance the design and evaluation of reactors.

The research reported herein:

- derives a mathematical relationship relating photon uptake to light intensity, flashing frequency, load factor, PSII concentration, turnover frequency, and I_s,

- applies the above relationship to algal cultures in which light is attenuated through the depth of the culture,
- demonstrates the use of the relationship for design of steady-state continuous reactors, and
- verifies the relationship by comparing it to experimental results.

6.3 Temporal Light Dilution Model Description

Most of the existing models were intended for use in natural environments. Reactors are ideally designed with temperature and light intensity cycles, cell densities, nutrients, mixing and other conditions set for near-optimal production. Under such conditions, photoinhibition would be minimized [27,49], photoacclimation need not be accounted for under steady-state conditions, and high cell densities allow for simplifying assumptions. Thus, a simpler, more useable model can be developed for reactor design.

The mathematical relationship is based on an "energy funnel" concept. This concept assumes that the photosynthetic apparatus of the algae has the capacity to store a quantity of photo-energy, C, measured in photons per unit area. This assumption is valid since the algae must have some storage capability to continue utilizing photons in the absence of light, making temporal dilution possible. The stored photo-energy is assumed to be utilized for cell energy at a constant rate as long as stored photo-energy is available for utilization. If the flashing light intensity and duration are sufficiently small, the "energy funnel" will never fill beyond capacity, thus no photons will be wasted (spill over). If the flux of photons per flash is greater than the energy funnel capacity, photon use efficiency will decrease.

The value of C has been proposed by Tennessen et al. [40] to be equivalent to the number of PSII sites per unit area. This theory is given merit in that the limiting reaction in photosynthesis was determined to be the reduction of cytochrome *f* by PSII and the molar ratio of cytochrome *f* to PSII is equal to unity [50,51].

6.4 Experimental Data

In order to compare the model to experimental data, the following parameters must be available for each combination of parameters: $I(z=0)$, f, ϕ, I_s or the continuous light growth curve, μ or u_p or productivity, and C or PSII content and cell density. Results presented by Phillips and Myers [39] contained sufficient information to compare the model. Further, the results were completely tabulated and cover a wide range of f and ϕ, from 1.5 – 144 Hz and 5 – 40 %, respectively. This was the primary data used for evaluating the validity of the relationship. The trends established by the relationship were also compared to experimental data given by Tennessen et al. [40], Terry [21], and Kok [38]. Because these researchers did not include all of the data necessary for the model, the model could not be quantitatively compared.

CHAPTER 7

TEMPORAL LIGHT DILUTION MODEL DEVELOPMENT

To date, mathematical models relating photosynthetic productivity to temporal light dilution have been too complex for general engineering design applications. These relationships took into account a number of variables, such as photoacclimation, that can be ignored or taken into account by some simpler means. In this chapter, a simpler relationship is developed that can be used for "first-cut" engineering calculations and to understand the relationship among the variables.

7.1 Continuous Light Model

Although this chapter's goal is a model relating productivity to temporal light dilution, a model relating productivity to continuous light is necessary for describing the underlying theory, model validation, and determining some of the variables from experimental data.

To develop this model the following assumptions are made. These assumptions are numbered as they will be referred to by number in future discussions.

1. An algal culture normal to a light source consists of a homogenously distributed concentration of photosynthetic units, *C*, measured in μmol of PSU's per unit area of light-harvesting pigment (LHP) (this will be discussed later in this section) (Fig. 7.1).

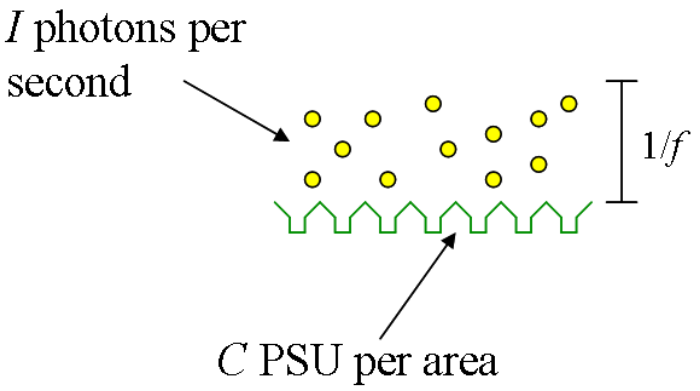

Figure 7.1. Visual representation of the model used for continuous and discontinuous light utilization models. The algal culture is treated as a collection of PSU's collecting a randomly distributed flux of photons.

2. The photons are homogenously distributed over the algal culture and are striking the culture at a rate of I_o μE m^{-2} s^{-1}.
3. The PSU's are all open and have a turnover frequency (rate at which a PSU can process a captured photon) of f Hz (Fig. 7.1).
4. The algal culture is very dense such that the quantity of PSU's per area is very large (C~10^{17} PSU m^{-2} s^{-1}).
5. Algal productivity, or specific growth rate, is proportional to the quantity of photons utilized.
6. The photon requirement, γ, necessary to activate a PSU, is equal to unity. This is a common assumption used in most models [26,48].

The probability, p, of a photon striking a PSU in one turnover period is given as

$$p = 1 - e^{-I_o / fC\gamma} \tag{8}$$

Since the concentration of PSU's is very large, by the central limit theorem, p becomes the fraction of PSU's filled in the culture. Because of Assumption 5,

$$\frac{\mu}{\mu_{\max}} = 1 - e^{-I_o/fC\gamma} \tag{9}$$

This is not a unique kinetic model; Dubinsky et al. and Sakshaug et al. obtained comparable relationships that were derived similarly to Eq. 9 [52,53]. Equation 9 generates a curve relating specific growth rate to I_o very similar to light saturation curves seen in the literature (Fig. 7.2).

It is important to note that C is measured in units of moles of PSU's per unit area of light-harvesting pigments, *not* the surface area of the algal culture. To account for this it is convenient to define C as

$$C = c\chi \tag{10}$$

where c is the *volumetric* density of PSU's, measured in moles of PSU's per volume of algal culture. χ is defined as the volume of algal culture per unit area of LHP. Since it is mostly the chlorophyll and other LHP's that contribute to the attenuation of light through a culture, χ can be assessed as

$$\chi = \frac{1}{(k\rho)_{LHP}} \tag{11}$$

and light attenuation through a culture defined as

$$I_z = I_o e^{-z/\chi} \tag{12}$$

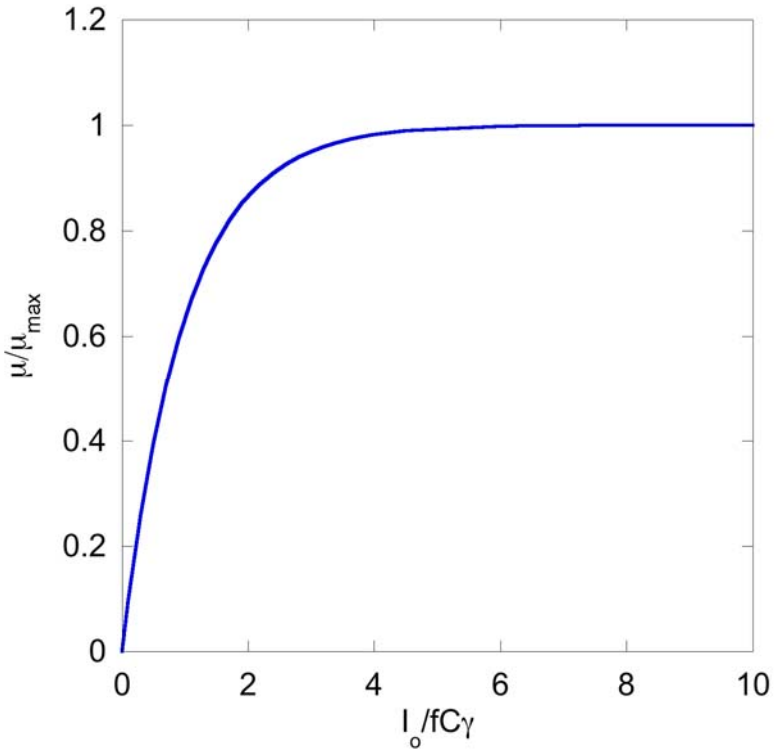

Figure 7.2. Relationship between specific growth rate and light intensity as predicted by Eq. 9.

7.2 Temporal Light Dilution Model

It is sometimes of value to make an assumption that does not represent actual phenomena, but creates a suitable approximation that can greatly simplify a model. For this reason, one more assumption will be made:

7. For the situation described in Assumption 1, each photon striking the culture strikes an open PSU until all of the PSU's are filled.

Assumption 7 removes the curvature from Fig. 7.2 and replaces it with a discontinuous linear relationship:

$$\frac{\mu}{\mu_{\max}} = \begin{cases} I_o / I_s & I_o < I_s \\ 1 & I_o \geq I_s \end{cases} \quad (13)$$

This is the same assumption made by Bush in the development of his relationship for continuous light and was shown in Section 6.1.1 to induce negligible error. Using Assumption 7 reduces the temporal light dilution relationship to the form of that of a filling reservoir (Fig. 7.3). A photon reservoir of capacity *C* is filled at a rate $I_z(t)$. The reservoir is emptied at a rate $fC\gamma$ when photons are stored in the reservoir and $I_z(t)$ when the reservoir is empty. If the stored photons exceed C, any additional photons are wasted, $I_w(t)$.

If it can be assumed that

8. The light intensity can be represented by a square wave of frequency *v*, with a duty cycle $\phi = t_f / v = t_f / (t_f + t_d)$ (Fig. 7.4),

then there are three solutions to I_u, the rate of photons being utilized. The solution depends on the magnitude of $I_z(t)$, *C*, and *f*.

7.2.1 Case 1: $(I_z - fC\gamma)\phi \leq C\upsilon, I_z\phi \leq fC\gamma$

This is the ideal case in which the PSU's are never overfilled and there is adequate time between each flash for all of the PSU's to return to their open state. Thus, all of the absorbed photons are used and

$$I_u = I_z\phi \quad (14)$$

Algae exposed to such conditions are termed fully light diluted.

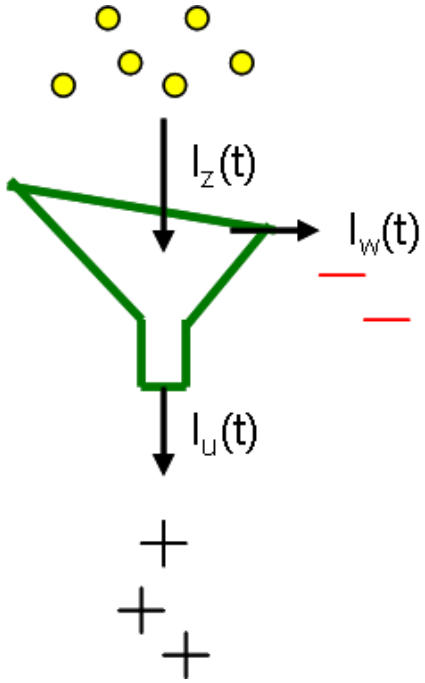

Figure 7.3. Visual representation of photon utilization model with Assumption 6.

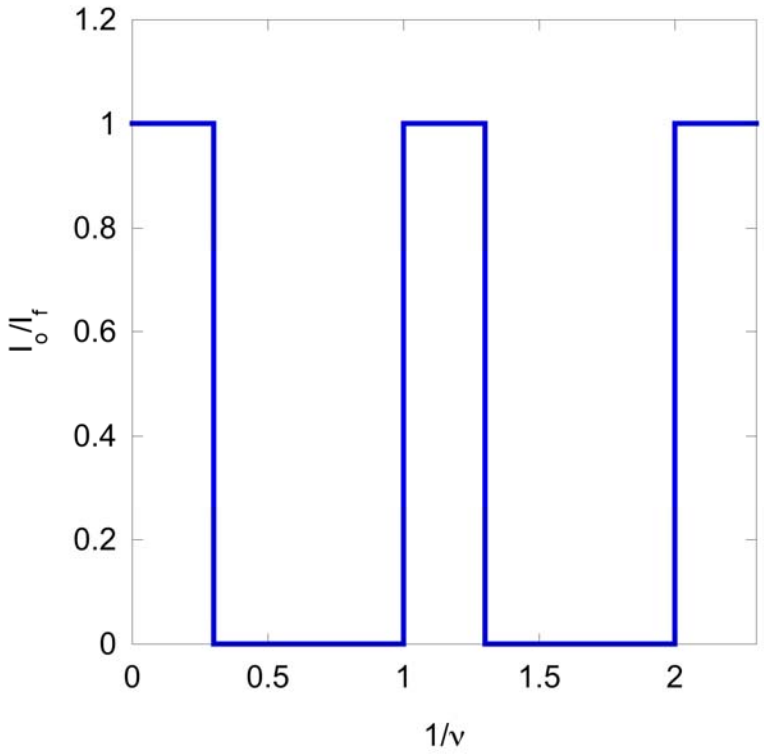

Figure 7.4. Square wave with a frequency ν and duty cycle $\phi = 0.3$.

7.2.2 Case 2: $C\upsilon < (I_z - fC\gamma)\phi, \upsilon \le f\gamma(1-\phi)$

In this case, the photon capacity is overfilled, but the dark time is sufficient for the PSU's to completely discharge. The photon utilization is then described as

$$I_u = C(\upsilon + f\phi\gamma) \tag{15}$$

Algae subjected to this case are termed partially light diluted.

7.2.3 Case 3: $f\gamma(1-\phi) < \upsilon, fC\gamma < I_z\phi$

This case represents the situation in which the dark time is insufficient to fully discharge the PSU's. The result is the photon reservoir never emptying at steady state, resulting in

$$I_u = Cf\gamma \tag{16}$$

This case results in algae that are termed fully light undiluted.

7.2.4 Defining u_p in Terms of Flashing Characteristics

Equations 14 - 16 describe the rates of photons being utilized with temporal dilution for a very thin culture of algae in which light attenuation through the culture is infinitesimally small. Most reactors capture most of the incident light, thus light attenuation is significant. Because the light intensity decreases exponentially through a culture, more than one of the cases may be observed in a single culture. At high light intensities, only partially diluted or fully undiluted situations are valid. As the light attenuates through the culture, temporal light dilution benefits become significant (fully light diluted). Partially light diluted and fully light undiluted situations will not coincide

in the same culture because the occurrence of these situations is dependent on constants such as v, ϕ, and f, not on I_z.

The depth into the culture at which fully light undiluted algae interfaces with fully lighted diluted algae will be called s_3, and the depth of the interface between partially light diluted algae and fully light diluted algae will be called s_2. s_3 occurs when $fC\gamma = \phi I_f e^{-z/\chi}$. This occurs when $z = s_3 = \chi \ln\left(\frac{\phi I_f}{fC\gamma}\right)$. s_2 occurs when $Cz(v + f\gamma\phi) = \phi I_f e^{-z/\chi}$. Solving for z, $z = s_2 = \chi \ln\left(\frac{\phi I_f}{C(v + f\gamma\phi)}\right)$.

Recall that the photon utilization, u_p, is defined as the ratio of photons consumed to the total photons available. Evaluating the photon utilization rate in mathematical form, similar to the method in which Bush derived his equation, yields

$$u_p^{(2)} = \frac{\int_0^{s_2} C(v + f\gamma\phi)dz + \phi\int_{s_2}^{\infty} I_z dz}{\phi\chi I_f} \tag{17}$$

and

$$u_p^{(3)} = \frac{\int_0^{s_3} Cf\gamma dz + \phi\int_{s_3}^{\infty} I_z dz}{\phi\chi I_f} \tag{18}$$

Evaluating the integrals of Eq. 17 and 18 yields

$$u_p^{(2)} = \frac{C(v + \phi f\gamma)}{\phi I_f}\left(\ln\left(\frac{\phi I_f}{C(v + \phi f\gamma)}\right) + 1\right) \tag{19}$$

and

$$u_p^{(3)} = \frac{fC\gamma}{\phi I_f}\left(\ln\left(\frac{\phi I_f}{fC\gamma}\right)+1\right) \tag{20}$$

Equations 19 and 20 are very similar in form to the Bush equation, the only differences being that $I_o = \phi I_f$ and $I_s = C\left(v+\phi f\gamma\right)$ or $I_s = Cf\gamma$.

7.3 Discussion

Recall that in fully light undiluted situations the dark time is insufficient to extract any benefit from the flashing effect, therefore the photon utilization rate in Eq. 20 should be identical to the Bush equation. Comparing the two equations, this would only be the case if $I_s \equiv Cf\gamma$.

I_s is not strictly defined, but it is generally agreed that it is the light intensity at which $d\mu/dI_o\big|_{I_o=0}$ intersects with μ_{max}, or

$$I_s = \frac{\mu_{\max}}{\left.\frac{d\mu}{dI_o}\right|_{I_o=0}} \tag{22}$$

If the light saturation curve follows Eq. 9, Eq. 21 reduces to $I_s = \mu_{\max}/\left(\mu_{\max}/fC\gamma\right) = fC\gamma$, thus Eq. 20 does resolve to the Bush equation. Further, given that $I_s \equiv fC\gamma$, Eq. 19 reduces to

$$u_p^{(2)} = \frac{Cv+\phi I_s}{\phi I_f}\left(\ln\left(\frac{\phi I_f}{Cv+\phi I_s}\right)+1\right) \tag{22}$$

This definition of I_s is nearly identical to that determined by Zonneveld, the only difference being that his was defined per algal cell, whereas it is defined here as per algal culture [48].

The equations can be unified into one equation in which I_u is defined as the minimum value of I_s, $Cv+\phi I_s$, and I_a ($I_u = \min(I_s, Cv+\phi I_s, I_a)$) and defining the photon utilization as

$$u_p = \frac{I_u}{I_a}\left(\ln\left(\frac{I_a}{I_u}\right)+1\right) \tag{23}$$

Equation 23 is of the same form as the Bush equation, but it is generalized to account for all light conditions, including intermittent illumination and the entire range of I_a, whereas the Bush equation was only valid for continuous illumination with $I_o \geq I_s$.

7.4 Correction Coefficient

Assumption 7 approximates the kinetic curve (Eq. 9) with a set of linear relationships. This is necessary to obtain an explicit relationship, but doing so can incur a large error, as much as 37%, and a total rms error of 14%. One solution to reduce the error associated with this assumption is to assume a proportionately larger value of I_s, by a factor of κ. By using $\kappa = 1.79$, the maximum error and total rms error are minimized to one half that obtained by using no correction coefficient (Fig. 7.5). There is no physical significance to setting $\kappa = 1.79$, it is simply a value that minimizes the error associated with Assumption 7.

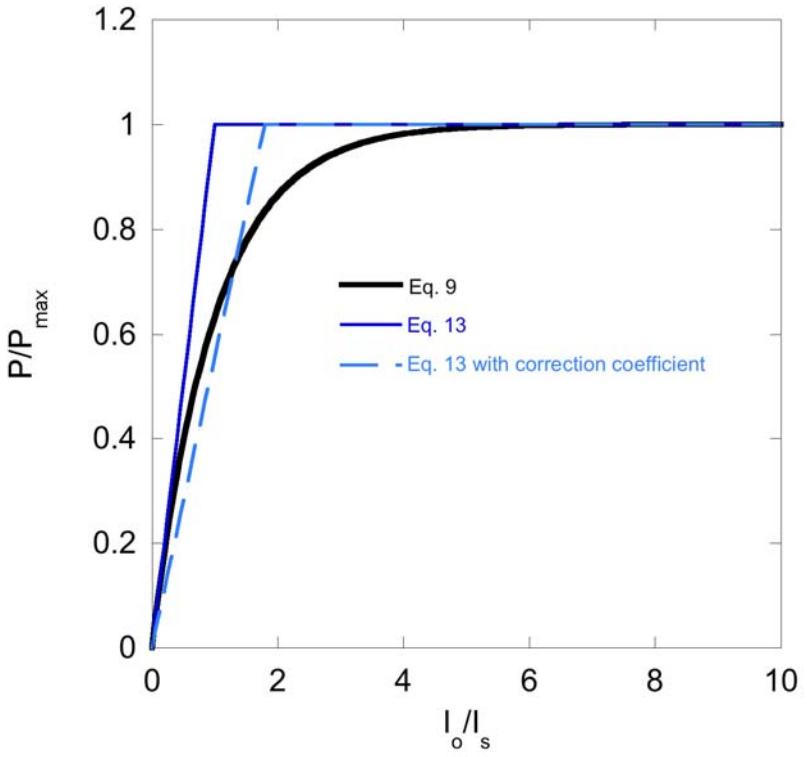

Figure 7.5. Comparison of Eq. 13 with and without the correction factor to Eq. 9.

CHAPTER 8

TEMPORAL LIGHT DILUTION MODEL VALIDATION

Results obtained by Phillips and Myers [39] will be used to validate the model obtained in Chapter 7 because their paper presented sufficient information to determine the model variables and compare the calculated results to the experimental results. Nothing in their paper could be found that would suggest the data are unreliable.

The model will be qualitatively compared to the results of other researchers, such as Kok [38], Tennessen et al. [40], and Terry [21] as well.

8.1 Determining *c*

Recall that *c* is the volumetric density of PSU's, specifically the volumetric concentration of PSII centers. Unfortunately Phillips and Myers did not calculate this value explicitly, but stated that chlorophyll contents were "within the range observed by Emerson and Arnold" [54]. From their data, the chlorophyll concentration for lights similar to that used by Phillips and Myers was between 2.45 and 17.5 μmol chlorophyll mL^{-1} of packed cells. From Phillips and Myers data, the cell concentration was 0.24 g mL^{-1}, resulting in 10.2 – 72.9 μmol chlorophyll g^{-1} of cells. From Emerson and Arnold's data, the chlorophyll / PSII ratio was between 250 and 390, thus the PSII per cell mass concentration would be 26.2 – 292 nmol PSII g^{-1} cells. Given that the experimental cell contained 5 mg of cells and had a lit volume of 25.5 cm^3, finally *c* can be determined to be between 5.13 and 57.2 μmol m^{-3}. The reactor had a thickness of 1 cm and attenuated

21% of the light. From this, χ was determined to be 0.042 m, thus C = 1.31 ± 1.09 μmol m^{-2}. The range of *c* is quite large, but it will be more accurately estimated in a later section to a value that falls within this range.

8.2 Determining *f*

The value of *f* can be determined by exposing the algae to very brief flashes of light and increasing the subsequent dark period until no further gain in photon utilization is observed. This experiment is observed from Phillips and Myers' data by comparing $\mu/(\phi I_f)$ (photon yield) to the dark period for $t_f = 1$ ms (Fig. 8.1). Since this is a specific growth rate saturating curve with respect to t_d, an exponential decay equation similar to Eq. 9 was applied to the data in the form

$$\frac{\mu}{\phi I_f} = \left(\frac{\mu}{\phi I_f}\right)_{\max}\left(1 - e^{-t_d/\tau}\right) \tag{24}$$

Following the arguments of the previous chapter, the saturating t_d is equivalent to τ, thus from Fig. 8.1, f = 125 Hz. This is similar to the value estimated by Phillips and Myers of 100 Hz.

8.3 Comparison to the Continuous Model

Now that *C* and *f* have been estimated, Eq. 9 can be compared to the continuous data of Phillips and Myers and is graphed in Fig. 8.2. The curves generated by the experimental data and Eq. 9 are very similar in form (Fig. 8.2), and choosing C =0.384 μmol m^{-2} (within the range of estimated values of *C*) results in the equation overlapping

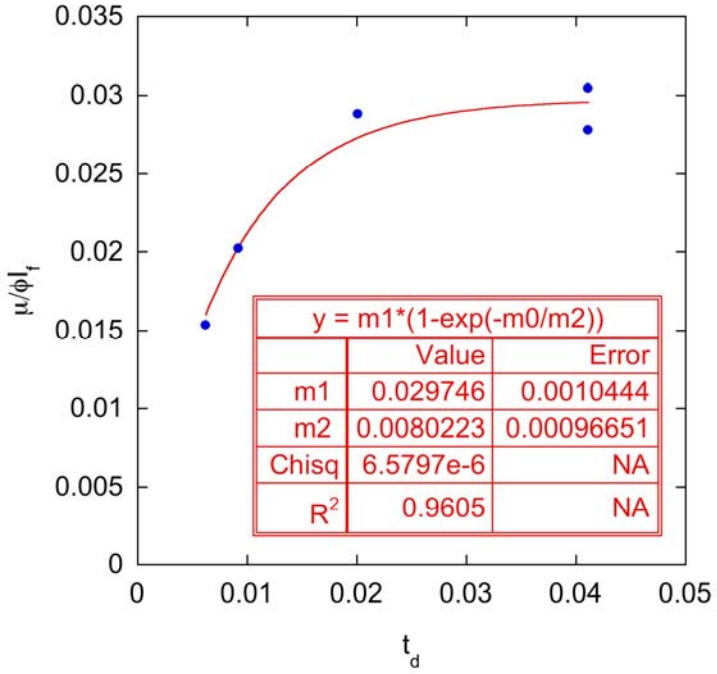

Figure 8.1. Photon yield as a function of dark time fore very short (1 ms) flashes, from Phillips and Myers [39]. The curve fit value of "m2" corresponds to the PSU turnover time of the algae used for their experiments.

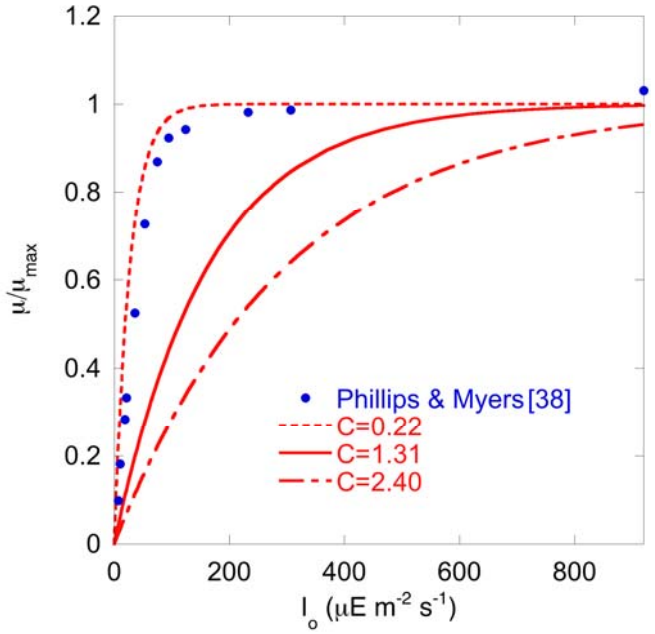

Figure 8.2. Comparison of Eq. 8 to the data of Phillips and Myers for the determined range of C [39].

nearly all of the data points, particularly compared to the relationships commonly used previously (Fig. 8.3).

8.4 Comparison to the Temporal Light Dilution Model

Phillips and Myers noted that the calculated and experimentally determined average light intensities differed somewhat due to discrepancies between the nominal values of t_f and t_d and the actual values. To more accurately compare the model to the data, the values of t_f and t_d were adjusted such that the calculated and experimental average light intensities became the same, hence the "nominal" t_f and t_d and "adjusted" t_f

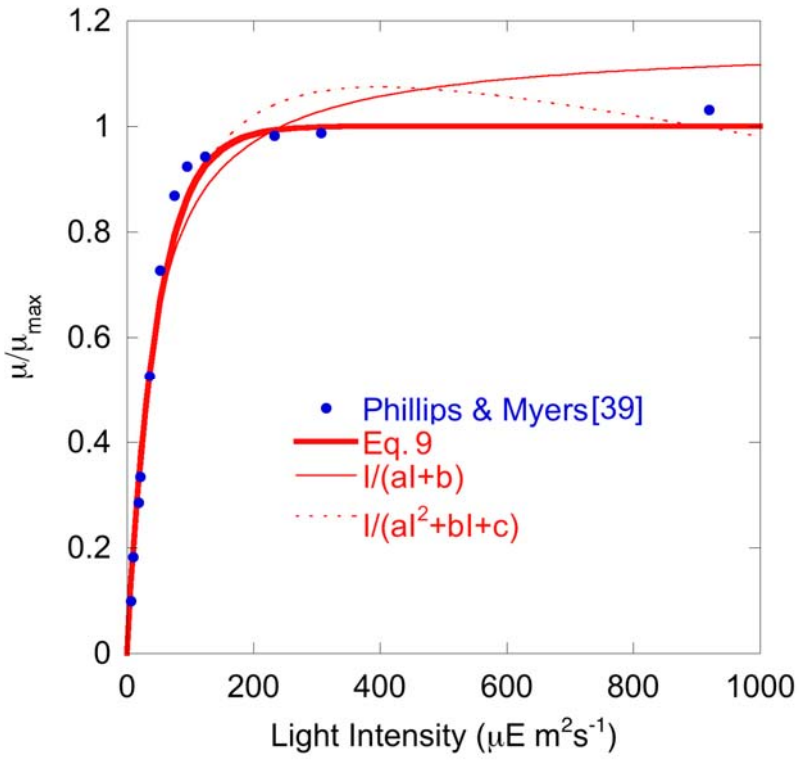

Figure 8.3. Comparison of best fits for three different models to the data of Phillips and Myers [39].

and t_d columns in Table 8.1.

Except for the experiments 69-72 and 79 in which $t_f \approx 1$ ms, only partial light dilution applies for all of the experiments. For the experiments with $t_f \approx 1$ ms, the algae experience partial light dilution through most of the reactor then full light dilution. However these experiments can also be treated as partially light diluted only with negligible error. Unfortunately, the data did not span enough values to observe solely fully light undiluted or fully light diluted experiments. Since all of the experiments can be assumed to be partially light diluted, the given values of v and ϕ along with the determined values of f and C are applied to Eq. 23 to calculate u_p for each experiment. The calculated relative specific growth rate is determined as

Table 8.1. Nominal and Adjusted Light and Dark Times from Phillips and Myers [39] Data.

Experiment No.	Nominal		Adjusted	
	t_f (ms)	t_d (ms)	t_f (ms)	t_d (ms)
82	66.7	600	65.8	601
81	66.7	266	68.3	264
80	66.7	100	67.2	99
75	16.7	316	15.6	317
73	16.7	150	16	151
74	16.7	67	15.8	67.9
77	16.7	39	15.1	40.6
66	4.2	163	4.05	163
67	4.2	79	3.61	79.6
65	4.2	37	3.9	37.3
68	4.2	17	3.93	17.2
78	4.2	10	3.79	10.4
70	1	41	0.91	41.1
72	1	41	0.9	41.1
69	1	20	0.9	20.1
71	1	9	0.84	9.2
79	1	6	0.79	6.2

$$\frac{\mu}{\mu_{\max}} = Yu_p \phi I_f \tag{25}$$

where Y is the photon yield. From Phillips and Myers' continuous light data, it was determined that $Y \approx 0.0292 \pm 0.005$ m^2 s μmol^{-1}.

The experimental results are compared to the relative specific growth rates calculated above in Fig. 8.4. The experimental error bars were taken from Phillips and Myers [55].

Figure 8.4 shows that while Eq. 23 does not exactly predict the results of

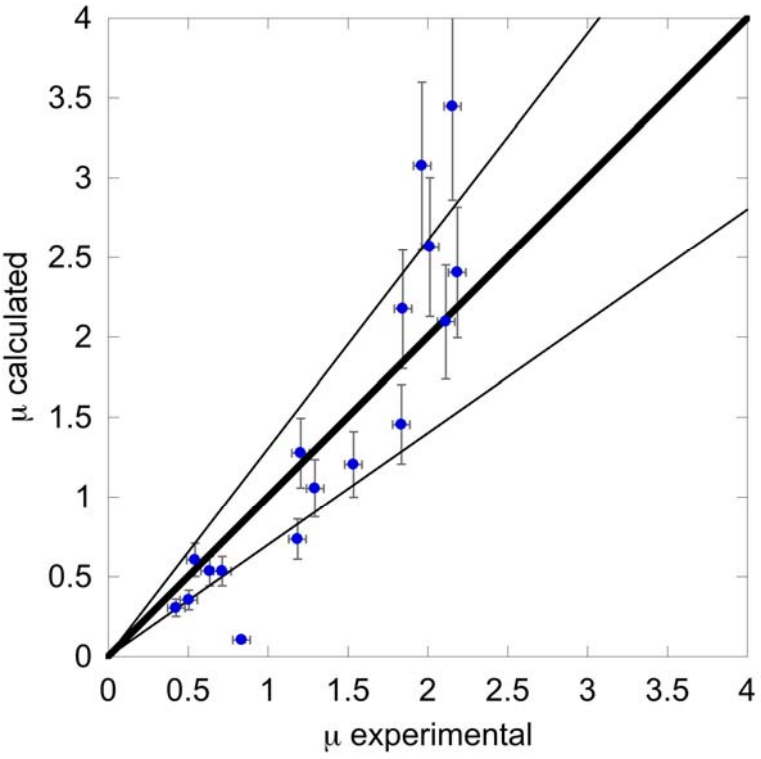

Figure 8.4. Comparison of light dilution model to data of Phillips and Myers [39].

Phillips and Myers, it generally mirrors the results, predicting the growth rate to within ±30% for most of the data points.

As mentioned in Section 7.4, the error associated with the model may be reduced by mulitplying I_s by a factor κ. Using the suggested value of 1.79 does not improve the accuracy of the model by any amount. Using $\kappa = 1.35$ reduces the error, but only by 1%. The reason the correction coefficient is ineffective is because the flash times for the experiments were sufficient to completely saturate the PSU's. Significant deviations between Eq. 9 and Eq. 13 only occur when the PSU's are partially saturated ($I_a \approx Cv + \phi I_s$). The differences between the experimental and calculated results can be attributed to three factors. First, unavoidable deviations are inherent in biological systems because of their complicated and dynamic responses to the environment. Large deviations are expected when a simple model is applied to such a complex process. Second, Phillips and Myers indicated "light leakage" in the experimental apparatus that yielded values of t_f and t_d that were longer and shorter, respectively, than the recorded values. Finally, and what is likely the largest contributor to the errors, Phillips and Myers observed variations in chlorophyll content of an order of magnitude from experiment to experiment, likely due to photoadaptation and photoinhibition of the algae during the experiments.

8.5 Model Comparison to Tennessen et al. and Terry

Tennessen et al. [40] conducted a series of experiments on tomato plant leaves using high-intensity (5000 μmol m^{-2} s^{-1}) red LED's with very short light pulses (10 – 3000 μs) and corresponding dark times such that the average light intensity was always 50 μmol m^{-2} s^{-1}. The result was effectively photosynthesis as a function of v with constant

ϕ and I_a. Employing Eq. 23 with C = 1.0 μmol m^{-2} (the value estimated by Tennessen et al.), the model closely predicts their data (Fig. 8.5).

Terry [21] observed a similar trend with *Phaeodactylum tricornutum*, except that the saturating frequency he observed was much lower (less than 6 Hz), and the various load factors (up to 0.5) he induced did not significantly affect this trend. Eq. 19 predicts this: the low saturating frequency v implies a correspondingly low PSU turnover frequency f, which would in turn limit the influence of ϕ, just as Terry observed.

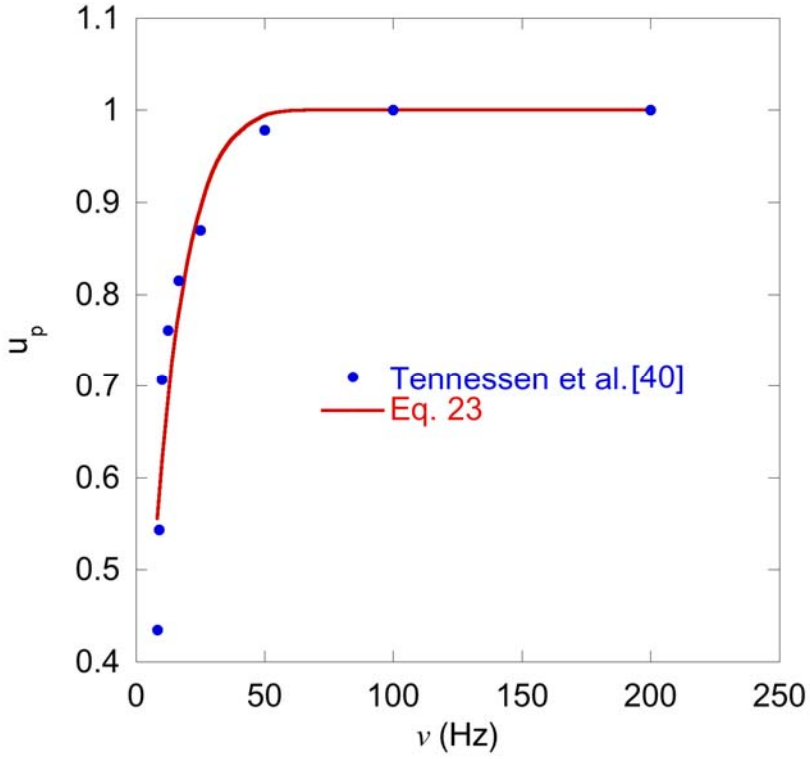

Figure 8.5. Comparison of experimental data of Tennessen et al. [40] to Eq. 23.

8.6 Model Comparison to Kok

The experiments completed by Kok [38] were similar to that of Phillips and Myers [39]. However, his results were not as completely detailed. What makes Kok's work valuable from the standpoint of comparing a photon utilization model was that he illustrated the effect of flash time, dark time, and incident light intensity on the effect of photon utilization (Fig. 8.6). In order for the temporal light dilution model to be considered valid, it should duplicate these results.

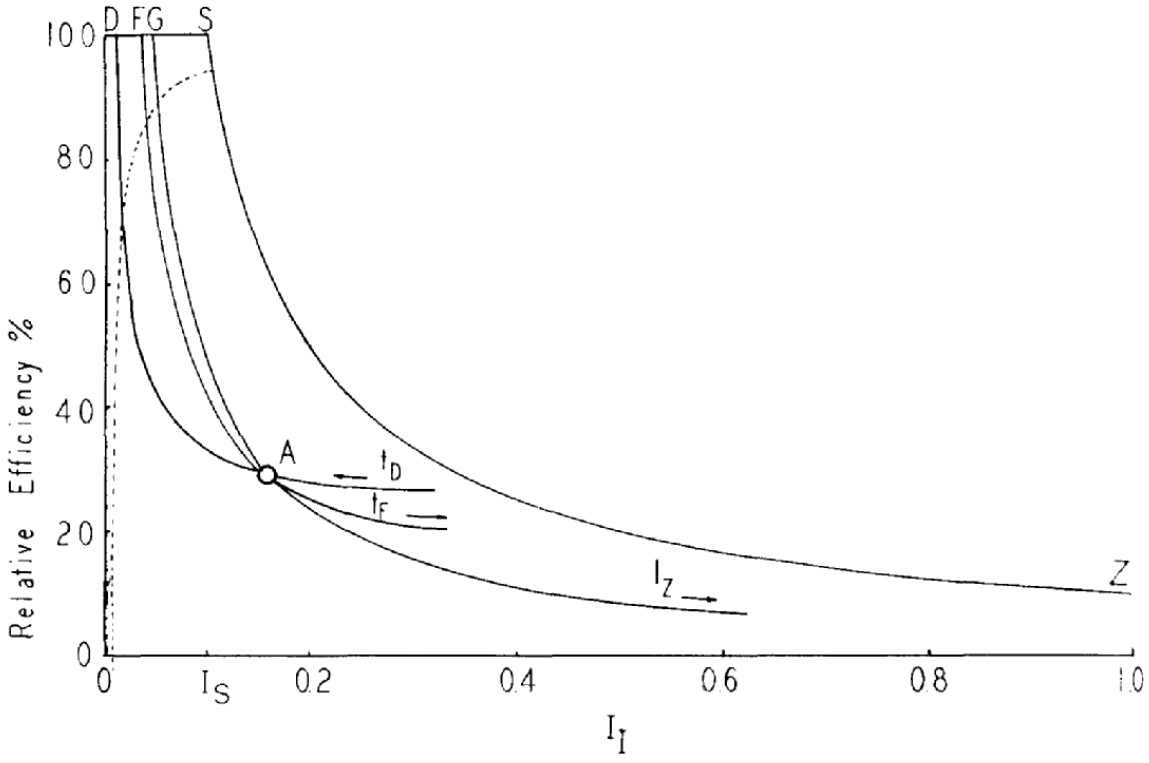

Figure 8.6. Fig. 5 from Kok (1953) predicting photon utilization as affected by t_f, t_d, and I_f (I_z). The abscissa represents the integrated light intensity (I_a) scaled to full sunlight.

Rewriting Eq. 19 in terms of t_f, t_d, and I_f yields

$$u_p = \frac{C + t_f I_s}{t_f I_f}\left(\ln\left(\frac{t_f I_f}{C + t_f I_s}\right) + 1\right) \tag{26}$$

To obtain the graph shown in Fig. 8.6, Kok started at point "A" where t_f = 16 ms, t_d = 84 ms, I_f = 1800 μE m^{-2} s^{-1}, and I_s = 180 μE m^{-2} s^{-1}, and determined the shape of the curves if t_f, t_d, or I_f were varied while holding the others values constant. Applying this to Eq. 26 and assuming C = 1 μmol m^{-2}, for convenience, yields the results shown in Fig. 8.7.

Figure 8.7 identically matches Kok's graph, except for the line of varying t_d.

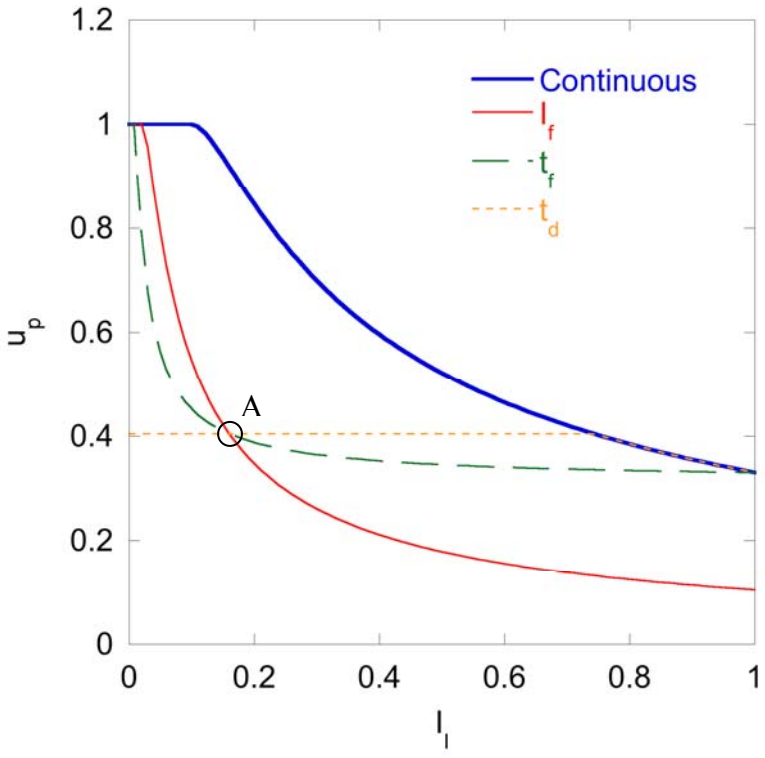

Figure 8.7. Photon uptake for varying I_f, t_f, and t_d according to Eq. 26.

Equation 26 predicts a flat line since it is independent of t_d, however Kok shows a curved line that flattens around point A. It is unclear why Kok generated this curve as he did. It contradicts results obtained by Phillips and Myers [39] in which increasing t_d did not increase the specific growth rate (and hence u_p), suggesting the flat line shown in Fig. 8.7 is correct.

CHAPTER 9

APPLICATION OF THE TEMPORAL LIGHT DILUTION MODEL

In this chapter, the relationship developed in Chapter 7 will be used to evaluate the performance of a reactor for the purposes of demonstrating its applicability to reactor design. Also, the general design recommendations will be made for the use of TLD in algal reactors.

9.1 Evaluation of the Temperature Control Reactor Design

The design of the temperature control reactors described in Chapters 2 through 6 were designed after the reactor used by Richmond and Cheng-Wu [8]. These reactors utilize rapid mixing of a dense algal culture to induce temporal light dilution. The effectiveness of this reactor at using the flashing effect will be evaluated here.

If the algae received no benefit from the intermittent illumination then $u_p \approx 0.34$ (I_s and I_o used for this calculation are determined below). With any benefit from intermittent illumination, u_p would increase.

Two characteristics of the reactor need to be determined: ϕ and v. In a reactor where random mixing is used to induce temporal light dilution, average values of ϕ and v are used since these values can vary significantly. Hu et al. suggested that the mean value of ϕ be calculated as the fraction of the reactor through which the light penetrates [37]. From photographs of light penetration into the reactors, it was determined that the sunlight penetrates roughly 8% of the reactor, thus $\phi \approx 0.08$.

To determine the flashing frequency observed by the algae, an experiment was devised in which a 0.6-cm orange plastic pellet was introduced into one of the reactors. This type of pellet was selected because it has a density comparable to water. The south side of the reactor was observed on a clear day for each time the pellet appeared. This was counted as one "flash" and the time required for 100 "flashes" was counted. From the time, a flashing frequency could be estimated. Since it was unlikely that the pellet could be observed every time it entered the lit zone of the reactor, this experiment provided a conservative flashing frequency. From this experiment, it was determined that $v = 0.55 \pm 0.02$ Hz.

The frequency of the light-dark cycle has been estimated based on turbulent fluid mechanics in vertical plate reactors by Richmond [56]. Extrapolating his estimates for reactors in the range of 0.375 cm to 6 cm to a 10-cm reactor gives a range of flashing frequencies from 0.1 to 3 Hz. However, since light penetrates into both sides of the reactor, the frequency should be twice that, or 0.2 to 6 Hz. The flashing frequency determined by the experiment above falls within this range, although closer to the lower end.

Characteristics of the algae, C and f, now need to be estimated. Chlorophyll (a and b) was extracted from samples according to the procedures suggested by Becker [57] using 90% methanol for six randomly selected dry samples. The resulting chlorophyll content was 26 mg g^{-1} dried algae. Melis et al. observed that dark green algal cultures (as opposed to yellow-green cultures) contain approximately 500 mol chlorophyll per mol of PSII, hence $c \approx 57$ μmol m^{-3} [31]. From the optical density data, χ was estimated to be

3.3 cm. Now C can be estimated to be 1.9 μmol m^{-2} and if f = 100 Hz, I_s = 190 μE m^{-2} s^{-1}. A similar value of I_s was observed by Melis et al. [31] for *Dunaliella salina*.

Applying Eq. 23, u_p = 0.36, therefore the mixing induced in the reactors did not significantly improve u_p. This is not surprising, since TLD effects in VPR's were not shown to be significant in reactors with thicknesses greater than 4 cm [37,56], and specific aeration rates (aeration flow rate / reactor volume) on the order of four [35]. Since the reactors were 10 cm thick with specific aeration rates of 0.7, their thickness would need to be reduced by more than half and aeration quadrupled to begin seeing improvements from TLD.

9.2 General Photobioreactor Design Considerations

In outdoor reactors, the saturating light intensity of the algae is commonly about one tenth of the incident light intensity [58]. The photon utilization fraction as a function of ϕ and v is illustrated in Fig. 9.1. Full photon utilization is only achievable when $\phi \leq I_s / I_o$ and v approaches f although the latter requirement is relaxed the smaller that ϕ is.

However, optimal conditions need not be attained to yield significant improvements in photon utilization. In situations without TLD, $u_p \approx 0.33$. To double photon utilization, $u_p \approx 0.66$, ϕ need only be less than 0.33 and $v/f \geq 0.66$. For smaller values of ϕ, v/f can be even smaller.

These results explain the contradiction between the predictions of Powell et al. [59] and the results of Hu et al. [37]. Powell et al. developed a model that integrated

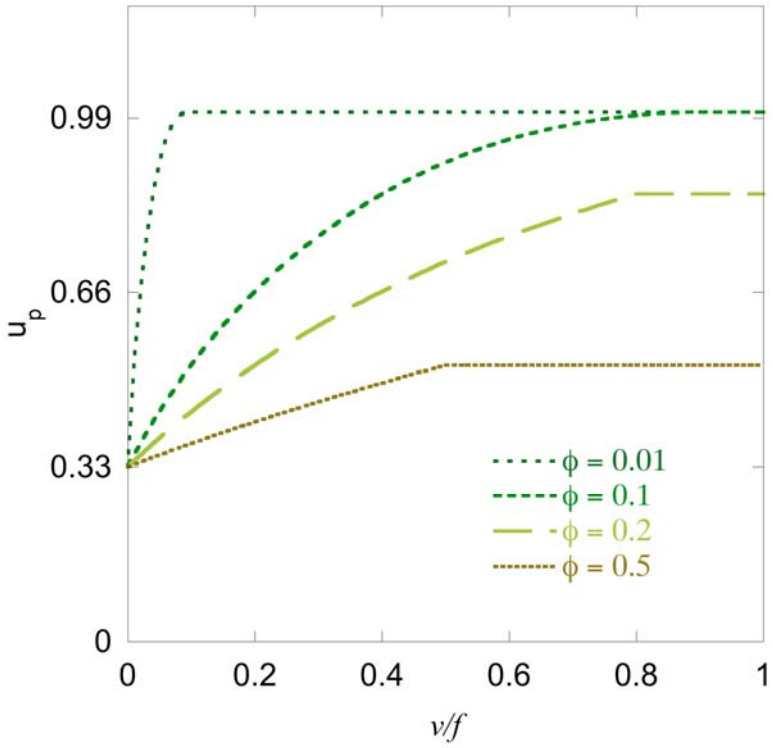

Figure 9.1. Photon utilization fraction as a function of flashing frequency normalized by the PSU turnover frequency for various load factors.

turbulent fluid mechanics with a probability model to predict the light/dark cycles of algae in a thin dense culture. Their results suggested that the variance of the light/dark cycles observed by the algae was so large that only a small fraction of algae would observe optimal light/dark cycles at any given time, thus rapid mixing was unlikely to yield significant improvements in production. However, Hu et al. clearly demonstrated that it did. Powell et al.'s prediction was inaccurate because, as was shown in Fig. 9.1, light/dark cycles can still yield large improvements in photon utilization even if the cycles are not optimal.

CHAPTER 10

TEMPORAL LIGHT DILUTION MODEL SUMMARY, CONCLUSIONS, AND FUTURE WORK

The Bush equation relates the fraction of photons utilized for photosynthesis to the incident continuous light intensity and the maximum photon utilization rate (I_s) of the algae. The work completed here generalized the equation to account for conditions in which the light is intermittent (flashing). The generalized equation is presented as

$$u_p = \frac{I_u}{I_a}\left[\ln\left(\frac{I_a}{I_u}\right)+1\right] \tag{23}$$

where I_u is dependent on the flashing conditions is always the minimum value of I_s, $Cv+\phi I_s$, and I_a ($I_u = \min\left(I_s, Cv+\phi I_s, I_a\right)$).

This model offers a simple means of taking into account algal characteristics (C and I_s) and optimizing a reactor that uses temporal light dilution for the algae. It was shown that C and I_s are related ($I_s = fC\gamma$), thus only two of the three variables need be determined, the third can be calculated.

The model was shown to successfully predict the experimental data of Phillips and Myers [39], Tennessen et al. [40], Terry [21], and Kok [38]. Only Phillips and Myers provided sufficient data to compare the model to each data point. The model predicted the experimental results to within ±30% for all but 3 of the 16 data points. The most probable cause of deviation is variation in the value of C among the experiments.

While the model definitely qualitatively simulates the results obtained by previous researchers, a set of future experiments should be devised on optically thick cultures of algae in which I_f, ϕ, v, C, and I_s are explicitly determined and the resulting productivities are compared to the values that Eq. 23 predicts to determine its quantitative accuracy.

Because of one of the assumptions made in the development of the model, a correction factor, κ, may reduce the error associated with that assumption, but no experimental data was available to demonstrate this. This correction factor is only of value when $I_a \approx Cv+\phi I_s$.

According to the model, many algae species can achieve maximum photon utilization with a flashing frequency above 100 Hz and a load factor not exceeding 10% for full sunlight. Algae with large I_s and C are more attractive for temporal light dilution applications because ϕ and v can be larger and smaller, respectively.

In deriving the model, it was shown that the growth rate of an algal culture with respect to incident light intensity can be described in the form of a Tessier kinetics formula:

$$\frac{\mu}{\mu_{\max}} = 1 - e^{-I_o/I_s} \tag{27}$$

This relationship appears to model experimental data very well in relatively dense algal cultures (as opposed to populations found in natural waters) and in which photoinhibition is not observed.

It is important to note that while temporal light dilution is a means of using high-intensity light (e.g. sunlight) more efficiently, it in no way improves the efficiency of the

photochemical pathways (i.e. any given PSU never utilizes photons, on average, at a rate more than I_s). As such, using concentrated light (either natural or artificial) in intermittent illumination would offer no improvement in areal productivity. Future reactors should, rather than attempt to temporally dilute the incident light, augment the location of the algae in such a way that its exposure to the incident light is intermittent. Vertical plate reactors described by Hu and Richmond [35], Hu et al. [36,37], and Richmond [56] are an example of this. Other reactors operating on a similar principle with appropriate flashing frequencies and load factors should yield comparable results.

REFERENCES

[1] Sheehan, J., Dunahay, T., Benemann, J., and Roessler, P., 1998, "A Look Back at the U.S. Department of Energy's Aquatic Species Program – Biodiesel from Algae," Technical Report No. NREL/TP-580-24190, National Renewable Energy Laboratory, Golden, CO.

[2] Zemke, P. E., Wood, B. D., Dye, D. J., Bayless, D. J., and Muhs, J. D., 2007, "Economic Analysis of a Vertical Sheet Bioreactor for Biodiesel Production," Proc. 2007 Energy Sustainability Conference, Long Beach, CA.

[3] Radmer, R., Behrens, P., Arnett, K., 1987. "Analysis of the Productivity of a Continuous Algal Culture System," Biotech. and Bioeng., 29, pp. 488-492.

[4] Andersson, A., Haecky, P., and Hagström, A., 1994, "Effect of Temperature and Light on the Growth of Micro- Nano- and Pico-plankton: Impact on Algal Succession," Marine Biol., 120(4), pp. 511-520.

[5] Lindström, K., 1984, "Effect of Temperature, Light, and pH on Growth, Photosynthesis and Respiration of the Dinoflagellate *Peridinium cinctum* FA. WESTII in Laboratory Cultures," Phycol., 20(2), pp. 212-220.

[6] Grobbelaar, J. U., and Soeder, C. J., 1985, "Respiration Losses in Planktonic Green Algae Cultivated in Raceway Ponds," Plankton Res., 7(4), pp. 497-506.

[7] Davis, E. A., Dedrick, J., French, C. S., Milner, H. W., Myers, J., Smith, J. H. C., and Spoehr, H. A., 1953, "Laboratory Experiments on Chlorella Culture at the Carnegie Institution of Washington Department of Plant Biology," *Algal Culture: From*

Laboratory to Pilot Plant, J.S. Burlew, ed., Carnegie Institution of Washington, Washington, DC, pp. 126-135, Chap. 9.

[8] Richmond, A., and Cheng-Wu, Z., 2001, "Optimization of a Flat-Plate Glass Reactor for Mass Production of *Nannochloropsis* sp. Outdoors," Biotech., 85, pp. 259-269.

[9] Sosik, H. M., and Mitchell, B. G., 1994, "Effects of Temperature on Growth, Light Absorption, and Quantum Yield in *Dunaliella tertiolecta* (Chlorophyceae)," Phycology, 30(5), pp. 833-840.

[10] Pierrot, D., Lewis, E., and Wallace, D. W. R., 2006, MS Excel Program Developed for CO2 System Calculations, ORNL/CDIAC-105a, Carbon Dioxide Information Analysis Center, Oak Ridge National Laboratory, Oak Ridge, TN, http://cdiac.ornl.gov/oceans/co2rprt.html.

[11] Leihr, S. K., 1988, "Mathematical Modeling of Carbon and Light-Limited Algal Biofilms," Ph.D dissertation, University of Illinois at Urbana-Champaign, Champaign, IL.

[12] Illman A. M., Scragg A. H., and Shales S.W., 2000, "Increase in Chlorella Strains Calorific Values When Grown in Low Nitrogen Medium," Enzym. and Microb. Technol., 27, pp. 631-635.

[13] Brown, T. L., LeMay, H. E., Jr., and Bursten, B. E., 2000, *Chemistry: The Central Science,* 8th ed., Prentice Hall, Upper Saddle River, NJ, pp. 145-186, Chap. 5.

[14] Coleman, H. W., and Steele, W. G., 1989, *Experimentation and Uncertainty Analysis for Engineers*, John Wiley and Sons, New York, pp. 30-32, Chap. 2.

[15] Borowitzka, M.A., and Borowitzka, L. J., eds., 1988, "*Dunaliella*," *Microalgal Biotechnology*, Cambridge University Press, New York, pp. 27-58.

[16] Zemke, P. E., Wood, B. D., and Dye, D. J., 2010, "Considerations for the Maximum Production of Triacylglycerol from Microalgae," Biomass and Bioenergy, 34, pp. 145-151.

[17] Stumm, W., and Morgan, J. J., 1981, *Aquatic Chemistry: An Introduction Emphasizing Chemical Equilibria in Natural Waters*, John Wiley and Sons, New York, p. 562, Chap. 9.

[18] Sorokin, C., and Krauss, R. W., 1958, "The Effects of Light Intensity on the Growth Rates of Green Algae," Plant Physiol., 33, pp. 109-113.

[19] Hall, D. O., and Rao, K. K., 1994, *Photosynthesis*, 5th ed., Cambridge University Press, New York, pp. 179-184, Chap. 8.

[20] Steele, J. H., 1965, "Notes on Some Theoretical Problems in Production Ecology," *Primary Productivity in Aquatic Environments*, C.R. Goldman, ed., University of California Press, Berkeley, pp. 383-398.

[21] Terry, K. L., 1986, "Photosynthesis in Modulated Light: Quantitative Dependence of Photosynthetic Enhancement on Flashing Rate," Biotech. and Bioeng., 28, pp. 988-995.

[22] Märkl, H., 1980, "Modelling of Algal Production Systems," *Algae Biomass*, G. Shelef, and C.J. Soeder, eds., North Holland Biomedical Press, Amsterdam, North Holland.

[23] Rubio, F. C., Camacho, F. G., Sevilla, J. M. F., Chisti, Y., and Grima, E. M., 2003, "A Mechanistic Model of Photosynthesis in Microalgae," Biotech. and Bioeng., 81(4), pp. 459-473.

[24] Eilers, P. H. C., and Peeters, J. C. H., 1988, "A Model for the Relationship Between Light Intensity and the Rate of Photosynthesis in Phytoplankton," Ecol. Model, 42, pp. 199-215.

[25] Burlew, J. S. ed., 1953, "Current Status of the Large-Scale Culture of Algae," Algal Culture: From Laboratory to Pilot Plant, Carnegie Institution of Washington, Washington, DC, pp. 3-23, Chap. 1.

[26] Zonneveld, C., 1998, "Photoinhibition as Affected by Photoacclimation in Phytoplankton: A Model Approach," Theor. Biol., 193, pp. 115-123.

[27] Eilers, P. H. C., and Peeters, J. C. H., 1993, "Dynamic Behaviour of a Model for Photosynthesis and Photoinhibition," Ecol. Model, 69, pp. 113-133.

[28] Chain, R. K., and Arnon, D. I., 1977, "Quantum Efficiency of Photosynthetic Energy Use," Proc. Natl. Acad. Sci., 74, pp. 3377-3381.

[29] Ley, A. C., and Mauzerall, D. C., 1982, "Absolute Absorption Cross Sections for Photosystem II and the Minimum Quantum Requirement for Photosynthesis in *Chlorella vulgaris*," Biochim. Biophys. Acta, 680, pp. 95-106.

[30] Osborne, B. A., and Geider, R. J., 1987, "The Minimum Photon Requirement for Photosynthesis," New Phyt., 106, pp. 631-644.

[31] Melis, A., Neidhardt, J., and Benemann, J. R., 1999, "*Dunaliella salina* (Chlorophyta) with Small Chlorophyll Antenna Sizes Exhibit Higher Photosynthetic

Productivities and Photon Use Efficiencies Than Normally Pigmented Cells," Appl. Phycol., 10, pp. 515-525.

[32] Gordon, J. M., and Polle, J. E. W., 2007, "Ultrahigh Bioproductivity from Algae," Appl. Microbiol. and Biotech., 96, pp. 969-975.

[33] Bayless, D. J., Vis-Chiasson, M. L., and Kremer, G. G., 2003, "Enhanced Practical Photosynthetic CO2 Mitigation," U. S. Patent No. 6,667,171 B2.

[34] Tredici, M. R., and Zittelli, G. C., 1998, "Efficiency of Sunlight Utilization: Tubular Versus Flat Photobioreactors," Biotech. and Bioeng., 57, pp. 187-197.

[35] Hu, Q., and Richmond, A., 1996, "Productivity and Photosynthetic Efficiency of *Spirulina plantensis* Affected by Light Intensity, Cell Density, and Rate of Mixing in a Flat Plate Reactor," Appl. Phycol., 8, pp. 139-145.

[36] Hu, Q., Guterman, H., and Richmond, A., 1996, "A Flat Inclined Modular Photobioreactor for Outdoor Mass Cultivation of Photoautotrophs," Biotech. and Bioeng., 51, pp. 51-60.

[37] Hu, Q., Zarmi, Y., and Richmond, A., 1998, "Combined Effects of Light Intensity, Light-Path, and Culture Density on the Output Rate of *Spirulina platensis* (Cyanobacteria)," Euro. J. Phycol., 33, pp. 165-171.

[38] Kok, B., 1953, "Experiments on Photosynthesis by Chlorella in Flashing Light," *Algal Culture: From Laboratory to Pilot Plant*, J.S. Burlew, ed., Carnegie Institute of Washington, Washington DC, pp. 63-75, Chap. 6.

[39] Phillips, J. N., Jr., and Myers, J., 1953, "Growth Rate of Chlorella in Flashing Light," Plant Physiol., pp. 152-161.

[40] Tennessen, D. J., Bula, R. J., and Sharkey, T. D., 1995, "Efficiency of Photosynthesis in Continuous and Pulsed Light Emitting Diode Irradiation," Photosynth. Res., 44, pp. 261-269.

[41] Park, K.-H., Kim, D.-I., and Lee, C.-G., 2000, "Effects of Flashing Light on Oxygen Production Rates in High-Density Algal Cultures," Microbiol. and Biotech., 10(6), pp. 817-822.

[42] Emerson, R., and Arnold, W., 1932, "A Separation of the Reactions in Photosynthesis by Means of Intermittent Light," Gen. Physiol., 15, pp. 391-420.

[43] Clendenning, K. A., and Ehrmantraut, H. C., 1950, "Photosynthesis and Hill Reactions by Whole *Chlorella* Cells in Continuous and Flashing Light," Arch. Biochem. 29, pp. 387-403.

[44] Weller, S., and Franck, J., 1941, "Photosynthesis in Flashing Light," Phys. Chem., 45(9), pp. 1359-1373.

[45] Rieke, F. F., and Gaffron, H., 1943, "Flash Saturation and Reaction Periods in Photosynthesis," Phys. Chem., 47, pp. 299-308.

[46] Matthijs, H. C. P., Balke, H., Van Hes, U. M., Kroon, B. M. A., Mur, L. R., and Binot, R. A., 1996, "Application of Light-Emitting Diodes in Bioreactors: Flashing Light Effects and Energy Economy in Algal Culture (*Chlorella pyrenoidosa*)," Biotech. and Bioeng., 50, pp. 98-107.

[47] Grobbelaar, J. U., 1991, "The Influence of Light/Dark Cycles in Mixed Algal Cultures on their Productivity," Bioresource Technol., 38, pp. 189-194.

[48] Zonneveld, C., 1997, "Modeling Effects of Photoadaptation on the Photosynthesis-Irradiance Curve," Theor. Biol., 186, pp. 381-388.

[49] Nedbal L, Tichy´ V., Grobbelaar J.U., Xiong, V.F., and Neori, A., 1996, "Microscopic Green Algae and Cyanobacteria in High-Frequency Intermittent Light." Appl. Phycol., 8, pp. 325-333.

[50] Gregory, R. P. F., 1989, *Photosynthesis*, Chapman and Hall, New York, pp. 83-94, Chap. 5.

[51] Hall, D. O., and Rao, K. K., 1994, *Photosynthesis*, 5th ed., Cambridge University Press, New York, pp. 51-53, Chap. 3.

[52] Dubinsky, Z., Falkowski, P. G., and Wyman, K., 1986, "Light Harvesting and Utilization by Phytoplankton," Plant Cell Physiol., 27(7), pp. 1335-1349.

[53] Sakshaug, E., Johnsen, G., Andresen, K., and Vernet, M., 1991, "Modeling of Light-Dependent Algal Photosynthesis and Growth: Experiments with the Barents Sea Diatoms *Thalassiosira nordenskioeldii* and *Chaetoceros furcellatus*," Deep-Sea Res., 38, pp. 415-430.

[54] Emerson, R., and Arnold, W., 1932, "The Photochemical Reaction in Photosynthesis," Gen. Physiol, 16, pp. 191-205.

[55] Phillips, J. N., Jr., and Myers, J., 1953, "Measurement of Algal Growth Under Controlled Steady-State Conditions," Plant Physiol., pp. 148-152.

[56] Richmond, A., 2003, *Handbook of Microalgal Culture*, Wiley-Blackwell, New York, pp. 149-151, Chap. 8.

[57] Becker, E. W., 1994, *Microalgae: Biotechnology and Microbiology*, Cambridge University Press, New York, pp. 58-59, Chap. 8.

[58] Goldman, J. C., 1979, "Outdoor Algal Mass Cultures – II. Photosynthetic Yield Limitations," Water Res., 13, pp. 119-136.

[59] Powell, C. K., Chaddock, J. B., and Dixon, J. R., 1965, "The Motion of Algae in Turbulent Flow," Biotech. and Bioeng., 7, pp. 295-308.

APPENDICES

APPENDIX A

STANDARD PROCEDURES

During the course of the experiments, as many as three technicians were maintaining the reactors and preparing samples. To eliminate variability as much as possible, standard procedures were developed and implemented. These procedures are detailed in this appendix.

A.1 Algae Dry Mass Preparation and Measurement

1. Wear gloves for all procedures in which skin may come into contact with algae to minimize contamination.
2. Thoroughly clean all containers and squeegee. Ensure the pH probe has been tested that day. If not, test it and calibrate if necessary.
3. **Write the date, time, technician initials, and sample labels** on the data sheet.
4. Remove lid from reactor and scrape inside walls of reactor with the squeegee. Be sure to thoroughly stir the bottom of the reactor with the squeegee to mix up settled algae. Remove and wipe down the squeegee.
5. Fill a 1-L Nalgene bottle with media and cap it with a lid.
6. Quickly move the sample(s) to the pH station and **record the pH** on the data sheet.
7. Fill two spectrophotometer (SP) cuvets with fresh media and place it in the slots of the SP. Autozero the SP at 806 nm. Fill another cuvet with the sample and place in the SP. Measure the optical density at 806 nm. **Write the optical density** on the data sheet. If the OD is higher than 0.5, it is necessary to dilute the sample. In this case,

write the optical density of the dilute solution AND the dilution factor.

8. Clean and thoroughly dry polycarbonate centrifuge bottles. **Record the dry weights of the bottles** (lid included) on the data sheet.
9. Fill the bottles with media to approximately 500 grams (lid included). Each bottle to be centrifuged much be within 0.1 grams of any other loaded bottle being centrifuged. **Record the final weights of the bottles** on the data sheet.
10. Prepare blank bottles with purified water if necessary according to step 7.
11. Load bottles in the centrifuge. Turn it on and go through necessary procedures to centrifuge the bottles at 7000 RPM for 7 minutes.
12. While the centrifuge runs, obtain a 50-mL centrifuge tube. **Label the tube with the date and sample description. Record the dry weight of the tube (cap included) on the data sheet.**
13. Remove the centrifuge bottles from the centrifuge and drain the supernatant into the sink. With a metal or plastic scoop, scrape most of the algae pellet from the bottles and place it in the 50-mL centrifuge tube.
14. Add a small (~25 mL) amount of hypersaline water (1.5 M NaCl) to one of the bottles and use the scoop to suspend the remaining algae in the bottle. Transfer the solution to the other bottle and repeat. Finally, pour the solution into the centrifuge tube.
15. Repeat step 12 until the centrifuge tube is filled to 50 mL. Place the lid on the tube and shake thoroughly.
16. Prepare a 50 mL centrifuge tube blank with purified water if necessary.
17. Place tube in the 50 mL centrifuge and centrifuge the tube at 3600 rpm for 20

minutes.

18. Measure the total volume of remaining algae solutions and **record on the harvest data sheet.** Dispose of remaining algae according to laboratory procedures.
19. Remove the centrifuge tube and pour off the supernatant into the sink. **Record the mass of the tube on the data sheet.**
20. Place the tube in the -80 ^{o}C freezer.

A.2 Daily Maintenance Procedures

1. Wear gloves for all relevant procedures to avoid skin contact with algae to prevent contamination.
2. From each of the three reactors, remove lid and pull the sparger from the solution. Using a piece of wire or other narrow device, clean debris out of and away from each of the holes in the sparger. Place the sparger back in the solution such that its orientation is diagonal from one corner of the reactor to the other and laying on the bottom of the reactor.
3. Visually check that the spargers in all three reactors appears to be sparging the same. Clean sparger(s) again if necessary. **Write technician initials on data sheet indicating that spargers have been cleaned and inspected.**
4. If necessary, with a non-cleaning sponge and a bucket of RO water, clean the dried algae from each of the reactor walls, trying not to deposit dried algae back into the solution. Replace the lids on the reactors.
5. Check the flow rates into each of the reactors. **Record each of the flow meter readings on the data sheet.** Adjust the flow meters as necessary such that the flow

into each of the reactors is the same. If adjustments are necessary, **record the new flow meter settings on the data sheet**.

A.3 Bomb Calorimetry Sample Preparation Procedures

1. Make sure mortar and pestle are clean and completely dry.
2. Place sample in mortar and grind to a powder with pestle.
3. Return the powder to its original container.
4. Use a paper towel and water to clean out the mortar and pestle.

A.4 Bomb Calorimetry Test Procedures

1. Open valves to the calorimeter under the sink. Run hot and cold water through the tap to bleed out room-temperature water
2. Obtain paper towels, beaker, tweezers, mortar and pestle, 0.0709 M Na2CO3 solution, isopropanol, 10 mL pipette, distilled water, squirt bottle, measuring stick, scoop, mass scale, and sample(s).
3. Ensure all equipment is clean and dry. If not, clean and dry dirty equipment.
4. Tare the mass scale. Place the bomb cal pail on the scale. Fill with water until the scale reads 2550 g. The mass should be within 1 g of 2550 g, but the closer the better. Place the pail in the calorimeter.
5. Place the crucible on the mass scale and tare it. Add 1/3 of the sample, or 0.5 g, whichever is less, to the crucible. **Record the mass of the sample, mi.** Install the crucible back onto the retaining wire. Throughout the rest of the experiment, DO NOT TARE THE SCALE.

6. Cut a length of fuse wire, approximately 10 cm. **Record the length of the wire, wi.** Tie the fuse wire into the holes and form the wire such that it dips into the sample, but does not touch the walls of the crucible.
7. Place the bomb insert into the bomb and screw the lid onto it.
8. Make sure the relief valve is closed. Place the oxygen feed fitting onto the oxygen bomb. Open the head valve, then slowly open the feed valve. Slowly load the bomb to 30 atmospheres. FAILURE TO SLOWLY PRESSURIZE BOMB CAN DISPLACE SAMPLE AND LEAD TO POOR RESULTS. Close both valves. Open the bleed valve, and remove the feed fitting.
9. Attach the bomb clamp to the oxygen bomb. Set the bomb into the pail. Release the clamp and shake all the water off the clamp into the pail.
10. Install the detonator wires into the bomb. Try not to remove water from the pail with fingers.
11. Swing the cover over the pail and lower it. Lower the thermometer into pail. Make sure the mixer falls into the pail.
12. Switch the calorimeter to ‘ON’. Make sure the calorimeter is set to ‘RUN’. Wait until the jacket temperature reaches the pail temperature, indicated by an audible clicking of the hot/cold water solenoids.
13. Check to make sure the jacket and pail temperatures are the same. **Record the temperature of the pail, Ti.**
14. Press and hold the ignite button until the red light goes out. If ignition has occurred, the temperature should begin to rise rapidly.

15. Wait 5 minutes to note the pail temperature. Wait 1 minute and check the pail temperature again. Repeat until the temperature remains steady for 2 minutes. **Record the temperature, Tf.**
16. Turn the calorimeter to 'Off'. Lift the thermometer. Lift the lid and swing away.
17. Remove the detonator wires. Use bomb clamp to lift the bomb out of the pail. Drain water off the top of the bomb into the pail.
18. Set the bomb on a flat surface. Crack the relief valve and wipe the bomb dry while it is venting.
19. When venting is complete, remove the lid, pull the core out, and set on the core stand. Remove the crucible and place on the mass scale. Pick out any pieces of wire, melted or not. **Record the mass, mf.**
20. Remove remaining wire, and straighten. **Record the length of remaining wire, wf.** Dispose of the wire so that it is not confused with future wire pieces.
21. Use a squirt bottle full of distilled water to liberally wash the core, bomb, and crucible. Pour the wash into a beaker. Use scoop to scrape loose caked soot. Add distilled water to the wash to make 50 mL.
22. Add a small amount of Methyl Orange to the beaker and swirl until dissolved. The solution should be red in color.
23. Fill a pipette to the 0-mL line with Na_2CO_3. Place the beaker under the pipette. Drip 0.5 mL at a time into the beaker and swirl continuously. Continue until liquid in the beaker turns orange or yellow. **Record the volume of titrant used, Tit.**

24. Pour out solution. Wash beaker with water and set aside. Wipe down and dry all bomb components and scoop with isopropanol. Drain water catch basin. FAILURE TO DRAIN CATCH BASIN CAN CAUSE THE CALORIMETER TO LEAK IN FUTURE EXPERIMENTS.
25. Repeat steps 4 – 24 until samples are completed.
26. Turn off water under cabinet. Leave the oxygen bomb insert hanging on the rack to avoid rusting. Return all tools and equipment.

A.5 Lipid Extraction Protocol

At no time during the protocol, should any plastic materials be used with the solvents. Many of the plastics release plasticizers or paraffin like fractions that interfere with the analysis. Use only glass pipettes, glass containers, Teflon coated caps and gas-tight syringes.

1. Take a clean 40-mL I-Chem style bottle (VWR P/N 15900-022), and add 15 mL of distilled water (by weight), then mark the bottom of the meniscus on the side of the bottle. This will be used to mark the final volume of solution for the analysis. Once marked, dump out the water and place in the oven to dry the glass before use. Label each bottle for their respective samples they will be containing.
2. Samples should be prepared as in Section A.3. Using a clean spatula, weigh out 200 mg of freeze dried algae sample into a test tube (16 x 125 mm Fisher P/N 14-961-30). Label the tube with its respective sample.

3. Prepare a solution of solvent for the extraction. This is prepared by adding equal volumes (usually 100 mL) of tetrahydrofuran, chloroform and hexane.
4. Using a 5-mL gas tight syringe, add 5 mL of the solvent mixture to each tube and sonicate using the microtip for about 10 seconds, three times each. Wipe off the sonicator tip between samples. **Make sure to wear adequate hearing protection.**
5. Place the test tubes in the Fisher Centrific Model 228 centrifuge and spin down the cell debris for approximately 1 minute. **Be careful, as there is always the possibility that a tube could break.**
6. Remove as much of the solvent as possible without disturbing the pelleted cell debris, and place in the premarked 40-mL I-Chem style bottle.
7. Repeat steps 4-6 two more times.
8. Bring the final volume of the extracted solution to 15 mL. Note that there may be some solvent left in the test tube after the final extraction. The solution should be capped and mixed, and is now ready for analysis.
9. Remove exactly 1 mL of the extract using a gas tight syringe and transfer to a GC vial with a Teflon septa (Fisher P/N 03-377-8D). Be sure to label the vials with by the samples they contain.
10. Add 10 μL of an internal standard of octacosane (10 mg dissolved in 1 mL of the solvent mixture). This will be used to confirm instrument performance and proper injection volume.
11. Add 50 μL of MSTFA to each GC vial.

A.6 GC Standard Preparation for Quantization

1. Prepare a stock standard solution as described below:

Heptadecane	50 uL
Myristic Acid	50 mg
Palmitic Acid	50 mg
Stearic Acid	50 mg
Stigmasterol	20 mg
Vegetable Oil	250 uL

2. Dissolve stock solution in 4 mL of solvent mix (THF:Chloroform:Hexane) as in Section A.5. Remove 10 uL, 25 μL, 50 uL and 100 μL and add to solvent in GC vial to make 1 mL total volume, then add 10 μL of internal standard to each. This prepares a maximal sample (100 μL) that contains the following:

Vegetable oil	5 μL/mL
Heptadecane	1 μL/mL
Myristic Acid	1 mg/mL
Palmitic Acid	1 mg/mL
Stearic Acid	1 mg/mL
Stigmasterol	0.4 mg/mL

APPENDIX B

CALCULATIONS

The equations used to calculate compound results (e.g. HRT, cell density, productivity) as well as measurement uncertainty are detailed below. Calculations justifying assumptions that were used in the chapters are also included.

For the determination of measurement uncertainties, e_r, the general formula

$$e_r = \left[\sum_{i=1}^{n} e_{X_i}{}^2 \left(\frac{\partial R}{\partial X_i} \right)^2 \right]^{1/2} \tag{28}$$

is used, where X_i denotes the associated variables used to calculate the result, R.

For the average calculations given in Table 4.2, and Table 4.4. the ranges represent confidence intervals of 95%. For data sets that were apparently random (AFEC, media density, repeated bomb calorimeter and GC experiments), Chauvenet's principle was applied to detect and remove aberrant data [14]. The precision limit, $\hat{e}$ was calculated as

$$\hat{e} = t_{95\%} S_X \tag{29}$$

unless otherwise specified below.

The measurement uncertainties given represent combined bias and precision uncertainties.

B.1 Hydraulic Retention Time

The HRT was calculated as:

$$\theta = \frac{V_R}{V_p} \tag{30}$$

A value of 29.5 ± 0.5 L was used for V_R since the reactors had a maximum capacity of 30 L as much as 1 L evaporated over the course of a day. The volume of media removed each day from the reactors, V_p, was calculated as

$$V_p = \frac{m_h + m_{c1} + m_{c2} + m_{rs}}{\rho_m} \tag{31}$$

where

m_h = Media mass obtained from reactor overflow

m_{c1} = Media mass from first centrifuge bottle

m_{c2} = Media mass from second centrifuge bottle

m_{rs} = Mass of sample remaining after centrifugation

ρ_m = Media density

The measurement uncertainty of θ is

$$e_\theta = \theta\left[\frac{{e_{V_r}}^2}{{V_r}^2} + \frac{{e_{\rho_m}}^2}{{\rho_m}^2} + \frac{4{e_{m_1}}^2}{\left(m_h + m_{c1} + m_{c2} + m_{rs}\right)^2}\right]^{1/2} \tag{32}$$

where

e_{V_r} = 0.5 L, based on up to 1 L of evaporation from each reactor per day

e_{ρ_m} = 4 g L^{-1}, based on 95% confidence of media density measurements

e_{m_1} = 0.005 g, based on mass scale measurement accuracy

B.2 Cell Density

The cell density, X, for each sample was calculated as the mass of the dry sample divided by the centrifuged sample volume:

$$X = \frac{\rho_m (m_d - m_e)}{m_{c1} + m_{c2}} \tag{33}$$

where

m_d = Mass of the dried sample (including tube)

m_e = Mass of the empty tube

and the cell density uncertainty is

$$e_X = X\left[\frac{e_{\rho_m}{}^2}{\rho_m^2} + \frac{e_{m_d}{}^2}{(m_d - m_e)^2} + \frac{e_{m_2}{}^2}{(m_d - m_e)^2} + \frac{2e_{m_1}{}^2}{(m_{c1} - m_{c2})^2}\right]^{1/2} \tag{34}$$

where

e_{m_d} = 0.05 g, based on variation in sample tube caps (95% confidence)

e_{m_2} = 0.00005 g, based on mass scale measurement accuracy

B.3 Mass Productivity

Mass productivity is defined as

$$P = V_R X / \theta \tag{35}$$

However, it can be simplified by substituting Eq. 30 for θ to obtain

$$P = V_p X = \frac{(m_h + m_{c1} + m_{c2} + m_{rs})X}{\rho_m} \tag{36}$$

The resulting mass productivity uncertainty is

$$e_P = P\left[\frac{4e_{m_1}^2}{m_h + m_{c1} + m_{c2} + m_{rs}} + \frac{e_X^2}{X^2} + \frac{u_{\rho_m}^2}{\rho^2}\right]^{1/2} \quad (37)$$

B.4 Energy Content

Two energy contents were calculated for each sample: total energy content, H_T, and ash-free energy content, H_{AF}. They were calculated from the bomb calorimetry results as

$$H_T = \frac{W(T_2 - T_1) - 2.3(l_2 - l_1) - \omega}{m_i} \quad (38)$$

and

$$H_{AF} = \frac{W(T_2 - T_1) - 2.3(l_2 - l_1) - \omega}{m_i - m_a} \quad (39)$$

where

W = Specific heat of the water, bucket, bomb, and internal components

T_1 = Initial water temperature

T_2 = Post-combustion water temperature

l_2 = Initial fuse wire length

l_1 = Post-combustion fuse wire length

ω = Titrant volume

m_i = Sample mass

m_a = Sample ash mass

The energy content uncertainty is

$$e_{H_{AF}} = H_{AF}\left[\frac{e_W^2\left(T_2 - T_1\right)^2 + 2e_T^2 + 10.58e_l^2 + e_\omega^2}{\left(W\left(T_2 - T_1\right) - 2.3\left(l_2 - l_1\right) - \omega\right)} + \frac{2u_{m1}^2}{\left(m_i - m_a\right)^2}\right]^{1/2} \quad (40)$$

where

e_W = 0.195 kJ/g, based on the certainty of 12 calibration points

e_T = 0.0025 ^{o}C, based on the minimum resolution of the thermometer

e_l = 0.5 mm, based on minimum resolution of the measuring stick

e_ω = 0.25 mL, based on the minimum quantity of titrant in which a color change could be observed

The presence of sulfur in samples combusted in a bomb calorimeter can bias the results. Calculations are given here to determine a maximum bias.

According to Table 3.1, the media was prepared with 1.25 g l^{-1} of $MgSO_4*7H_2O$, the only source of sulfur. Prepared samples were typically obtained from 1.6 L of media, containing a total of 2 g of $MgSO_4*7H_2O$ (0.26 g of S). It is very improbable that the algae incorporated all of the available sulfur from the media, but assuming such will establish a bias upper limit. The smallest sample taken had a dry mass of 0.8 g of algae, resulting in f_s = 0.26 / 0.8 = 32.5% sulfur content. Sulfur content bias is calculated as

$$b_s = -\frac{13.7 f_s}{m_s} \quad (41)$$

Given that the smallest m_s = 0.25 g, the maximum bias would be 18 cal g^{-1}, less than 0.4% of the lowest sample energy content.

B.5 Energy Productivity

The energy productivity, E, is simply the product of P and H_T, both of which have an associated mean value and variance. Because P and H_T are independent of each other, it can be assumed that the covariance of the two values is zero. Then

$$\overline{E} = \overline{P}\overline{H}_T \tag{42}$$

and

$$S_E = \left[\overline{P}^2 S_{H_T}^2 + \overline{H}_T^2 S_P^2 + S_{H_T}^2 S_P^2\right]^{1/2} \tag{43}$$

where

$\overline{E}$ = Mean energy productivity

$\overline{P}$ = Mean mass productivity

$\overline{H}_T$ = Mean total energy content

S_E = Energy productivity standard deviation

S_{H_T} = Total energy content standard deviation

S_P = Mass productivity standard deviation

B.6 TAG and FFA Content

Four compounds were sought out from the GC results: glycerin, octacosane, FFA, and TAG. To quantify them, the GC software was used to integrate the area under the resulting curves and compare them to the area under the curves generated by standard samples (see Appendix A.6).

For glycerin, the peaks were integrated from 4.75 to 5.25 min., for octacosane, 18.75 – 19.25 min., for FFA, 10 – 15 min., and for TAG, from 30 – 35 min. Glycerin and

octacosane were not compared to standards, only relative to each other, but FFA and TAG were compared to obtain actual concentrations.

From the standards, the conversion factors from area to mg of FFA and TAG, c_{FFA} and c_{TAG}, were (9.26 ± 1.33) × 10^6 au/mg and (1.84 ± 0.35) × 10^6 au/mg, respectively[4]. The FFA and TAG concentration, $\lambda_{FFA,TAG}$, was calculated as

$$\lambda_{FFA,TAG} = \frac{V_{sol}}{m_{sol}}\left[\frac{A_{FFA}}{c_{FFA}} + \frac{A_{TAG}}{c_{TAG}}\right] \tag{44}$$

where

V_{sol} = Total solvent volume (mL)

m_{sol} = Total solute mass (mg)

A_{FFA} = Area under peaks corresponding to FFA's (au)

A_{TAG} = Area under peaks corresponding to TAG's (au)

The measurement uncertainties associated with A_{FFA} and A_{TAG} were estimated in Section 3.11 to be ±5% of their values. The measurement uncertainty for λ is

$$e_\lambda = \lambda\left[\frac{e_{V_{sol}}^2}{V_{sol}^2} + \frac{e_{m_{sol}}^2}{m_{sol}^2} + \frac{e_A^2\left(c_{TAG}^2 + c_{FFA}^2\right)}{\left(A_{FFA}c_{TAG} + A_{TAG}c_{FFA}\right)^2} + \frac{e_{c_{FFA}}^2 A_{FFA}^2 c_{TAG}^4 + e_{c_{TAG}}^2 A_{TAG}^2 c_{FFA}^4}{\left(A_{FFA}c_{TAG} + A_{TAG}c_{FFA}\right)^2}\right]^{1/2} \tag{45}$$

in which

$e_{V_{sol}}^2$ = 0.5 mL

$e_{m_{sol}}^2$ = 0.2 mg

[4] au = arbitrary units

APPENDIX C

EXPERIMENTAL DATA

The data collected throughout the course of the experiment, including the reactor and sample data, bomb calorimetry data, GC data, and the calculated cell densities and productivities, are documented in Tables C1 – C4.

Data that has been crossed out was omitted because it was determined to be aberrant data. FFA and TAG data points that are highlighted in bold were biased by a factor of 1.66 because of an accidental change that was made to the GC equipment. The final FFA and TAG data that are reported take this factor into account. For data points that are the averages of 2 or more data points, the standard deviations are presented in parentheses.

Table C1. Daily reactor and sample data.

Sample	Sample Time (PM)	Aeration (lpm)	Insolation (MJ/m^2-day)	pH	OD (806 nm)	Sample Volume (l)	Harvested Volume (l)	Dry Cell Mass (g)	Cell Density (g/l)	Dry Time (days)
8/1 NTC	17:30	23		7.51	1.41	1.542	N/A	1.109	0.72	3
8/1 CTC	17:30	25		7.43	1.11	N/A	N/A	0.529	0.683	
8/1 VTC	17:30	25		7.68	N/A	N/A	N/A	N/A		
8/2 NTC	19:30	20		7.84	2.56	1.537	N/A	1.156	0.752	3
8/2 CTC	19:30	21		7.75	1.18	1.542	N/A	1.324	0.859	3
8/2 VTC	19:30	20		7.78	1.38	1.543	N/A	1.917	1.243	3
8/3 NTC	14:30	26		7.66	2.23	1.539	N/A	1.174	0.763	3
8/3 CTC	14:30	21		7.5	1.95	1.540	N/A	0.998	0.649	3
8/3 VTC	14:30	22		7.7	~~3.941~~	1.542	N/A	1.616	1.049	3
8/4 NTC	15:17	20		7.54	1.11	1.542	N/A	0.973	0.631	3
8/4 CTC	15:17	20		7.37	1.02	1.534	N/A	0.763	0.498	3
8/4 VTC	15:17	20		7.89	2.02	1.540	N/A	1.377	0.895	3
8/5 NTC	3:17	18		7.31	0.85	1.540	N/A	0.961	0.62	2
8/5 CTC	3:17	20		7.20	0.62	1.538	N/A	1.403	0.91	2
8/5 VTC	3:17	20		7.72	1.79	1.529	N/A	0.929	0.61	2
8/6 NTC	2:48	20		7.11	1.07	1.539	N/A	0.825	0.54	3
8/6 CTC	2:48	20		7.08	0.98	1.541	N/A	0.844	0.55	3
8/6 VTC	2:48	20		7.68	2.02	1.540	N/A	1.462	0.95	3
8/7 NTC	2:51	20		7.17	0.96	1.610	0.565	0.983	0.61	3
8/7 CTC	2:51	19		7.06	0.92	1.542	0.904	1.060	0.69	3
8/7 VTC	2:51	21		7.61	1.85	1.543	0.612	1.443	0.94	3
8/8 NTC	3:15	19		7.52	1.00	1.543	0.673	0.805	0.52	3
8/8 CTC	3:15	20		7.78	0.93	1.536	0.848	0.836	0.54	3
8/8 VTC	3:15	20		8.00	1.83	1.542	0.589	1.367	0.89	3
8/9 NTC	3:20	20		7.48	1.06	1.543	0.692	0.792	0.51	2
8/9 CTC	3:20	20		7.94	1.02	1.542	0.815	0.848	0.55	3
8/9 VTC	3:20	18		7.92	1.84	1.542	0.596	1.261	0.82	2

Sample	Sample Time (PM)	Aeration (lpm)	Insolation (MJ/m^2-day)	pH	OD (806 nm)	Sample Volume (l)	Harvested Volume (l)	Dry Cell Mass (g)	Cell Density (g/l)	Dry Time (days)
8/10 NTC	3:25	20		7.31	1.54	1.543	0.617	0.792	0.51	3
8/10 CTC	3:25	20		7.77	1.31	1.539	0.706	1.040	0.68	3
8/10 VTC	3:25	20		7.64	2.10	1.540	0.608	1.355	0.88	3
8/11 NTC	3:00	20		7.30	1.05	1.599	0.803	0.861	0.54	3
8/11 CTC	3:00	19		7.71	1.50	1.543	0.803	1.153	0.72	3
8/11 VTC	3:00	20		7.48	1.88	1.541	0.605	1.325	0.86	3
8/12 NTC	3:45	20		7.22	1.12	1.539	0.638	0.799	0.52	3
8/12 CTC	3:45	18		7.62	1.66	1.541	0.771	1.291	0.84	3
8/12 VTC	3:45	22		7.45	1.93	1.541	0.632	1.348	0.87	3
8/13 NTC	4:00	18		7.76	1.13	1.541	0.606	0.831	0.54	3
8/13 CTC	4:00	21	22.7	8.09	1.83	1.538	0.604	1.332	0.87	2
8/13 VTC	4:00	18		7.90	1.82	1.540	6.191	1.322	0.86	2
8/14 NTC	3:30	19		6.94	1.26	1.540	0.613	0.920	0.60	5
8/14 CTC	3:30	20	23.4	7.16	2.23	1.540	0.644	1.515	0.98	3
8/14 VTC	3:30	20		6.94	1.74	1.542	1.402	1.139	0.74	3
8/15 NTC	3:30	20		6.98	1.27	1.542	0.604	0.894	0.58	3
8/15 CTC	3:30	19	17.8	7.46	2.34	1.542	0.614	1.779	1.15	3
8/15 VTC	3:30	19		7.24	1.76	1.539	0.602	1.168	0.76	3
8/16 NTC	3:00	N/A		N/A	1.40	N/A	1.035	N/A	N/A	2
8/16 CTC	3:00	N/A	21.0	N/A	3.13	N/A	0.482	N/A	N/A	2
8/16 VTC	3:00	N/A		N/A	1.85	N/A	0.935	N/A	N/A	2
8/17 NTC	3:00	20		7.31	1.45	1.534	0.804	1.040	0.68	2
8/17 CTC	3:00	22	22.6	7.58	2.62	1.535	0.674	1.919	1.25	2
8/17 VTC	3:00	23		7.28	1.80	1.540	1.082	1.226	0.80	2
8/18 NTC	2:45	18		7.37	1.66	1.539	1.194	1.204	0.78	3
8/18 CTC	2:45	19	22.5	7.53	2.36	1.538	0.636	2.068	1.34	2
8/18 VTC	2:45	18		7.10	1.55	1.542	1.233	1.260	0.82	3
8/19 NTC	3:10	20		7.05	2.12	1.540	0.748	1.314	0.85	3

Sample	Sample Time (PM)	Aeration (lpm)	Insolation (MJ/m^2-day)	pH	OD (806 nm)	Sample Volume (l)	Harvested Volume (l)	Dry Cell Mass (g)	Cell Density (g/l)	Dry Time (days)
8/19 CTC	3:10	20	23.9	7.23	3.41	1.538	0.606	2.132	1.39	3
8/19 VTC	3:10	20		6.89	1.92	1.541	1.158	1.254	0.81	3
8/20 NTC	3:20	15		7.37	2.08	1.539	0.879	1.310	0.85	2
8/20 CTC	3:20	17	24.0	7.46	3.19	1.535	0.622	2.221	1.45	3
8/20 VTC	3:20	17		7.31	2.12	1.538	1.127	1.178	0.77	3
8/21 NTC	3:05	20		7.42	2.10	1.537	0.640	1.384	0.90	3
8/21 CTC	3:05	20	23.7	7.60	3.21	1.538	0.605	2.279	1.48	2
8/21 VTC	3:05	20		7.23	2.01	1.537	1.310	1.135	0.74	3
8/22 NTC	4:00	20		7.41	2.20	1.537	0.643	1.486	0.97	3
8/22 CTC	4:00	20	22.5	7.40	3.60	1.537	0.611	2.383	1.55	5
8/22 VTC	4:00	20		6.97	1.89	1.539	1.242	1.087	0.71	5
8/23 NTC	8:45	20		7.10	2.48	1.539	0.735	1.531	0.99	2
8/23 CTC	8:45	20	9.8	7.33	3.59	1.538	0.608	2.325	1.51	2
8/23 VTC	8:45	20		7.08	1.83	1.540	0.870	1.091	0.71	2
8/24 NTC	3:30	20		7.10	2.35	1.540	0.631	1.541	1.00	2
8/24 CTC	3:30	20	15.3	7.35	3.34	1.537	0.699	2.273	1.48	3
8/24 VTC	3:30	20		7.06	1.44	1.540	1.173	1.044	0.68	3
8/25 NTC	3:30	21		7.57	2.34	1.540	0.652	1.634	1.06	5
8/25 CTC	3:30	22	21.0	7.50	3.46	1.539	5.651	2.336	1.52	3
8/25 VTC	3:30	20		7.20	1.75	1.539	0.592	1.120	0.73	2
8/26 NTC	3:15	22		7.62	2.53	1.532	1.052	1.613	1.05	3
8/26 CTC	3:15	22	22.9	7.78	2.99	1.538	1.271	1.933	1.26	3
8/26 VTC	3:15	22		7.36	1.80	1.541	0.650	1.044	0.68	2
8/27 NTC	3:00	22		7.55	2.60	1.537	1.321	1.646	1.07	2
8/27 CTC	3:00	21	22.8	7.61	3.10	1.538	0.875	2.038	1.32	2
8/27 VTC	3:00	22		7.45	2.38	1.539	1.187	1.146	0.75	2
8/28 NTC	3:00	22		7.71	2.65	1.536	0.592	1.757	1.14	3
8/28 CTC	3:00	22	20.3	7.45	3.22	1.537	1.177	2.086	1.36	2

Sample	Sample Time (PM)	Aeration (lpm)	Insolation (MJ/m^2-day)	pH	OD (806 nm)	Sample Volume (l)	Harvested Volume (l)	Dry Cell Mass (g)	Cell Density (g/l)	Dry Time (days)
8/28 VTC	3:00	21		7.21	2.15	1.539	1.339	1.236	0.80	2
8/29 NTC	3:30	22		7.42	2.75	1.539	0.761	1.779	1.11	2
8/29 CTC	3:30	22	13.6	7.49	2.95	1.538	1.047	2.150	1.40	2
8/29 VTC	3:30	22		7.26	1.91	1.540	0.984	1.155	0.75	2
8/30 NTC	3:30	22		7.73	2.72	1.539	1.573	1.752	1.14	2
8/30 CTC	3:30	22	20.8	7.62	3.14	1.537	0.967	2.118	1.38	2
8/30 VTC	3:30	22		7.40	1.94	1.539	1.594	1.224	0.80	2
8/31 NTC	3:30	22		7.81	3.02	1.539	0.602	1.839	1.19	2
8/31 CTC	3:30	22	22.0	7.74	3.31	1.539	0.677	2.161	1.40	5
8/31 VTC	3:30	22		7.54	2.16	1.538	0.727	1.233	0.80	2
9/1 NTC	3:10	21		7.69	2.96	1.537	0.699	1.892	1.23	2
9/1 CTC	3:10	21	21.2	7.63	3.59	1.536	0.695	2.237	1.46	2
9/1 VTC	3:10	22		7.45	2.10	1.541	0.668	1.233	0.80	2
9/2 NTC	3:15	24		7.26	2.95	1.536	0.702	1.905	1.24	2
9/2 CTC	3:15	22	21.5	7.47	3.81	1.538	0.621	2.392	1.55	2
9/2 VTC	3:15	24		7.06	2.17	1.537	0.546	1.297	0.84	2
9/3 NTC	3:15	25		7.49	2.96	1.538	0.973	2.021	1.31	2
9/3 CTC	3:15	24	19.2	7.39	3.49	1.538	0.609	2.418	1.57	2
9/3 VTC	3:15	24		7.19	2.24	1.537	0.619	1.234	0.80	2
9/4 NTC	2:55	N/A		7.49	3.04	1.539	0.613	2.014	1.31	2
9/4 CTC	2:55	N/A	20.6	7.41	3.42	1.537	0.733	2.445	1.59	2
9/4 VTC	2:55	N/A		7.28	2.52	1.538	0.744	1.492	0.97	2
9/5 NTC	8:15	24		7.03	2.35	1.540	0.696	2.045	1.33	2
9/5 CTC	8:15	22	11.0	7.01	3.66	1.537	0.620	2.408	1.57	2
9/5 VTC	8:15	22		6.85	3.05	1.540	0.559	1.474	0.96	2
9/6 NTC	4:45	N/A		7.83	2.93	1.538	0.656	2.058	1.34	2
9/6 CTC	4:45	N/A	15.9	7.68	3.31	1.536	0.768	2.368	1.54	2
9/6 VTC	4:45	N/A		7.62	2.34	1.538	0.710	1.374	0.89	2

Sample	Sample Time (PM)	Aeration (lpm)	Insolation (MJ/m^2-day)	pH	OD (806 nm)	Sample Volume (l)	Harvested Volume (l)	Dry Cell Mass (g)	Cell Density (g/l)	Dry Time (days)
9/7 NTC	4:30	24		7.27	2.98	1.536	0.627	1.960	1.28	2
9/7 CTC	4:30	23	18.0	7.19	3.78	1.534	0.658	2.426	1.58	2
9/7 VTC	4:30	24		7.05	2.49	1.540	0.696	1.560	1.01	2
9/8 NTC	3:15	24		7.15	2.94	1.538	0.865	2.100	1.37	2
9/8 CTC	3:15	24	21.3	7.14	3.57	1.538	0.809	2.495	1.62	2
9/8 VTC	3:15	24		7.01	2.52	1.536	0.818	1.515	0.99	2
9/10 NTC	N/A	24		7.41	3.48	1.539	2.360	2.448	1.59	2
9/10 CTC	N/A	24	19.4	7.31	3.81	1.538	1.916	2.787	1.81	2
9/10 VTC	N/A	24		7.12	3.22	1.540	2.355	2.104	1.37	2
9/12 NTC	16:45	24		7.22	3.63	1.540	3.189	2.453	1.59	2
9/12 CTC	16:45	24	20.2	7.09	3.83	1.535	3.211	2.778	1.81	2
9/12 VTC	16:45	24		7.09	3.52	1.542	3.187	2.196	1.42	2
9/14 NTC	15:30	24		7.40	3.43	1.539	2.990	2.537	1.65	2
9/14 CTC	15:30	24	12.6	7.53	3.81	1.536	2.982	2.867	1.87	2
9/14 VTC	15:30	23		7.50	3.85	1.538	2.980	2.187	1.42	2
9/16 NTC	N/A	24		7.22	3.27	1.539	3.473	2.415	1.57	2
9/16 CTC	N/A	24	18.3	7.19	3.51	1.538	3.423	2.853	1.85	2
9/16 VTC	N/A	24		7.11	3.24	1.535	3.445	2.187	1.42	2
9/18 NTC	N/A	N/A		7.15	3.43	1.540	3.192	2.508	1.63	2
9/18 CTC	N/A	N/A	19.1	6.99	3.75	1.537	3.186	2.939	1.91	2
9/18 VTC	N/A	N/A		6.97	3.64	1.536	3.185	2.344	1.53	2
9/20 NTC	15:00	24		7.18	3.30	1.538	3.132	2.378	1.55	2
9/20 CTC	15:00	24	18.5	7.00	3.65	1.539	3.148	2.789	1.81	2
9/20 VTC	15:00	23		7.05	3.75	1.539	3.143	2.467	1.60	2
9/21 NTC	15:00	24		7.12	3.12					
9/21 CTC	15:00	24		7.06	3.44					
9/21 VTC	15:00	24		7.11	3.63					
9/22 NTC	15:00	24		7.79	3.21					

Sample	Sample Time (PM)	Aeration (lpm)	Insolation (MJ/m^2-day)	pH	OD (806 nm)	Sample Volume (l)	Harvested Volume (l)	Dry Cell Mass (g)	Cell Density (g/l)	Dry Time (days)
9/22 CTC	15:00	24		7.78	3.27					
9/22 VTC	15:00	24		7.87	4.26					
9/23 NTC	16:00	28		7.69	3.35					
9/23 CTC	16:00	28		7.51	3.50					
9/23 VTC	16:00	28		7.61	3.74					
9/24 NTC	15:00	27		7.46	3.32	1.540	0.710	2.226	1.45	2
9/24 CTC	15:00	26	18.2	7.40	3.45	1.537	0.948	2.405	1.56	2
9/24 VTC	15:00	26		7.42	3.79	1.540	1.227	2.357	1.53	2
9/25 NTC	15:00	26		7.39	3.42	1.540	0.969	2.288	1.49	2
9/25 CTC	15:00	26	17.6	7.37	3.55	1.540	0.942	2.410	1.57	2
9/25 VTC	15:00	26		7.43	3.88	1.535	1.084	2.318	1.51	2
9/26 NTC	15:00	27		7.57	3.54	1.540	0.871	2.344	1.52	2
9/26 CTC	15:00	24	17.4	7.46	3.79	1.539	0.727	2.480	1.61	2
9/26 VTC	15:00	26		7.53	3.84	1.540	0.644	2.375	1.54	2

Table C2. Bomb calorimetry data.

Sample	Test Date	Sample Mass (g)	Temperature Change (K)	Wire Consumed (cm)	Titrant (ml)	Ash Content (g)	Total Energy Content (kJ/g)		Ash-free Energy Content (kJ/g)	
8/6 CTC	9/20	0.26	0.37	6.9	0.5	0.1				
8/6 CTC	9/20	0.26	0.355	8.1	1	0.1	12.07	(0.35)	20.21	(0.85)
8/6 CTC	10/23	0.32	0.43	5.8	1.25	0.14				
8/6 NTC	10/22	0.27	0.44	7.3	1.75	0.08				
8/6 NTC	10/27	0.27	0.49	3.8	2.25	0.04	14.04	(2.17)	19.21	(0.97)
8/6 NTC	10/28	~~0.22~~	~~0.295~~	~~5.1~~	~~1~~	~~0.08~~				
8/6 VTC	10/24	0.46	0.87	7.2	5	0.11				
8/6 VTC	10/27	0.46	0.85	8.1	4.5	0.12	16.33	(0.39)	21.68	(0.62)
8/6 VTC	10/28	0.46	0.83	7.7	3.25	0.11				
8/9 CTC	10/8	0.29	0.435	7.1	1.25	0.11				
8/9 CTC	10/24	0.29	0.42	3.7	1.5	0.1	13.10	(0.25)	20.49	(0.85)
8/9 CTC	10/27	0.28	0.425	7.4	1.25	0.1				
8/9 NTC	9/25	0.25	0.42	8	1.5	0.07				
8/9 NTC	10/8	0.25	0.355	4.2	2	0.09	13.84	(1.17)	20.61	(1.18)
8/9 NTC	10/22	0.26	0.425	7.8	2	0.09				
8/9 VTC	10/2	0.41	0.74	7.4	4.5	0.13				
8/9 VTC	10/23	0.41	0.75	4.8	4.25	0.11	16.09	(0.15)	22.43	(0.79)
8/9 VTC	10/27	0.46	0.84	7.7	5.25	0.12				
8/12 CTC	10/27	0.42	0.75	7.9	4	0.11				
8/12 CTC	10/28	0.42	0.755	4.3	3.5	0.11	15.61	(0.42)	21.35	(0.26)
8/12 CTC	10/28	0.39	0.67	7.9	3.5	0.11				
8/12 NTC	10/23	0.28	0.48	7.9	2.5	0.08				
8/12 NTC	10/27	0.28	0.485	7.4	2.25	0.08	14.95	(0.30)	21.03	(0.26)
8/12 NTC	10/29	0.27	0.45	7.4	2	0.08				
8/12 VTC	10/8	0.41	0.78	8	5	0.11				
8/12 VTC	10/21	0.41	0.78	8.5	5.25	0.11	16.82	(0.08)	22.47	(0.79)
8/12 VTC	10/28	0.51	0.975	8.1	5.75	0.11				

Sample	Test Date	Sample Mass (g)	Temperature Change (K)	Wire Consumed (cm)	Titrant (ml)	Ash Content (g)	Total Energy Content (kJ/g)	Ash-free Energy Content (kJ/g)
8/15 CTC	10/6	0.52	0.825	5.3	4.5	0.17		
8/15 CTC	10/21	0.53	0.81	4.6	5.5	0.18	13.99 (0.42)	20.68 (0.19)
8/15 CTC	10/23	0.56	0.91	7.5	5.25	0.17		
8/15 NTC	9/25	0.28	0.465	6.5	1.5	0.11		
8/15 NTC	10/3	0.26	0.44	5.9	1.5	0.09	14.90 (0.28)	23.36 (0.65)
8/15 NTC	10/27	0.26	0.45	7.4	2	0.09		
8/15 VTC	10/22	0.38	0.705	6.8	4.5	0.1		
8/15 VTC	10/26	0.38	0.71	4.8	5.25	0.1	16.33 (0.23)	21.98 (0.63)
8/15 VTC	10/27	0.37	0.675	7.5	3.5	0.09		
8/18 CTC	10/14	0.54	1.015	6.8	7.5	0.12		
8/18 CTC	10/21	0.5	0.92	7.8	6.5	0.11	16.37 (0.23)	21.01 (0.33)
8/18 CTC	10/23	0.59	1.08	7.6	6.25	0.13		
8/18 NTC	9/20	0.34	0.66	8	3.5	0.1		
8/18 NTC	10/28	0.34	0.605	8.2	3	0.09	16.29 (0.74)	22.28 (1.69)
8/18 NTC	10/28	0.45	0.82	7.5	3.75	0.11		
8/18 VTC	9/20	0.38	0.745	7.4	5	0.1		
8/18 VTC	9/20	0.37	0.72	7.9	4	0.09	17.12 (0.20)	22.90 (0.51)
8/18 VTC	10/6	0.44	0.84	5.4	6	0.11		
8/21 CTC	9/25	0.56	1.025	8.7	7.5	0.14		
8/21 CTC	10/3	0.54	0.97	4.6	6.5	0.13	16.79 (1.28)	22.13 (1.50)
8/21 CTC	10/27	~~0.6~~	~~1.235~~	~~5.9~~	~~7.5~~	~~0.14~~		
8/21 NTC	10/2	0.46	0.91	7.1	6	0.1		
8/21 NTC	10/2	0.47	0.885	5.3	6	0.12	16.96 (0.47)	22.29 (0.17)
8/21 NTC	10/8	0.45	0.85	7.4	5	0.11		
8/21 VTC	9/20	0.36	0.705	8.4	4.5	0.08		
8/21 VTC	10/15	0.36	0.725	6.3	4.5	0.07	17.01 (0.93)	22.04 (0.17)
8/21 VTC	10/28	0.41	0.74	5.6	3	0.11		
8/24 CTC	10/6	0.54	0.97	5.2	7.5	0.11		

Sample	Test Date	Sample Mass (g)	Temperature Change (K)	Wire Consumed (cm)	Titrant (ml)	Ash Content (g)	Total Energy Content (kJ/g)		Ash-free Energy Content (kJ/g)	
8/24 CTC	10/22	0.51	0.98	7.4	7	0.11	16.51	(0.55)	20.91	(0.85)
8/24 CTC	10/28	0.57	1.07	7.2	6.5	0.12				
8/24 NTC	10/8	0.47	0.93	7.1	6.5	0.1				
8/24 NTC	10/24	0.47	0.935	8	6.5	0.09	17.50	(0.07)	21.89	(0.30)
8/24 NTC	10/29	0.51	1.005	7.6	6.25	0.1				
8/24 VTC	9/25	~~0.33~~	~~0.645~~	~~6.8~~	4	~~0.1~~				
8/24 VTC	10/3	0.33	0.64	8	4	0.08	17.39	(0.42)	22.94	(1.63)
8/24 VTC	10/14	0.35	0.71	8.6	4.5	0.06				
8/27 CTC	9/18	0.52	0.96	8.5	7	0.1				
8/27 CTC	10/3	0.51	0.955	5.8	7.5	0.12	16.57	(0.27)	20.79	(0.79)
8/27 CTC	10/15	0.56	1.065	6.9	8	0.1				
8/27 NTC	10/14	0.51	1.01	5.4	7.5	0.1				
8/27 NTC	10/15	0.5	1.01	5.5	7	0.1	17.57	(0.33)	22.02	(0.31)
8/27 NTC	10/21	0.57	1.11	7.2	7.75	0.12				
8/27 VTC	10/2	0.37	0.735	8.1	4.5	0.08				
8/27 VTC	10/2	0.36	0.68	4.8	4.5	0.1	17.19	(0.42)	22.52	(0.56)
8/27 VTC	10/8	0.42	0.825	7.7	5.5	0.09				
8/30 CTC	9/18	0.545	0.96	8	4	0.15				
8/30 CTC	9/18	~~0.52~~	~~0.92~~	~~8.7~~	~~4.5~~	~~0.07~~	15.39	(0.39)	19.75	(1.72)
8/30 CTC	10/14	0.54	0.91	4.9	6	0.13				
8/30 NTC	9/18	0.5	0.945	6.2	5.5	0.09				
8/30 NTC	10/8	0.5	0.965	5.1	7	0.12	16.90	(0.19)	21.64	(1.09)
8/30 NTC	10/21	0.6	1.14	6.1	6	0.14				
8/30 VTC	10/6	0.37	0.755	4.2	5	0.06				
8/30 VTC	10/26	0.37	0.74	7.7	4.5	0.09	17.82	(0.24)	21.93	(1.25)
8/30 VTC	10/28	0.4	0.8	4.1	5.25	0.06				
9/2 CTC	10/8	0.55	1.005	4.6	6	0.12				
9/2 CTC	10/26	0.55	1.01	7.4	4.25	0.13	16.41	(0.28)	21.15	(0.35)

Sample	Test Date	Sample Mass (g)	Temperature Change (K)	Wire Consumed (cm)	Titrant (ml)	Ash Content (g)	Total Energy Content (kJ/g)	Ash-free Energy Content (kJ/g)
9/2 CTC	10/27	0.55	1.04	7.5	6.5	0.12		
9/2 NTC	10/23	0.6	1.18	6.4	7	0.13		
9/2 NTC	10/27	0.56	1.115	7.1	7	0.1	17.37 (0.31)	21.88 (0.40)
9/2 NTC	10/28	0.54	1.04	8.5	5.5	0.12		
9/2 VTC	10/3	0.43	0.83	7.1	5.5	0.11		
9/2 VTC	10/8	0.41	0.8	6.8	5	0.1	17.15 (0.09)	22.59 (0.48)
9/2 VTC	10/27	0.45	0.87	5.1	5	0.1		
9/5 CTC	10/24	0.58	1.015	8	4	0.16		
9/5 CTC	10/27	0.55	1.01	8	5.5	0.13	15.85 (0.38)	21.30 (0.09)
9/5 CTC	10/29	0.55	0.98	5.3	4.5	0.14		
9/5 NTC	10/6	0.56	1.1	7.2	8	0.12		
9/5 NTC	10/24	0.55	1.1	9	6.5	0.11	17.44 (0.22)	22.28 (0.27)
9/5 NTC	10/27	0.55	1.07	6.1	6.5	0.13		
9/5 VTC	10/22	0.47	0.92	8	4.25	0.09		
9/5 VTC	10/28	0.49	0.98	9.2	4.5	0.12	17.23 (0.49)	22.31 (1.01)
9/5 VTC	10/28	0.45	0.85	7.7	4	0.11		
9/8 CTC	10/3	0.53	0.905	7.8	4.5	0.15		
9/8 CTC	10/27	0.54	0.935	7.6	4	0.15	15.12 (0.20)	20.89 (0.44)
9/8 CTC	10/29	0.56	0.945	7.7	4.5	0.15		
9/8 NTC	10/8	0.53	1.005	8.8	7	0.12		
9/8 NTC	10/24	0.54	1.025	6.3	6	0.1	16.98 (0.33)	20.87 (0.70)
9/8 NTC	10/28	0.55	1.075	4.2	7	0.08		
9/8 VTC	10/14	0.5	1.005	7.3	7	0.11		
9/8 VTC	10/15	0.51	1.03	7.2	6.5	0.1	17.61 (0.39)	22.45 (0.30)
9/8 VTC	10/23	0.52	1.01	8.3	6.75	0.12		
9/25 CTC	10/29	0.75	1.42	8.7	7.75	0.16		
9/25 CTC	10/29	0.75	1.385	5.2	6.5	0.17	16.27 (0.60)	21.09 (0.33)
9/25 CTC	10/31	0.77	1.35	4.2	5.5	0.19		

Sample	Test Date	Sample Mass (g)	Temperature Change (K)	Wire Consumed (cm)	Titrant (ml)	Ash Content (g)	Total Energy Content (kJ/g)	Ash-free Energy Content (kJ/g)
9/25 NTC	10/29	0.76	1.555	7.7	9.25	0.14		
9/25 NTC	10/29	0.75	1.52	4.3	8.5	0.14	17.94 (0.28)	22.00 (0.37)
9/25 NTC	10/31	0.71	1.41	7.6	7.5	0.13		
9/25 VTC	10/29	0.77	1.565	7.6	8	0.13		
9/25 VTC	10/29	0.75	1.505	7.5	8	0.16	18.00 (0.17)	22.30 (0.51)
9/25 VTC	10/31	0.72	1.47	5.1	8	0.14		
Calibration	9/20	0.69	2.025	7.5	4.5	0		
Calibration	10/3	0.67	2	5.8	5	0		
Calibration	10/6	0.68	2.01	8.4	5	0		
Calibration	10/8	0.59	1.75	4.5	4	0		
Calibration	10/21	0.565	1.665	4.6	3	0		
Calibration	10/23	0.61	1.81	7.6	4	0		
Calibration	10/24	0.65	1.945	7.8	4.5	0		
Calibration	10/27	0.63	1.905	7.1	4.5	0		
Calibration	10/27	0.58	1.735	5.2	3.75	0		
Calibration	10/28	0.67	1.985	5.6	4.5	0		
Calibration	10/29	0.65	1.89	3.2	4.5	0		
Calibration	10/31	0.67	2	5.4	4.5	0		

Table C3. GC data.

Sample	Test Date	Glycerin Area (10^-5)	Octacosane Area (10^-5)	FFA Area (10^-5)	TAG Area (10^-5)	FFA & TAG Content (%)
8/5 CTC	11/25	61.0	15.6	8.2	22.5	1.65
8/5 NTC	12/8	68.0	30.5	1.9	18.4	0.96
8/5 VTC	12/8	80.7	31.6	6.1	24.8	1.58
8/8 CTC	12/1	59.9	15.0	1.5	14.6	~~0.76~~
8/8 NTC	12/12	67.4	8.2	5.0	11.2	0.89
8/8 VTC	12/8	100.2	34.7	1.7	28.8	1.40
8/11 CTC	12/9	123.9	30.2	2.5	25.6	1.33
8/11 NTC	12/8	95.3	31.5	1.8	23.4	1.17
8/11 VTC	12/8	130.5	32.3	1.0	34.4	1.59
8/14 CTC	12/19	212.4	21.3	4.6	50.8	**1.57**
8/14 NTC	12/8	143.3	34.5	2.0	30.0	1.47
8/14 VTC	12/9	118.1	27.7	3.0	31.2	1.61
8/17 CTC	12/9	188.4	25.9	1.9	34.4	1.66
8/17 NTC	12/12	146.3	9.4	4.1	23.7	1.37
8/17 VTC	12/19	168.9	20.5	4.4	52.5	**1.60**
8/20 CTC	12/19	183.5	21.1	4.6	59.2	**1.79**
8/20 NTC	12/19	208.5	24.3	5.1	70.2	**2.10**
8/20 VTC	12/8	119.9	35.5	5.2	36.5	2.02
8/23 CTC	12/1	155.4	14.5	1.2	39.0	1.80
8/23 NTC	12/8	143.2	36.4	1.8	39.1	1.86
8/23 VTC	12/8	130.2	35.4	2.3	42.5	2.04
8/26 CTC	12/9	134.0	30.6	3.5	34.5	1.79
8/26 NTC	12/12	133.2	10.4	3.7	32.3	1.71
8/26 VTC	12/19	200.5	23.4	6.2	65.8	**~~3.38~~**
8/29 CTC	12/9	175.8	32.8	2.2	43.6	2.09
8/29 NTC	12/9	190.1	30.7	2.4	45.6	2.19
8/29 VTC	12/9	134.4	32.1	7.1	34.4	2.08

Sample	Test Date	Glycerin Area (10^-5)	Octacosane Area (10^-5)	FFA Area (10^-5)	TAG Area (10^-5)	FFA & TAG Content (%)
9/1 CTC	12/1	181.2	11.6	2.2	48.6	2.31
9/1 NTC	12/8	173.9	35.1	1.3	40.9	1.90
9/1 VTC	12/1	149.6	13.0	2.8	51.4	2.48
9/4 CTC	11/25	191.8	12.2	2.4	52.2	2.48
9/4 NTC	11/25	148.8	14.2	4.2	47.2	2.41
9/4 VTC	12/1	159.9	12.2	3.1	45.6	2.25
9/7 CTC	12/1	191.7	14.3	1.3	44.7	2.07
9/7 NTC	12/1	191.8	13.4	2.0	52.7	2.47
9/7 VTC	12/8	161.3	30.6	2.6	34.1	1.70
9/24 CTC	12/1	166.1	15.6	1.6	39.5	
9/24 CTC	12/19	230.3	18.7	2.3	69.6	1.90 (0.72)
9/24 NTC	12/8	68.0	30.2	1.2	16.1	
9/24 NTC	12/12	183.0	10.5	1.6	39.0	1.49 (0.95)
9/24 NTC	12/19	250.9	20.0	2.8	63.9	
9/24 VTC	11/25	193.4	13.3	5.5	50.8	
9/24 VTC	12/9	162.9	31.2	6.8	42.6	2.38 (0.31)
9/24 VTC	12/19	236.9	21.2	7.4	64.0	
Standard, 0.75%	11/30		14.6	~~12.6~~	~~20.4~~	
Standard, 1.125%	11/30		14.4	14.1	28.1	
Standard, 1.88%	11/30		15.0	24.6	47.9	
Standard, 3.75%	11/30		14.0	42.7	89.9	
Standard, 5.63%	11/30		13.6	68.5	133.0	
Standard, 7.50%	11/30		12.2	93.7	~~163.8~~	

Table C4. HRT and productivity data.

Sample	Hyrdaulic Retention Time (days)	Mass Productivity (g/day)	Energy Productivity (kJ/day)	TAG/FFA Productivity (mg/day)
8/5 NTC	N/A	N/A		
8/5 CTC	N/A	N/A		
8/5 VTC	N/A	N/A		
8/6 NTC	19.5	N/A		
8/6 CTC	19.5	N/A		
8/6 VTC	19.5	N/A		
8/7 NTC	13.8	1.33		
8/7 CTC	12.3	1.68		
8/7 VTC	13.9	2.02		
8/8 NTC	13.5	1.16		10.3
8/8 CTC	12.6	1.30		9.8
8/8 VTC	14.1	1.89		26.4
8/9 NTC	13.4	1.15	15.9	
8/9 CTC	12.7	1.30	17.0	
8/9 VTC	14.0	1.75	28.1	
8/10 NTC	13.9	1.11		
8/10 CTC	13.4	1.52		
8/10 VTC	14.0	1.89		
8/11 NTC	12.5	1.29		15.1
8/11 CTC	12.5	1.69		22.4
8/11 VTC	14.0	1.85		29.3
8/12 NTC	13.8	1.13	16.9	
8/12 CTC	13.0	1.94	30.3	
8/12 VTC	13.8	1.90	32.0	
8/13 NTC	14.0	1.16		
8/13 CTC	14.0	1.85		
8/13 VTC	3.9	6.64		

Sample	Hyrdaulic Retention Time (days)	Mass Productivity (g/day)	Energy Productivity (kJ/day)	TAG/FFA Productivity (mg/day)
8/14 NTC	13.9	1.29		18.9
8/14 CTC	13.7	2.15		33.6
8/14 VTC	10.2	2.17		34.9
8/15 NTC	14.0	1.24	18.5	
8/15 CTC	13.9	2.49	34.8	
8/15 VTC	14.0	1.62	26.5	
8/16 NTC	N/A	N/A		
8/16 CTC	N/A	N/A		
8/16 VTC	N/A	N/A		
8/17 NTC	12.8	1.59		21.8
8/17 CTC	13.6	2.76		45.8
8/17 VTC	11.4	2.09		33.5
8/18 NTC	11.0	2.14	34.8	
8/18 CTC	13.8	2.92	47.8	
8/18 VTC	10.8	2.27	38.8	
8/19 NTC	13.1	1.95		
8/19 CTC	14.0	2.97		
8/19 VTC	11.1	2.20		
8/20 NTC	12.4	2.06		43.2
8/20 CTC	13.9	3.12		55.8
8/20 VTC	11.3	2.04		41.3
8/21 NTC	13.8	1.96	33.2	
8/21 CTC	14.0	3.17	53.3	
8/21 VTC	10.5	2.10	35.8	
8/22 NTC	13.8	2.11		
8/22 CTC	14.0	3.33		
8/22 VTC	10.8	1.96		
8/23 NTC	13.2	2.26		42.0

Sample	Hyrdaulic Retention Time (days)	Mass Productivity (g/day)	Energy Productivity (kJ/day)	TAG/FFA Productivity (mg/day)
8/23 CTC	14.0	3.24		58.5
8/23 VTC	12.4	1.71		34.9
8/24 NTC	13.8	2.17	38.0	
8/24 CTC	13.4	3.31	54.6	
8/24 VTC	11.1	1.84	32.0	
8/25 NTC	13.7	2.33		
8/25 CTC	4.2	10.92		
8/25 VTC	14.1	1.55		
8/26 NTC	11.6	2.72		46.6
8/26 CTC	10.7	3.53		63.3
8/26 VTC	13.7	1.48		50.2
8/27 NTC	10.5	3.06	53.8	
8/27 CTC	12.4	3.20	53.0	
8/27 VTC	11.0	2.03	34.9	
8/28 NTC	14.1	2.43		
8/28 CTC	11.1	3.68		
8/28 VTC	10.4	2.31		
8/29 NTC	13.0	2.55		55.9
8/29 CTC	11.6	3.61		75.5
8/29 VTC	11.9	1.89		39.4
8/30 NTC	9.6	3.54	59.9	
8/30 CTC	12.0	3.45	53.1	
8/30 VTC	9.6	2.49	44.4	
8/31 NTC	14.0	2.56		
8/31 CTC	13.5	3.11		
8/31 VTC	13.2	1.82		
9/1 NTC	13.4	2.75		52.3
9/1 CTC	13.4	3.25		75.0

Sample	Hyrdaulic Retention Time (days)	Mass Productivity (g/day)	Energy Productivity (kJ/day)	TAG/FFA Productivity (mg/day)
9/1 VTC	13.6	1.77		43.9
9/2 NTC	13.4	2.78	48.2	
9/2 CTC	13.9	3.36	55.1	
9/2 VTC	14.4	1.76	30.2	
9/3 NTC	11.9	3.30		
9/3 CTC	14.0	3.38		
9/3 VTC	13.9	1.73		
9/4 NTC	13.9	2.82		67.8
9/4 CTC	13.2	3.61		89.6
9/4 VTC	13.1	2.21		49.8
9/5 NTC	13.4	2.97	51.8	
9/5 CTC	13.9	3.38	53.6	
9/5 VTC	14.3	2.01	34.6	
9/6 NTC	13.7	2.94		
9/6 CTC	13.0	3.55		
9/6 VTC	13.3	2.01		
9/7 NTC	13.9	2.76		68.1
9/7 CTC	13.7	3.47		71.6
9/7 VTC	13.4	2.26		38.6
9/8 NTC	12.5	3.28	55.7	
9/8 CTC	12.8	3.81	57.6	
9/8 VTC	12.7	2.32	40.9	
9/10 NTC	15.4	6.20		
9/10 CTC	17.4	6.26		
9/10 VTC	15.4	5.32		
9/12 NTC	12.7	7.53		
9/12 CTC	12.6	8.59		
9/12 VTC	12.7	6.74		

Sample	Hyrdaulic Retention Time (days)	Mass Productivity (g/day)	Energy Productivity (kJ/day)	TAG/FFA Productivity (mg/day)
9/14 NTC	13.2	7.47		
9/14 CTC	13.3	8.43		
9/14 VTC	13.3	6.42		
9/16 NTC	12.0	7.87		
9/16 CTC	12.1	9.20		
9/16 VTC	12.0	7.09		
9/18 NTC	12.7	7.71		
9/18 CTC	12.7	9.03		
9/18 VTC	12.7	7.20		
9/20 NTC	12.8	7.22		
9/20 CTC	12.8	8.49		
9/20 VTC	12.8	7.50		
9/24 NTC	13.3	3.25		48.3
9/24 CTC	12.1	3.89		74.0
9/24 VTC	10.8	4.23		100.9
9/25 NTC	12.0	3.73	66.9	
9/25 CTC	12.1	3.89	63.2	
9/25 VTC	11.5	3.95	71.2	
9/26 NTC	12.4	3.67		
9/26 CTC	13.2	3.65		
9/26 VTC	13.7	3.37		

APPENDIX D

COPYRIGHT PERMISSION

The following pages contain e-mail correspondences from Tina McDowell, Editor and Publications Officer, for the Carnegie Institution of Washington, regarding permission to use Fig. 5 from Kok [38] (Fig. 8.6).

Gmail Peter Zemke <pezemke@gmail.com>

Copyright Permission

2 messages

Peter Zemke <pezemke@gmail.com> **Wed, Mar 10, 2010 at 2:30 PM**
To: tmcdowell@ciw.edu

Dear Ms. McDowell,

As I stated to you on the phone earlier today, I am in the process of preparing my dissertation in the Department of Mechanical Engineering at Utah State University. I hope to complete it in May of this year.

I am requesting your permission to include one figure from page 70 of the book published by the Carnegie Institute of Washington in 1953, titled *Algal Culture: From Laboratory to Pilot Plant,* by B. Kok and edited by J.S. Burlew. I intend to use the figure in my dissertation as shown in the attachment. I will include acknowledgments and/or appropriate citations to their work as shown in the attachment and copyright and reprint rights information in a special appendix. The citation will appear at the end of the manuscript as shown. Please advise me of any changes you require.

Please indicate your approval of this request via e-mail, fax, or letter, attaching any other form or instruction necessary to confirm permission. If you charge a reprint fee for use of your material, please indicate the charge and how you would prefer to receive the fee. If you have any questions, feel free to contact me.

Kind regards,

Peter Zemke

PhD Candidate
Mechanical & Aerospace Engineering
Utah State University
4130 Old Main Hill
Logan, UT 84322-4130

T: (435) 232-7708
F: (435) 797-1099

Zemke Copyright Permission.pdf
32K

Tina McDowell <tmcdowell@ciw.edu> **Thu, Mar 11, 2010 at 5:18 AM**
To: Peter Zemke <pezemke@gmail.com>

Carnegie has no objection to your use of the stated material. Please note that it's Carnegie InstituTION

[Quoted text hidden]

--
Tina McDowell
Carnegie Instituion for Science
1530 P St. NW
Washington, DC 20005
202-939-1120
www.CarnegieScience.edu
Follow us on twitter http://CarnegieScience.edu/twitter
Become our facebook fan http://CarnegieScience.edu/facebook

CURRICULUM VITAE

PETER EDWIN ZEMKE

May 2010

EDUCATION

Ph.D in Mechanical Engineering, Department of Mechanical & Aerospace Engineering, Utah State University, Logan, UT. *Research interests:* Optimization of algal photobioreactors, anaerobic digester process engineering, theoretical modeling of bioreactors. *Dissertation:* Mathematical Modeling of Light Utilization and the Effects of Temperature Cycles on Productivity in a Steady-State Algal Photobioreactor. *Chair:* Professor Byard D. Wood. May 2010.

M.S. in Mechanical Engineering, Department of Mechanical & Aerospace Engineering, Utah State University, Logan, UT. *Research interests:* Hybrid solar lighting, solar water heating, radiation-induced convection, natural convection. *Thesis:* Adaptation of Hybrid Solar Lighting Technology for Use in Solar Domestic Hot Water. *Chair:* Professor Byard D. Wood. December 2005.

B.S in Mechanical Engineering, Department of Mechanical & Aerospace Engineering, Utah State University, Logan, UT. *Emphasis:* Thermal / Fluids. December 2005.

PUBLICATIONS

Journals

Zemke PE, Dye DD, Wood BD, 2010. Considerations for the Maximum Production Rates of Triacylglycerol from Microalgae. *Biomass & Bioenergy* 34: 145 - 151.

Conferences

Gale JA, Zemke PE, Wood BD, Sunderland S, Weeks SA, 2009. Comparison of Induced Sludge Bed (Blanket) Anaerobic Reactor to Vertical Plug Flow Technology for Animal Manure Digestion, *Proceedings of the 2009 Western Nutrient Management Conference*, Salt Lake City, UT.

Zemke PE, Dye DD, Wood BD, Bayless DJ, Muhs JD, 2007. Economic Analysis of a Vertical Sheet Algal Bioreactor for Biodiesel Production, *Proceedings of the 2007 Energy Sustainability Conference,* Long Beach, CA.

Zemke PE, Wood BD, 2006. Hybrid Solar Lighting May Have Another Utility: Solar Water Heating, *Proceedings of the 2006 International Solar Energy Conference*, Denver, CO.

Posters

Zemke PE, Gale JA, 2009. Thermodynamics of a Full-Scale Anaerobic Digestion Process, *2009 Intermountain Graduate Student Symposium*, Logan, UT.

Zemke PE, 2004. Solar Hybrid Lighting, *2004 ASME Regional Student Conference*, Denver, CO.

Presentations

Zemke PE, Gale JA, 2009. Upstream Methods of Hydrogen Sulfide Mitigation in Anaerobic Digesters, *2009 Institute of Biological Engineering Regional Conference*, Logan, UT.

Zemke PE, 2009. A Review of the Design, Operation, and Performance of a Lab-Scale Vertical Sheet Photobioreactor, *2008 Intermountain Graduate Student Symposium*, Logan, UT.

ADDITIONAL RESEARCH

Sunderland Dairy Anaerobic Digester Retrofit Project, Utah State University (PI: Byard Wood). Designed biogas collection system and instrumentation, and over-pressure safety devices. Engineered solution to a design flaw in the effluent heat recovery unit. Collected and analyzed performance data to evaluate the system. Conducted analysis and made recommendations for economical operation in winter months.

RELATED SKILLS

Experimental:
- Bomb calorimetry
- Algal culturing techniques
- Biogas handling & sampling
- Lipid extraction & gas chromatography
- Particle Image Velocimetry (PIV)
- Basic machining & carpentry
- General laboratory practices

Computer:
- CFD (Fluent)
- Programming (Fortran, Matlab)
- Graphics (Solid Edge)
- Office Applications (Microsoft Office, iWork, Open Office)
- Math (Maple, Matlab)

AWARDS AND TITLES

Graduate researcher of the year, Department of Mechanical & Aerospace Engineering, 2008-2009 school year.

Subject matter expert, 2009 Hill Air Force Base Energy Forum, Biomass session.

Second place, Old Guard Poster Competition, 2004 ASME Regional Student Conference, Denver, CO.

PREVIOUS WORK EXPERIENCE

Mechanical engineer (short-term contract), Sustainable Energy Systems, Reno, NV – Jan. – Feb. 2009. Used numerical modeling to incorporate climate and experimental data to assess the heating requirements for a combined heat and power system at a gold leaching operation.

Engineering Intern, Aerojet, Clearfield, UT – May – Dec. 2002, May – Aug. 2003, May – Dec. 2005. Applied structural, dynamic, thermodynamic, and fluid engineering analyses to liquid rocket system components and subsystems maintenance.

AFFILIATIONS

American Society of Mechanical Engineers, 2000 - present

REFERENCES

Dr. Byard Wood, Department Head, Mechanical & Aerospace Engineering, Utah State University, 4130 Old Main Hill, Logan, UT 84322. *Phone:* (435) 797-2868, *Email:* byard.wood@usu.edu

Jody Gale, Extension Agent, Richfield Utah State University Extension, 250 N. Main Cnty Adm Bldg, Richfield, UT 84701. *Phone:* (435) 893-0470, *Email:* jody.gale@usu.edu

Dr. Ron Sims, Department Head, Biological and Irrigation Engineering, Utah State University, 4105 Old Main Hill, Logan, UT 84322. *Phone:* (435) 797-3156, *Email:* rcsims@engineering.usu.edu

Dr. Shaun Dustin, Energy Dynamics Lab, 1695 N Research Parkway, Logan, UT 84341. *Phone:* (435) 770-7816, *Email:* shaun.dustin@energydynamicslab.com